Reply to anonymous referee nr. 1 (review acpd-15-C589-2015):

We thank the reviewer for the helpful comments which we think have helped to improve the manuscript significantly. Especially, by removing the grammatical errors and misleading statements the revised manuscript will be easier to understand for the reader. The detailed replies on the reviewers comments are given below and structured as follows. Reviewer comments have bold letters, are labeled, and listed always in the beginning of each answer. The reviewer comments are followed by the author's comments including if necessary revised parts of the paper. The revised parts of the paper are written in quotation marks and italic letters.

Major Comments:

1. *The necessity for a more thorough literature review*.

a) The authors use of the catch-all term, '3-D effect' could be better formalized in the introduction (Which are you accounting for? Which are you not accounting for?)

➔ We thank the reviewer for highlighting this lack of information. Now, we have included the following part to the introduction:

"Within the present study, the focus lies on those 3-D radiative effects that are related to the horizontal photon transport between cloud and surface due to isotropic reflection of the incident radiation on the bright sea ice. The goal is to quantify the magnitude and horizontal extent of those 3-D effects as well as their influence on cloud retrievals from the visible wavelength range with a high spatial resolution. In reality, such surface 3-D radiative effects will be combined with cloud 3-D radiative effects due to cloud inhomogeneities."

➔ Additionally, we have included a new Figure (Reply-Figure 1), illustrating the effect of the horizontal photon transport between surface and cloud layer to better describe the 3-D radiative effect we are investigating here. The manuscript is adjusted as follows:

"…In this study, only the latter case is considered, namely, the 3-D radiative effects related to the pathway of the photons between cloud and surface. Horizontal photon transport in the layer between surface and cloud smoothes the abrupt decrease of the surface albedo from large values above sea ice to low values above the open water. For measurements without clouds (Fig. 4f, green in Fig. 6) we could not find similar areas with enhanced γ_λ above the water close to the ice edge. The theory explaining the 3-D radiative effect, which cause the enhancement of γ_λ, is illustrated in Fig. 7. The incident radiation ($F_0 \cdot \cos(\Theta)$) impinges on the cloud, where scattering and absorption processes take place. Part of the incident radiation is transmitted through the cloud and scattered into the direction of the ice edge (bold black arrow). Sea ice acts similar to a Lambertian reflector and reflects the incoming radiation almost uniformly in all directions (grey arrows). The reflected radiation penetrates the cloud at a certain altitude (red or blue arrows), from where parts of it are scattered into the observation direction. Without sea ice in the vicinity of the measurements, the reflected radiance would be influenced only by the cloud and dark ocean water. The measured nadir radiance $I^{\uparrow}$ above the cloud parcel is enhanced due to the additional radiation reflected from the sea ice into the direction of the last scattering point in the cloud. This effect is significant only for cloudy cases, because of the weak scattering efficiency of the clear atmosphere compared to that of clouds. If we compare the 3-D effect for clouds of different altitude (Fig. 7), the horizontal photon path of the reflected radiation is extended (compare for cloud A (red) and cloud B (blue)). Hence, the range of the 3-D effect increases with cloud altitude."

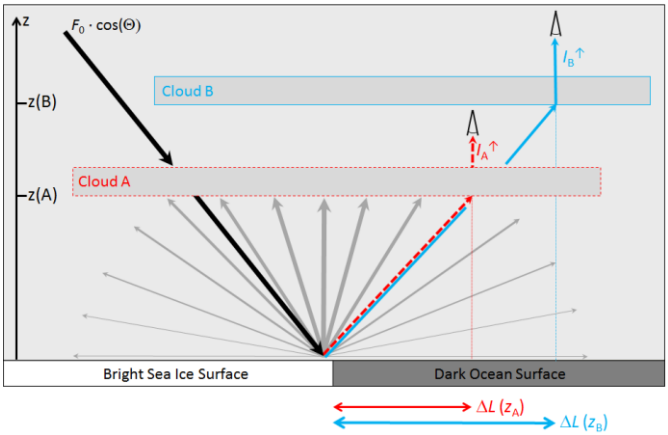

Reply-Figure 1: Sketch of the 3-D radiative effects between clouds at two different altitudes and the surface in the vicinity of an ice edge. The arrows illustrate the pathway of the photons between source, cloud, surface, and sensor.

b) Variability of the Arctic surface albedo: The Lindsay and Rothrock paper cited (page 1423) does not emphasize solely the large variability seasonally, but also monthly. This variability is a great consideration in how important the 3-D effects presented in the manuscript are important in practice (see major comment #2). This point is given only a brief, summary statement that is well into the paper (page 1444). …

➔ Thanks for this suggestion as it clearly motivates the investigation of the 3-D radiative surface effects in Arctic regions. In the revised manuscript the statement on the monthly variability in the Arctic surface albedo is included in the introduction:

"The mean values for the cloud-free portions of individual cells range from 0.18 to 0.91 and were found to be highly variable at monthly and annual time scales (Lindsay and Rothrock, 1994)."

"However, even when ice and ice-free areas are perfectly separated by the retrieval algorithms, 3-D radiative effects may still affect the cloud retrieval over ice-free pixels close to the ice edge. With respect to the large temporal and spatial variability of the Arctic surface albedo as described by Lindsay and Rothrock (1994), the investigation of the 3-D effects becomes even more important…."

… I disagree with the author's statement that near-infrared snow/ice surface albedo decreases only slightly compared to the visible (see, for example, measurements shown in Platnick et al., (2001; reference(s) listed at end of review)). In fact, the reduced variability in bright snow/ice surface conditions at near-infrared channels is the reason why satellite algorithms do not use the 645 nm wavelength channel to retrieve cloud properties over snow/ice, but rather the 1.2 micron plus 1.6 micron channel in the case of MODIS (Platnick et al., 2001; 2003; Krijger et al., 2011), as the authors have done.

➔ The reviewer is completely right. By mistake, we switched the words "slightly" and "significantly" in the original manuscript. Thank you for pointing at this. We revised this sentence and included also quantitative albedo values for the wavelength 1.6 µm.

"These differences significantly decrease in the near-infrared wavelength range (α_{water} = 0.01 and α_{snow} = 0.04 at λ = 1.6 µm wavelength; Bowker et al., 1985), but still slightly alter the radiative transfer."

… I also note that the authors cited the Krijger results, from which I also draw my finding that the literature review needs more thorough treatment.

➔ We totally agree with the reviewer. A couple of references, e.g. necessary to discuss the problems of cloud retrieval in arctic regions, have not been addressed in the original manuscript. This is changed in the revised version. In particular, based on the references suggested by the reviewers, it is clear that we overemphasized the difficulties of cloud retrievals over bright surfaces and were wrong with the statement that cloud retrievals are not possible over ice surfaces. The reason for our misleading statement was that we focused only on the measurements with the imaging spectrometer AisaEAGLE, which covers only wavelength in the range from 400 nm to 1000 nm. For this spectral range, cloud retrievals over ice surfaces in fact are not possible without additional information (as it is stated by Krijger et al., 2011). But of course it has to be mentioned that this is only valid for the visible wavelength range and can be overcome by introducing near-infrared wavelength channels. We thank the reviewer for highlighting this lack of information, which necessarily must confuse the reader. We revised the relevant parts in the manuscript (also with respect to your later comments on MODIS) and introduced a series of new references including Platnick et al. (2001, 2004), Platnick and King (2003), and Krijger et al. (2011).

> *"A highly variable Arctic surface albedo as observed during the VERDI campaign complicates the cloud retrieval introduced by Bierwirth et al. (2013). In fact, retrievals of cloud microphysical and optical properties using only visible wavelengths are strongly biased by a bright surface (Platnick et al., 2001, 2004; Platnick and King, 2003; Krijger et al., 2011). To overcome this limitation, near-infrared channels are introduced in the retrieval algorithms instead of the visible channel used over dark surfaces. E.g., for MODIS the 1.6 µm band reflectance is applied as a surrogate for the traditional non-absorbing band in conjunction with a stronger absorbing 2.1 or 3.7 µm band (Platnick et al., 2001, 2004; Platnick and King, 2003). However, an accurate separation between sea ice and open water needs to be performed before the retrieval algorithms are applied. Operational algorithms such as that for MODIS use NOAA's (**N**ational **O**ceanic and **A**tmospheric **A**dministration) microwave-derived daily 0.25° **N**ear Real-Time **I**ce and **S**now **E**xtent (NISE) dataset (Armstrong and Brodzik, 2001; Platnick and King, 2003) to identify snow- or ice-covered scenes."*

c) The applicability of the selected cloud retrieval algorithm to Arctic conditions: The authors apply the method of Werner et al. (2013) to Arctic conditions. I think their point here is that the Werner cloud retrieval (developed for trade cumuli over an ocean surface impacted by thin, overlying cirrus) is also applicable to Arctic conditions, given good cloud clearing. I would like to see more discussion of the support for their retrieval band combination (in line with comments of 1b as well).

➔ The choice of the method by Werner et al. (2013) is justified by the following points. We refer to Werner et al (2013), because the general approach using ratios instead of absolute radiances was applied here as well. Second, the method is not restricted to cases when cirrus is above the aircraft (we have chosen data with clear sky conditions above the aircraft) but also improves retrieval uncertainties in this cases. It further improves the retrieval technique from Bierwirth et al. (2013) by using ratios of radiances instead of total radiance only. In comparison to the retrieval grid, derived by the two-wavelength retrieval from Bierwirth et al. (2013), the ratio method further results in a better orthogonality of the τ and r_{eff} solution space (please notice Reply-Figure 2). This leads to a better separation of the τ and r_{eff} solution space. For airborne investigations of τ and r_{eff} with large spatial coverage and high spatial resolution (as we want to perform it in future studies), this will result in a better accuracy of the retrieved values. To make our decision using the ratio method by Werner et al. (2013) more clear, we included the following part in the revised manuscript:

"The retrieval grid is constructed from the simulated γ_λ at 645 nm wavelength on the abscissa and the ratio of γ_λ at 1525 and 579 nm wavelength on the ordinate. This wavelength and the wavelength ratio was chosen in order to improve the retrieval method by Bierwirth et al. (2013). The choice of wavelength follows the method presented by Werner et al. (2013). This method creates a retrieval grid with a more separated solution space for τ and r_{eff} than the classic two-wavelength method by Nakajima and King (1990) or Bierwirth et al. (2013). Furthermore, it effectively corrects the retrieval results for the influence of overlying cirrus and reduces the retrieval error for τ and r_{eff} caused by calibration uncertainties (Werner et al., 2013). For airborne investigations of τ and r_{eff} with large spatial coverage and high spatial resolution, this will result in a higher accuracy of the retrieved cloud properties."

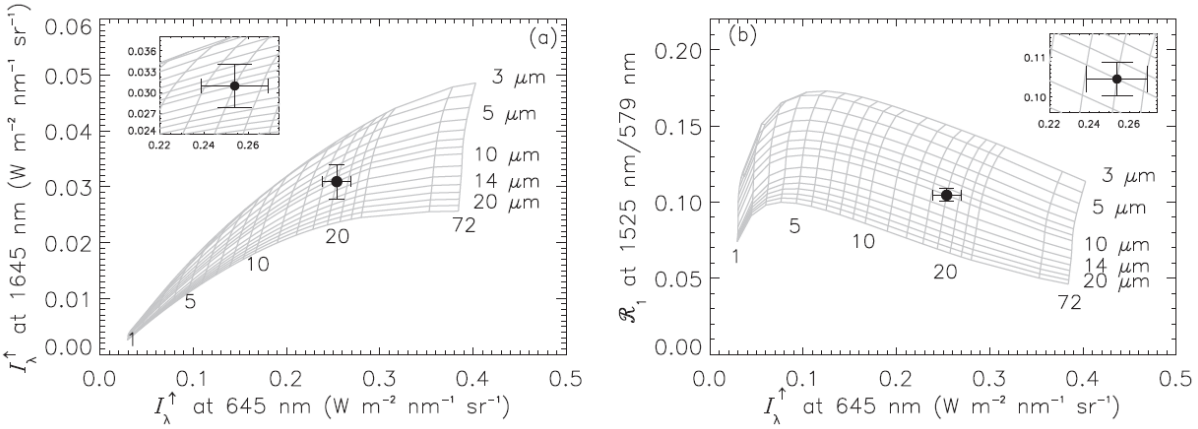

Reply-Figure 2: Comparison of classical two-wavelength retrial method by Nakajima and King (1990) and ratio method by Werner et al. (2013). Graphs adapted from Werner et al. (2013), not included in the manuscript.

2. *Meeting the challenge of interpreting the theoretical results to those that are important in practice*.

As mentioned in preamble, the authors have presented very detailed simulations. However, it is difficult to draw the practical implications from the simulations. In my opinion, this is due to the following reasons: uncertainty analysis, spatial averaging, and organization of paper (see comments 1a and 1b above, and comment 3 below). In particular, while I find Fig 15 interesting, I don't agree that it could be used (as is) to correct the retrieved cloud optical thickness and particle size, due to the many assumptions, different scale factor, and the choice of your retrieval wavelengths.

➔ We have revised the manuscript with regard to your suggestion. Please find our revisions below in subsections a-c.

➔ With regard to Figure 15, we agree with the reviewer that our statement about a possible "correction" is too ambitious. In fact, due to the large number of parameters changing the 3D-effect (shape, size, distribution of ice flows, cloud properties) and appropriate assumptions to be made, a corrections seems only reasonable when all parameters are known. In that case, a correction is not necessary anymore as the entire scene will have been accurately modeled with radiative transfer simulations anyway. Therefore, we removed this statement.

a) Uncertainty analysis and interpretations – This comment derives from what I feel is missing from the article, or hypothesis/findings which could be better set up (in introduction) and summarized (in conclusion). …

➔ With regard to this comment and in line with your later comments on the length of the paper, we revised the introduction and summary as well. The hypothesis and findings should now be better clarified. With regard to this topic, the main changes for the introduction are:

"… Within the present study, the focus lies on those 3-D radiative effects, which are related to the horizontal photon transport between cloud and surface that occurs due to isotropic reflection of the incident radiation on the bright sea ice. The goal is to quantify the magnitude and horizontal extent of those 3-D effects, as well as their influence on cloud retrievals from the visible wavelength range with a high spatial resolution. In reality, such surface 3-D radiative effects …"

➔ With respect to the revision of the summary, please see the information given under 2c.

… For example, in comment 1b, I noted the relative importance of incorrect surface albedo assumption (or unaccounted for natural variability in the surface albedo) on the modeled radiance fields to the 3-D effects. It would not require numerous, detailed calculations to provide, for instance a value for upwelling irradiance over your assumed dark ocean value (plus a reasonable 5% for a measurement uncertainty) and compare it to the measured and modeled (average) values shown in Figure 6. Similarly, uncertainty bars (or even, better, retrieval values derived from your measurements) would be beneficial to interpreting Figure 15 (in addition to spatial averaging that I comment on below). …

➔ We hope we got the point right that this comment addresses uncertainties with respect to the accurate value of sea-ice albedo. Actually, this is what we already tried to discuss at Page 1435 Line 28 – Page 1436 Line 6 in the old manuscript. To make this point more clear, we revised this part and elaborate it in more detail.

"**Furthermore, simulations with varied values of the surface albedo were performed (not shown). Based on the measurement uncertainty of AisaEAGLE, the surface albedo of the dark ocean water and bright sea ice was varied by ± 6 %. Over the dark ocean area, the simulations show almost identical results with differences far below 1 % in γ_λ. Compared to the measurement uncertainties, those differences in the surface albedo are of less significance for ΔL. Indeed, the albedo has a larger effect over the sea-ice surface (up to 10 %) due to changing the albedo value relative with 6 %, which corresponds to an absolute change of ± 0.05 compared to 0.002 absolute change for the water surface. For the investigations presented here, the effect over the dark ocean area is relevant only.**"

➔ Additionally, we present the results of the sensitivity study with respect to uncertainties in surface albedo here: See Reply-Figure 3. To confirm that a measurement error in the albedo is of less importance for ΔL, please see Reply-Figure 3. The blue line represents simulations with an ice albedo of $\alpha_{ice} = 0.91$ and a water albedo of $\alpha_{water} = 0.042$. The red line represents the same simulation, except changes in the albedo of minus 6 % ($\alpha_{ice} = 0.8554$) over the ice surface and plus 6 % ($\alpha_{water} = 0.04452$) over the dark ocean surface. The 6 % error was chosen with respect to the measurement uncertainty of AisaEAGLE. Compared to the measurement uncertainties from the cases presented in the manuscript (Reply-Figure 4), over the dark ocean water, differences due to uncertainties in the surface albedo covered area are of less significance. Over the sea-ice surfaces, the difference of 6 % has a larger effect due to the larger value of the sea-ice albedo. However, for our investigations only the effect over the dark ocean covered area is of interest.

Considering the number of Figures included in the manuscript, we do not present Reply-Figure 3 in the revised manuscript, but give the numbers of the sensitivity study.

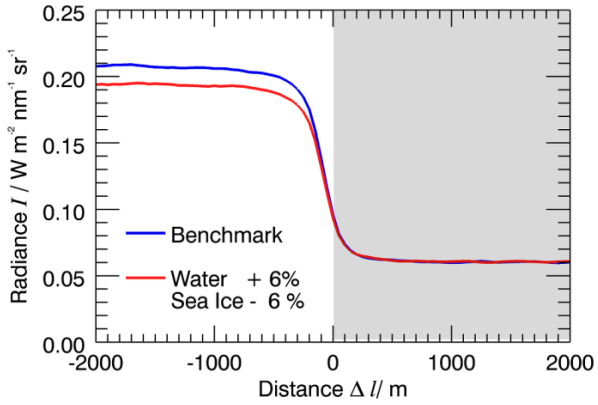

Reply-Figure 3: (not included in the resubmitted manuscript)

➔ We have revised Figures 6 and 15 including measurement uncertainties. The uncertainty range is illustrated by dotted lines, which represent the standard deviation from the measurements and simulations, calculated for each distance to the ice edge.

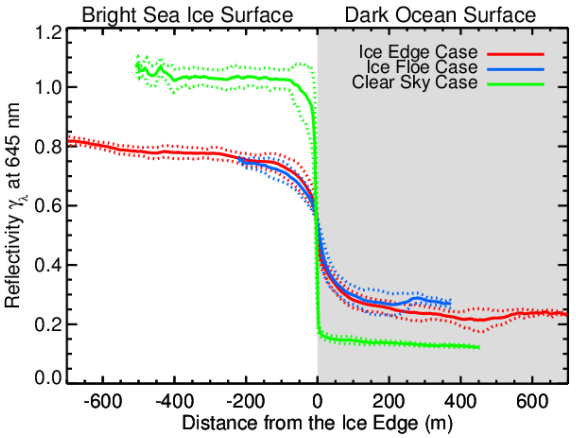

Reply-Figure 4: Revised Figure 6

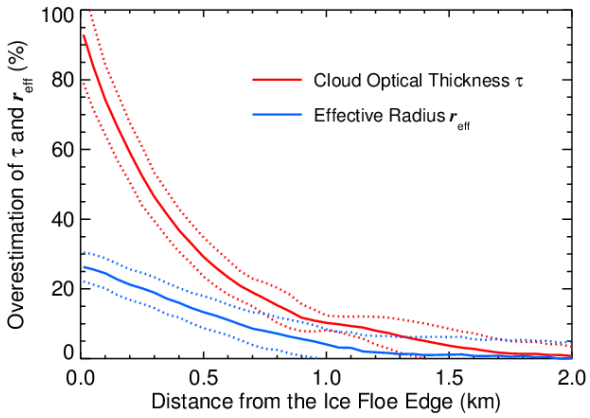

Reply-Figure 5: Revised Figure 15 (now 16)

… Again, only because you remark on MODIS in your article, I mention that the MODIS operational cloud retrieval has associated uncertainties, which include those due to spectral surface albedo (implemented since collection 5; current version is collection 6), which could accompany Figure 1 and support the valid point that retrievals of clouds over snow/ice are challenging. (see Platnick et al., 2004). This could be used to strengthen the statement, "We estimate the cloud optical thickness from the MODIS image to be in the range…" (page 1428).

➔ A discussion about the uncertainties of MODIS retrieval is given in the revised manuscript. See reply above. Furthermore, "We estimate the cloud optical thickness from the MODIS image to be in the range…" was a rather poor choice of wording. Since we had a detailed look at the level-2 MODIS products (see Reply-Figure 6), which gave us quantitative numbers of τ in the surroundings of the measurement area, we changed it to the following:

"τ was obtained from AisaEAGLE measurements above open water far from any ice edge using the retrieval method presented by Bierwirth et al. (2013). An average value of τ = 5.3 ± 0.5 was derived, which agrees with the MODIS level-2 product showing values for τ between 0.02 and 15.5 (τ = 3.6 ± 2.5) in the investigated area."

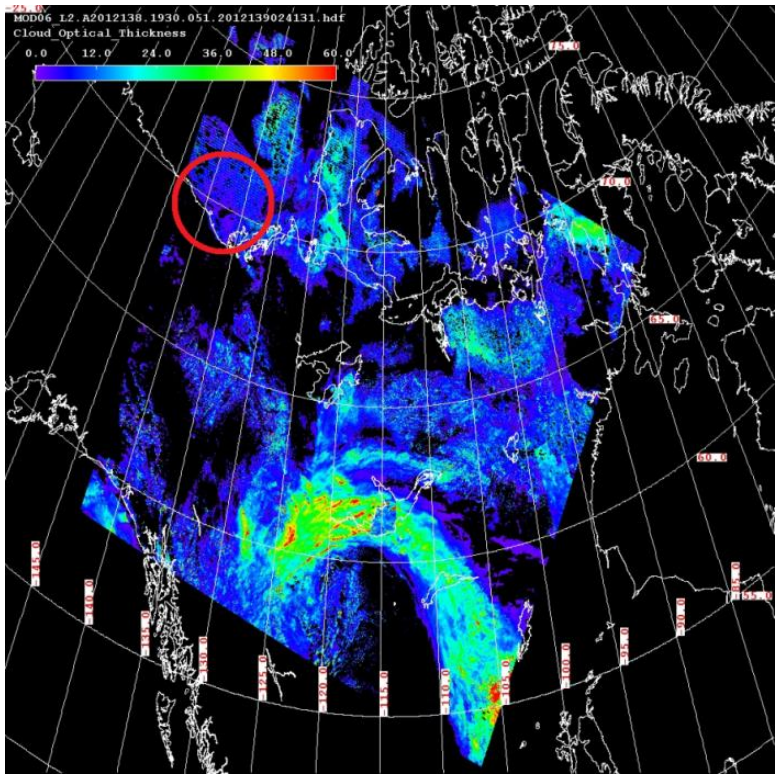

Reply-Figure 6: Level-2 MODIS product. Cloud optical thickness.

b) Spatial averaging – In general, the authors conclude the horizontal transfer of radiation is detectable within a distance of ~ 2km or less from ice edge, with various dependencies on cloud properties, and ice floe size/shape/area and proximity of individual ice floes to adjacent ice floes. Have you considered spatially averaging your results from 50 m pixels to 1 km pixels, to more closely align with the pixel size of operational imagers, such as MODIS, which you reference in your manuscript?

➔ The reviewers suggestion points at a topic worth for detailed discussion. However, even if it might not be pointed out clear enough in the original manuscript, our intention of the study was not to relate the observed effects to satellite observations of different scales. Therefore, we did not vary the spatial scaling but focused on the full resolution obtained with AisaEAGLE. To transfer those investigations to satellite retrievals, several crucial changes would have to be applied to our current work, e. g. changing our wavelength choice, which is not possible for the limited measurements of AisaEAGLE. In contrast, at the moment we rather want to use the full capacity of the spatial resolution of the imaging spectrometer AisaEAGLE to investigate the 3-D radiative effects on small horizontal scales. During future projects, when also the AisaHAWK (see comment 1c) is available, we will be able to perform the retrieval also with near-infrared wavelength. For those measurements and reason of comparisons, it would be valuable to investigate the scaling of observations to the pixel size of operational satellite imagers. However in a first attempt, we scaled the AisaEagle observations to a 50 times larger grid. For the case with the elongated ice edge, presented in Fig. 4a of the original manuscript, this results in a pixel size of 180 m into the flight direction by 220 m across the flight direction. Please see Reply-Figure 7. The pixels next to the ice edge show still enhanced and reduced radiances. Furthermore, the smooth decrease can still be observed from the cross section presented in Reply-Figure 7b.

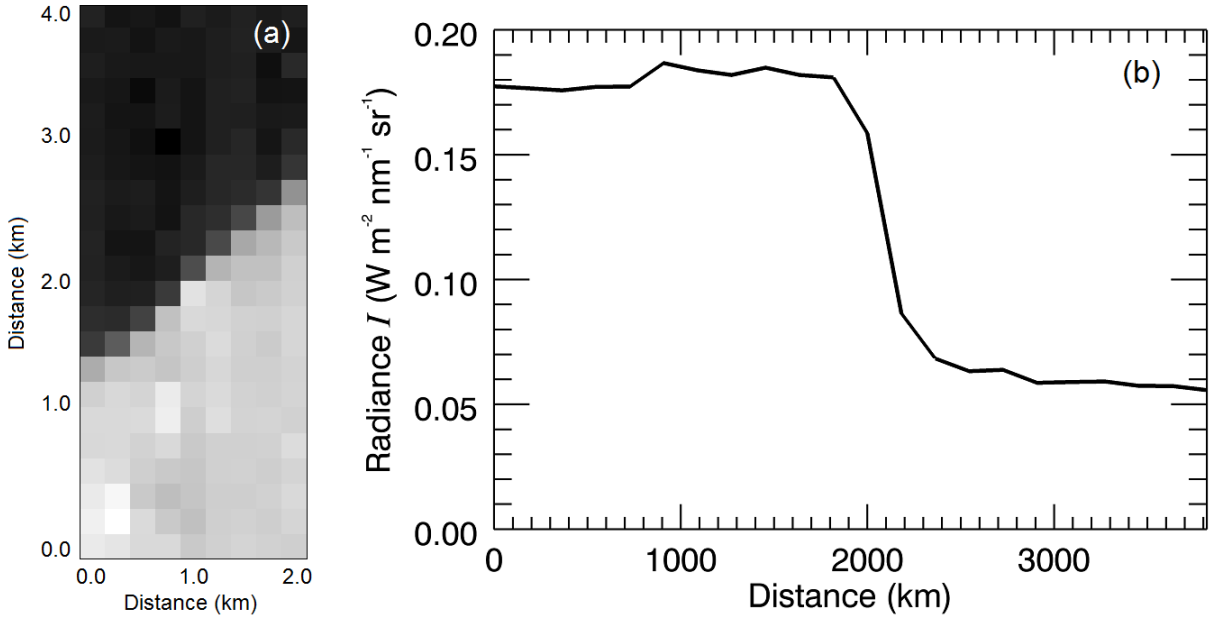

Reply-Figure 7: a) Scaled image of the measurement case from Fig. 4a in the original manuscript. b) Cross section into the direction of flight for the center pixel of the image. Not included in the resubmitted manuscript.

c) Organization of paper – The paper is long, but the most significant challenge to reading the paper comprehensively come from a lack of organization, which, by necessity, then results in multiple instances of redundant prose. In section 4 (model studies) could you, instead, present the material by the physical dependency you are trying to quantify versus the current approach of model case studies organized from basic to more complicated? I feel this will reduce the length, and also make clearer the distinction between ΔL and ΔLcrit, and their usage throughout the article. …

➔ We started to replace all variables (cloud optical thickness, effective radius, upwelling radiance radiance, downwelling irradiance, …) by its symbols (τ, r_{eff}, $I_\lambda^\uparrow$, $F_\lambda^\downarrow$, …). Furthermore, we agree that Section 4 was way too long. We revised this section and significantly shortened it, especially by removing most of the repetitions or summarizing them in Section 4.2 (repetition of input parameters such as τ, cloud altitude or geometrical thickness) and 4.2.1 (general findings such as the description of the enhanced or reduced reflectivity in the vicinity of ice edges). Furthermore, we have resorted single paragraphs, which makes this section even shorter and avoids unnecessary back and forth switching between the single parameters. Now, we complete the investigations of a single parameter, before discussing the next one (ice edge length, sea-ice area,…). By revising the Section, we also hope that it is more clear to the reader and that the original order of the single investigations (straight edge, single circular flow, group of flows, real scenario) is from basic to complex scenarios.

… In section 6 (summary and conclusions), I also feel tightening the prose (perhaps even by half!) and summarizing the results by general impact, versus re-iterating specific results would be much more effective. As another example, a prime motivation for your approach (that a simplified albedo field is necessary in a general characterization of the individual influences), is not presented until the last page of the article. Overall, while I am sensitive to the fact that this request I onerous, I think it is necessary.

➔ We agree with the reviewer that the summary in many instances was not written efficiently. We tried to follow the suggestions by the reviewer, revised this section and shortened it by almost the half summarizing only the most important results from the main part.

3. *What is your source of near-ir measurements*?

Section 2 discusses the instruments, and spectral range of AisaEAGLE (400-970 nm). What is your source of near-ir measurements? Section 5 discusses simulations at near-ir wavelength where liquid water absorbs (hence sensitivity to particle size), necessary for the cloud retrievals. While the authors mention the further work expanding the implications of this study to retrievals of cloud properties in the Arctic region, the results of this paper would be improved through a couple of your own results (adding a few derived points to the simulated curve in Figure 15, for example).

➔ This comment by the reviewer may have evolved from a misunderstanding due to an insufficient introduction of this section. The reviewer is right that AisaEAGLE only covers the visible wavelength range of up to almost 1000 nm. However, in Section 5 no measurements were applied at all. The whole study is based on radiative transfer simulations as our measurements do not cover the wavelength needed to apply the retrieval method by Werner et al. (2013). We still have done this study as outlook with regard to future studies, when a near-infrared imaging spectrometer (AisaHAWK, 1000-2500 nm wavelength) might be available. Intelligible, this is a legitimate question, since this information was not included in the manuscript yet. We have revised the manuscript and added a few more words at the point in the manuscript where we introduce the retrieval method by Werner et al. (2013).

"To quantify the magnitude of this overestimation, a synthetic cloud retrieval is investigated. The retrieval is based on simulations only in order to investigate also the uncertainties of retrieved r_{eff}, which cannot be derived from the current setup of AisaEAGLE measurements during VERDI. The limitation of AisaEAGLE to visible wavelengths restricts the retrieval to τ (Bierwirth et al., 2013). However, near-infrared measurements might be available by use of additional imaging spectrometers such as the AisaHAWK. Therefore, this study addresses both quantities τ and r_{eff}. To do so, the retrieval based on forward simulations is applied to the γ_λ field of a 3-D simulation where the cloud optical properties are known exactly."

Minor Comments:

1. Multiple instances of "ground overlaying cloud", in text and in figure captions, is confusing terminology. Replace instead with "overlying cloud", or simply "cloud" (or some variation of these) given that we know clouds are above the surface.

➔ The reviewer is right. "Ground overlaying" is a bad choice to characterize low-level clouds, which are touching the ground. However, we could not find an appropriate word, so we decided to replace "ground overlaying" by "low-level" and to add the altitude in quantitative numbers, from which it should become clear that the cloud is touching the ground. We changed it at each point where it occurred in the manuscript.

*"For a low-level cloud at 0–200 m altitude, as observed during the Arctic field campaign **VER**tical **D**istribution of **I**ce in Arctic clouds (VERDI) in 2012, an increase of the cloud optical thickness τ from 1 to 10 leads to a decrease of ΔL from 600 to 250 m."*

"From the two measurement cases presented here (τ = 5, h_{cloud} = 0–200 m), a distance ΔL of 400 m was observed."

***"Figure 8.** Simulated mean γ_λ across an ice edge for clear-sky conditions as well as for low-level clouds between 0 and 200 m altitude, τ = 1/5/10, and r_{eff} = 15 µm. …"*

***"Figure 10.** (a) Distance ΔL as a function of the cloud base altitude h_{cloud} for a cloud with a geometrical thickness of Δh_{cloud} = 500 m and different τ. (b) Distance ΔL as a function of the cloud geometrical thickness Δh_{cloud} for a low-level cloud with cloud base at h_{cloud} = 0 m and different τ."*

2. The sentence "the low Sun in summer and its absence in winter combined with usually high surface albedo…" could lead to confusion. All clouds warm in the absence of sunlight, irrespective of cloud altitude or surface albedo. I think what you are trying to say is that for conditions of low Sun and high surface albedo, the terrestrial warming dominates the reflective cooling. Could fix by re-formulating sentence, or removing the "absence in winter" part. It's just semantics.

➔ That is true. The wording we have used in the former manuscript could be misleading. We followed your suggestion and removed the part "absence in winter".

"However, the low Sun in summer combined with a usually high surface albedo lead to a dominance of the terrestrial (infrared) radiative warming of low clouds (Intrieri et al., 2002b; Wendisch et al., 2013)."

3. Lindsay and Rothrock (1994) analysed albedo in 200 km^2 cells (not 20 km^2) – page 1423.

➔ We corrected this mistake.

"Using Advanced Very High Resolution Radiometer (AVHRR) data from the polar-orbiting satellites NOAA-IO and NOAA-11, Lindsay and Rothrock (1994) analyzed the albedos of 145 different 200 km^2 cells in the Arctic."

4. The ending sentence to one paragraph ("The individual 3-D effect of heterogeneous surfaces in cloud free situations…"), should be moved to the starting sentence of the following paragraph – (page 1424).

➔ The last sentence belongs to the next paragraph. We changed this according to the reviewers suggestion.

5. obverse – observe (page 1426)

➔ corrected

6. status – stratus (page 1427)

➔ corrected

7. Remove an extra "each" (page 1430).

➔ removed

8. Two suggested wording changes for "Furthermore, the simulations…of the mean nadir radiance *for* a certain area…or if the enhancement is*, on* average*,* counterbalanced" (page 1432-1433).

➔ We followed the reviewers suggestion.

> *"Furthermore, the simulations are used to clarify whether these 3-D radiative effects result in an enhancement of the mean γ_λ for a certain area or if the enhancement is, on average, counterbalanced by the decrease of γ_λ above the sea ice."*

9. relative – relatively (page 1434).

➔ corrected

10. Suggested wording change "As a reference also a clear-sky scenario was *also* simulated…" (page 1434).

➔ We revised the whole section (please see comments above), for which reason this sentence was removed.

11. Missing word "This results from the reduction *in* contrast between the dark.." (page 1435).

➔ Word "in" included

12. Misplaced text? From "On the other hand, the decrease of …" through end of paragraph would be better incorporated two paragraphs preceeding. (page 1435).

➔ We followed the reviewers suggestion and moved this part up. Furthermore, we changed the order of ΔL and ΔL_{crit} (now ΔL_{HPT}) to avoid an unnecessary back and forth switching, as it was before.

"To compare the results with the measurement example in Fig. 6, the distance ΔL_{HPT} defined by Eq. (3) is analyzed. $\gamma_{\lambda,water}$ is set to the IPA values above water. For the cases presented in Fig. 8, ΔL_{HPT} increases with increasing τ from 100 m at τ = 1 to 250 m at τ = 5 and to 300 m at τ = 10. This shows that the horizontal photon transport increases with τ due to increased scattering inside the cloud layer.
In contrast to ΔL_{HPT}, the distance ΔL defined by Eq. (4) decreases from 600 m (at τ = 1.0) to 400 m (at τ = 5.0) and to 250 m (at τ = 10.0). The decrease of ΔL suggests that the area in which γ_λ is enhanced and a cloud retrieval might be biased is smaller for optically thick clouds. This is related to the decrease in contrast between cloud covered sea ice and cloud covered ocean if τ increases. The difference Δ(IPA) between $\gamma_{\lambda,ice}$ and $\gamma_{\lambda,water}$ decreases from γ_λ = 0.87 for the clear-sky case to γ_λ = 0.44 for τ = 10, mainly due to the increasing reflection of incoming radiation by the cloud. If τ increases, $\gamma_{\lambda,water}$ increases which results in a higher uncertainty range exceeding the γ_λ enhancement also in areas closer to the ice edge. Therefore, the γ_λ enhancement becomes less significant for a cloud retrieval compared to the measurement uncertainties. Since we aim to retrieve τ above water areas enclosed by ice floes, in the following ΔL is used to quantify the 3-D effects."

13. One too many clouds? "For an increasing cloud altitude of a cloud…" (page 1436).

➔ We removed one "cloud" after altitude.

"For an increasing altitude of a cloud with a geometrical thickness of 500 m, ΔL increases from…"

14. proofs – proves (page 1437).
➔ corrected

15. Word change "To quantify the influence…we *quantified* ΔL." (page 1437).

➔ The reviewer is right. "quantified" fits better than "analyzed". We changed this according to your suggestion.

16. Awkward sentence "For all values of *simulated* optical thickness…". Use instead, perhaps, "For simulations at all optical thicknesses, …"(page 1437).

➔ We revised this by the following:

"For all simulated τ, ΔL increases with an increasing radius of the ice floe, …"

17. Define SDs (page 1441).

➔ We defined SD as standard deviation.

18. kind of – approximately (page 1445).

➔ We changed this according to the reviewers suggestion.

19. Incorrect statement "The different patterns of overestimation …suggest that the 3-D effects can be larger at absorbing wavelengths" (page 1445).

➔ The reviewer is right. The statement is the wrong way round and contradicts the statements given before. Accordingly, we revised this part.

"Furthermore, Fig. 16 shows that the overestimation of τ increases approximately exponentially starting at about 1.5 km distance, while the overestimation of r_{eff} increases more slowly and only extends up to a distance of 1.0 km. This indicates that the magnitude of the 3-D effects depends on the wavelengths. In all simulations shown in Sect. 4.2, a wavelength of 645 nm was used for the retrieval of τ. However, the retrieval of r_{eff} also requires simulations at 1 525 nm in the absorption band of liquid water. Therefore, the smaller magnitude and horizontal extent of the overestimation of r_{eff} compared to the magnitude and horizontal extent of the overestimation of τ suggest that the 3-D effects will be smaller at absorbing wavelengths."

20. weather –whether (page 1447).

➔ Corrected

Figure Comments:

1. Suggest replacing the color bar in Figure 4 with a more dynamic scale range, or (even though I don't usually suggest doing this!), utilize different scale ranges for Figure 4e-f, than 4a-d.

➔ We revised this Figure (see below Reply-Fig. 8) and color-coded the images, which contain the ice masks. Due to the use of reflectivities instead of radiances, the span between extreme values became closer, which supports the use of the same legend for each image. The mentioned narrow bright bands around the sea-ice edges should now be easier to identify.

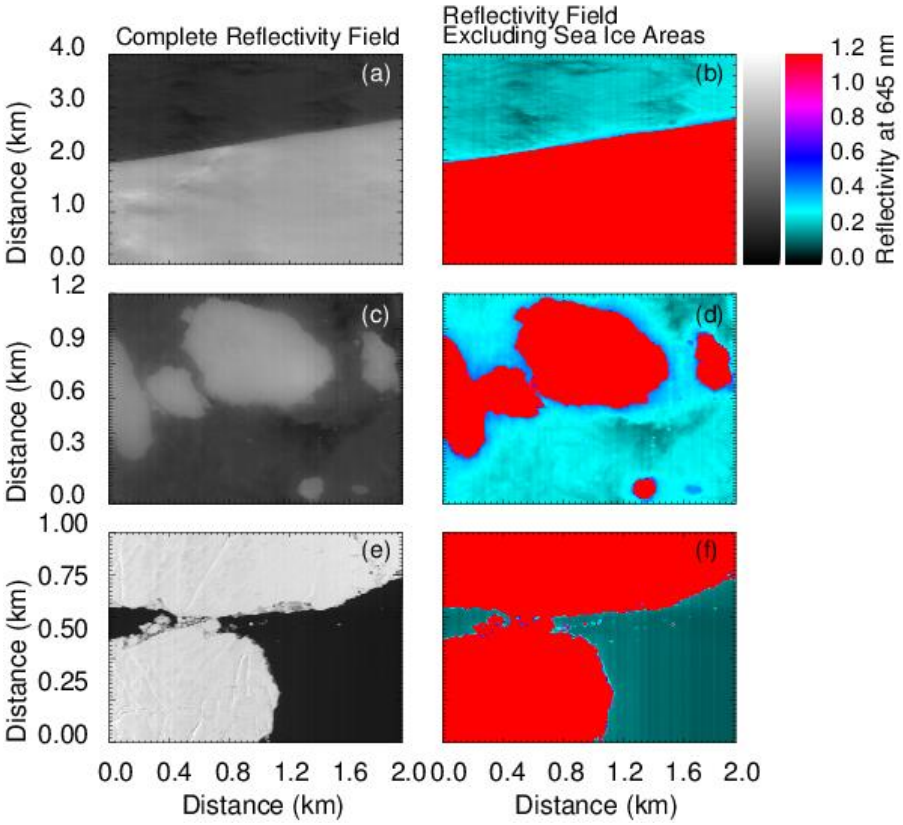

Reply-Figure 8: Revised Figure 4.

2. For all figures with units, please place units in open parentheses (), instead of after a slash.

➔ According to this comment, we revised all Figures and placed all units in open parentheses now.

3. Figure 5 – this is an incredible result!

➔ Thank you very much. We are encouraged to read this comment.

4. Figures 8a-b – It is difficult to interpret various curves, on left hand side of each plot.

➔ That is true. In the former graphs it was difficult to distinguish between the single curves, especially on the left side of each panel. We tried to fix this, using different colors for curves of different cloud optical thickness. The separation between both should be better now. Please view Reply-Fig. 9.

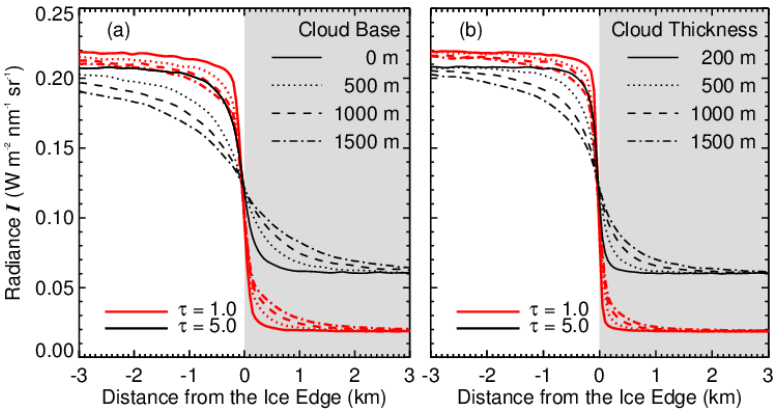

Reply-Figure 9: Revised Figure 8 (now Fig. 9)

5. Figure 10 – check your symbols, especially the curve for tau=1 and tau=10, as currently this plot contradicts your results in Figure 9.

➔ We thank the reviewer for highlighting this mistake. Indeed, not Figure 10 (now Fig. 11) was wrong, but Figure 9 (now Fig 10). We revised this Figure, See Reply-Fig. 10a. Additionally, we included the simulations for clouds with different geometrical thickness in a second panel (b).

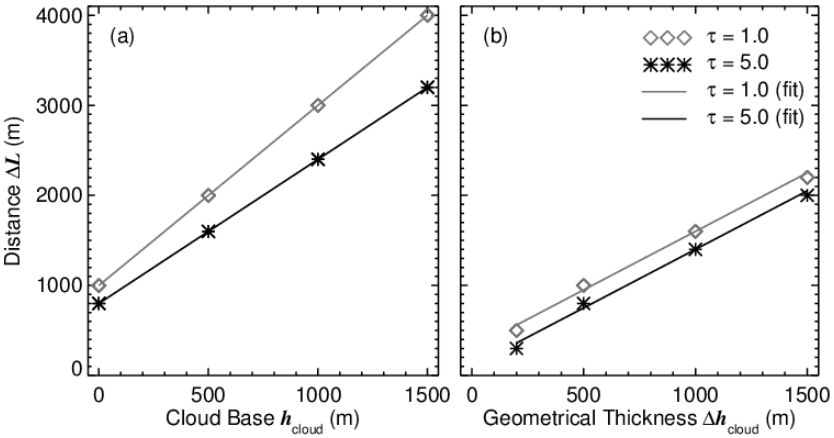

Reply-Figure 10: Revised Figure 9 (now Figure 10): *"(a) Distance ΔL as a function of the cloud base altitude h_{cloud} for a cloud with a geometrical thickness of Δh_{cloud} = 500 m and different τ. (b) Distance ΔL as a function of the cloud geometrical thickness Δh_{cloud} for a low-level cloud with cloud base at h_{cloud} = 0 m and different τ."*

6. Figure 14 – Perhaps revisit this figure if you decide on an alternative wavelength combination for your results.

➔ As we kept the wavelength choice as it was (please see our comments above), we have not revised this figure.

Reply to anonymous referee nr. 2 (review acpd-15-C651-2015):

We thank the reviewer for the helpful comments which we think have helped to improve the manuscript significantly. Especially, by removing the grammatical errors and misleading statements the revised manuscript will be easier to understand for the reader. The detailed replies on the reviewers comments are given below and structured as follows. Reviewer comments have bold letters, are labeled with the page number and line from the discussion paper, and are listed always in the beginning of each answer. The reviewer comments are followed by the author's comments with an explanation if necessary and revised parts of the paper. The revised parts of the paper are written in quotation marks and italic letters.

Sequential comments:

Page 1424, Lines 20-25: I don't quite agree with this point. The fact that the Zinner et al. (2010) paper found weak 3D effects for stratocumulus clouds does not rule out strong 3D effects for many observations of Arctic stratus clouds. This is because while the Zinner et al. (2010) simulations used a 45_ solar zenith angle, numerous studies pointed to much stronger 3D effects for the lower solar elevations that are quite frequent for Arctic clouds (see, for example, Loeb and Davies 1997, Loeb and Coakley 1998, Horvath et al. 2014, Grosvenor and Wood 2014).

➔ The reviewer comment is right. We did not adequately discuss the study by Zinner et al. (2010) and missed referring to results of other studies. We revised this part and included also the reference to Loeb and Davis (1996) and Grosvenor and Wood (2014).

> *"For a solar zenith angle (Θ) of 45°, Zinner et al. (2010) found that the remote sensing of stratocumulus was not biased by 3-D effects, while that of scattered cumulus was sensitive to horizontal heterogeneities. This leads to the assumption that retrievals of cloud microphysical and optical properties can be treated by 1-D simulations if the distance to ice-open water boundaries is sufficiently large. However, measurements in Arctic regions are often performed for solar zenith angles larger than 45°. In such cases, 3-D radiative effects generated by the cloud structures become important. Using plane-parallel 1-D simulations of clouds, Loeb and Davis (1996) stated that the cloud optical thickness shows a systematic shift towards larger values with increasing solar zenith angle. This dependence is still weak (≤ 10 %) for thin clouds (τ ≤ 6) and Θ ≤ 63°. Grosvenor and Wood (2014) confirmed this statement. They investigated MODIS satellite retrieval biases of τ and stated that τ is fairly constant between Θ = 50° and ≈ 65–70°, but then increases rapidly with an increase of over 70 % between the lowest and highest Θ."*

Page 1428, Lines 1-5: I recommend adding some qualifying words here, as the results only show that retrievals are not possible using the wavelengths used in this paper. However, using other wavelengths such as 1.2 micron can enable retrievals for some water clouds over frozen surfaces (Platnick et al. 2001) even if the retrieval accuracy is lower.

➔ We agree with the reviewer. Of course it has to be mentioned that our statement is only valid for the visible wavelength range and can be overcome by introducing near-infrared wavelength channels. We revised the relevant parts in the manuscript and introduced methods, which are using the near-infrared channels to retrieve cloud optical properties above ice surfaces.

> *"A highly variable Arctic surface albedo as observed during the VERDI campaign complicates the cloud retrieval introduced by Bierwirth et al. (2013). In fact, retrievals of cloud microphysical and optical properties using only visible wavelengths are strongly biased by a bright surface (Platnick et al., 2001, 2004; Platnick and King, 2003; Krijger et al., 2011). To overcome this limitation, near-infrared channels are introduced in the retrieval algorithms instead of the visible channel used over dark surfaces. E.g., for MODIS the 1.6 µm band reflectance is applied as a surrogate for the traditional non-absorbing band in conjunction with a stronger absorbing 2.1 or 3.7 µm band (Platnick et al., 2001, 2004; Platnick and King, 2003). However, an accurate separation between sea ice and open water needs to be performed before the retrieval algorithms are applied. Operational algorithms such as that for MODIS use NOAA's (**N**ational **O**ceanic and **A**tmospheric **A**dministration) microwave-derived daily 0.25° **N**ear Real-Time **I**ce and **S**now **E**xtent (NISE) dataset (Armstrong and Brodzik, 2001; Platnick and King, 2003) to identify snow- or ice-covered scenes."*

➔ Furthermore, at each time when we are talking about the fact that retrievals are not possible over bright sea ice surfaces, we included "for the visible wavelength range".

Page 1435 lines 9-13, and Page 1447 lines 13-15: I recommend mentioning that having stronger 3D effects for larger optical thicknesses is similar to the behaviors discussed earlier in the context of aerosol measurements near bright clouds. For example Marshak et al. (2008) found stronger "bluing" (3D enhancement near clouds) at shorter wavelengths, where the Rayleigh optical thickness is larger.

➔ This is a good suggestion. The dependence of the radiance enhancement to cloud optical thickness enhancement due to the ice floes in our study is comparable to the enhancement of the AOD due to the clouds in the study from Marshak et al. (2008), although the geometry differs and additional reasons for the bluing are discussed in literature. And the reviewer is right. There are more comparable studies (Kobayashi et al. (2000), Koren et al. (2007), …) , which are dealing with the "twilight zone" around clouds. Out of them, following the reviewers suggestion, we included a reference to Marshak et al. (2008).

> ***"****Similar investigations are presented by Marshak et al. (2008) with respect to aerosol-cloud interactions. In the vicinity of clouds, they found that the radiance in cloud-free columns is increased due to a cloud-induced enhancement of the Rayleigh scattering.****"***

Page 1435, lines 21-27: I recommend mentioning the additional consideration that, because of the nonlinearity of the optical thickness vs. reflectance curve, the same 5% relative change in reflectance implies a larger relative change in retrieved optical thickness for thicker clouds than for thinner clouds. In other words, it may help to determine Delta_I using a lower threshold for thick clouds than for thin clouds. For example, depending on solar elevation and other conditions, a 5% reflectance-difference threshold could be optimal for cloud optical depths around 1, but a 3.5% reflectance-difference threshold may be optimal for CODs around 5 and a 2% reflectance-difference threshold may work best for CODs around 10. It may even be worth including some results based on such dynamic thresholds into the paper.

➔ This is in fact a good suggestion. According to your idea, we have also tested the results of Figure 7 (now Figure 8) with different thresholds of 5 % (at $\tau = 1$), 3.5 % (at $\tau = 5$), and 2 % (at $\tau = 10$). This results in an increase of ΔL at $\tau = 5/10$ from 400 m/250 m to approximately 500 m/450 m. However, the reflectivity-difference threshold of 5 % (now adapted to 6 % with regard to Schäfer et al. (2013)) between IPA and 3-D simulations is chosen with respect to the measurement uncertainty of the imaging spectrometer AisaEAGLE. Indeed, the same measurement uncertainty causes then larger effects for clouds of higher optical thickness. Otherwise, the measurement uncertainty of the instrument is a reasonable value for the threshold, whereas it is difficult to justify the use of 3.5 %, 3 %, or some other values. However, we have revised this part to better clarify the use of ΔL_{crit} *(now* ΔL_{HPT}*)* and ΔL. In this context we have also revised the statement on the threshold choice. The revisions we made are:

"Over the water-covered area, an enhancement of γ_λ was measured close to the ice edge; while over the ice-covered area, γ_λ is reduced near the ice edge. We define two distances measured from the ice edge to quantify the enhancement effect. The first distance ΔL_{HPT} is introduced to quantify the range of horizontal photon transport. It characterizes the distance at which the transition from high $\gamma_{\lambda,ice}$ to low $\gamma_{\lambda,water}$ is $1/e^3$ of the initial difference between the mean γ_λ above ice ($\gamma_{\lambda,ice}$) and the mean γ_λ above open water ($\gamma_{\lambda,water}$):

$$\gamma_{\lambda,water}(\Delta L_{HPT}) = \gamma_{\lambda,water} + 1/e^3 \cdot \Delta IPA, \qquad (3)$$

with $\Delta IPA = \gamma_{\lambda,ice} - \gamma_{\lambda,water}$. By including ΔIPA, ΔL_{HPT} quantifies the range of horizontal photon transport independent on the difference of the surface albedo contrast. For the scene from Fig. 4a, ΔL_{HPT} indicated by the enhancement of γ_λ over the water surface extends to a distance of 200 m from the ice edge.
Furthermore, a second distance to the ice edge ΔL is defined for which $\gamma_{\lambda,water}$ is enhanced by 6 % of the average γ_λ above open water.

$$\gamma_{\lambda,water}(\Delta L) = \gamma_{\lambda,water} + 0.06 \cdot \gamma_{\lambda,water}. \qquad (4)$$

The choice of the threshold results from the radiance measurement uncertainty (± 6 %) of the imaging spectrometer AisaEAGLE. Using this definition, ΔL is independent of γ_λ measured above the ice surface. It only accounts for the significance of the enhancement with respect to the measurement uncertainty. If the enhancement is higher than the measurement uncertainty, a cloud retrieval might be significantly biased when using the contaminated measurements. Therefore, ΔL is a measure for the horizontal extent within which the 3-D effects bias the cloud retrieval in the vicinity of an ice edge. For the special case of the measured γ_λ in Fig. 6, the $\Delta L = 300$ m. Above open water, all measurements within that transition zone cannot be used for the cloud retrieval as the enhanced γ_λ will positively bias the retrieved τ."

"To compare the results with the measurement example in Fig. 6, the distance ΔL_{HPT} defined by Eq. (3) is analyzed. $\gamma_{\lambda,water}$ is set to the IPA values above water. For the cases presented in

Fig. 8, ΔL_{HPT} increases with increasing τ from 100 m at τ = 1 to 250 m at τ = 5 and to 300 m at τ = 10. This shows that the horizontal photon transport increases with τ due to increased scattering inside the cloud layer. In contrast to ΔL_{HPT}, the distance ΔL defined by Eq. (4) decreases from 600 m (at τ = 1.0) to 400 m (at τ = 5.0) and to 250 m (at τ = 10.0). The decrease of ΔL suggests that the area in which γ_λ is enhanced and a cloud retrieval might be biased is smaller for optically thick clouds. This is related to the decrease in contrast between cloud covered sea ice and cloud covered ocean if τ increases. The difference Δ(IPA) between $\gamma_{\lambda,ice}$ and $\gamma_{\lambda,water}$ decreases from γ_λ = 0.87 for the clear-sky case to γ_λ = 0.44 for τ = 10, mainly due to the increasing reflection of incoming radiation by the cloud. If τ increases, $\gamma_{\lambda,water}$ increases which results in a higher uncertainty range exceeding the γ_λ enhancement also in areas closer to the ice edge. Therefore, the γ_λ enhancement becomes less significant for a cloud retrieval compared to the measurement uncertainties. Since we aim to retrieve τ above water areas enclosed by ice floes, in the following ΔL is used to quantify the 3-D effects."

Page 1442, lines 5-6: It appears to me that in Figure 12 the spread of radiance distributions over sea and ice are much larger for Scenario 1 than for scenarios 2-4. So I suggest some correction or clarification, for example by describing what is meant by "spread".

➔ The reviewer is right. The spread of radiance (now reflectivity) distributions over bright sea ice and dark ocean water are much larger for Scenario 1. This is due to the smaller floe size in Scenario 2-4, compared to Scenario 1. Therefore, the large radiance/reflectivity values from Scenario 1 cannot be reached by Scenario 2-4. We revised this part to better clarify the reason for the different results.

"… All γ_λ values that are not included in the single water peak, result from the 3-D effects. Above ice, the distributions of Scenario 2-4 are shifted to lower γ_λ compared to Scenario 1. This is because the diameter of the floes is even smaller than in Scenario 1. Thus, the large reflectivity values of Scenario 1 cannot be reached by Scenario 2-4 (compare Fig. 11)…."

➔ Furthermore, we had to revise the whole fourth section with regard to the other reviews. The part with respect to our comment on the "spread" is not included anymore.

Page 1441, lines 17-18: It is a very interesting observation that 3D effects reduce the scene average reflection, and I wonder if the authors could offer an explanation for this. For example, could 3D surface-cloud interactions involving double surface reflection explain the reduction?

➔ The radiation, which reaches the cloud after its reflection on the sea ice will be scattered again by the cloud into several directions. Of course, part of it is also scattered into the direction of the dark ocean surface. There, due to the low albedo, most of the radiation will be absorbed and not reflected back into the direction of the cloud. This part of absorption does not exist in the IPA simulations. This results in a lower scene average reflection for the 3-D simulations compared to the IPA simulations, which leads to a lower ratio $R_{3D/IPA}$. To address this mechanism more clearly to the reader, we included the following sentences.

"This reduction originates from the absorption of the radiation, which is scattered by the cloud base back into the direction of the dark ocean surface. This part of absorption does not exist in the IPA simulations, which in comparison leads to a lower scene average reflection in the 3-D simulations."

Page 1454, Table 1: Either in the table or somewhere in the text it would be important to discuss the level of Monte Carlo simulation uncertainty. Most importantly, how do they compare to the deviations from 100% in Table 1?

➔ It is true that we missed to discuss the level of Monte Carlo uncertainty. In the revised manuscript we have included a quantitative value.

> ***"**2.2·10^9 photons were used in each single model run, which resulted in a noise level of the 3-D simulations less than 1 %. This value is much lower than the measurement uncertainties of AisaEAGLE.**"***
>
> *"Yet, the overall 3-D effect is relatively small with $R_{3\text{-}D/IPA}$ ranging from 96.5 to 98.4 %, but is still significantly above the noise level of the 3-D simulations."*

Page 1443, lines 21-23: I suggest considering another possible explanation for the Figure 13 frequency distributions being broader in the observations than in the simulations: the possibility that clouds may have been at a higher altitude or were geometrically thicker in reality than in the simulations. In order to support or disqualify this hypothesis, it would help to mention the top height (and/or thickness) of observed clouds, for example by discussing results from the AMALi lidar mentioned in Page 1426. Alternatively, the simulations could be repeated assuming higher cloud altitudes.

➔ We agree with the reviewer that the reason for the broader frequency distributions of the observations compared to the simulations is not well discussed in the original manuscript. However, we think that it is not likely that the broadening is due to differences in the cloud top altitude, rather than due to cloud base altitude and cloud-inhomogeneity effects. The cloud top is well defined by measurements with the AMALi, whereas AMALi cannot see the cloud base. Therefore, we performed some tests with a different altitude of the cloud base. Additionally, we slightly varied the surface albedo. Doing so, we could achieve a better agreement between simulation and observation.
Furthermore, in the revised manuscript we changed the normalization of the distributions in Fig. 13 (now Fig. 14) to a total value of one. This makes the comparison more meaningful and highlights the different radiative effects. A broadening of the dark ocean water and sea-ice peak may result from both sea ice edge effect and cloud heterogeneities. However, while surface effects will fill up the gap between the two peaks only, clouds inhomogeneities can also result in values smaller (over water) and higher (over sea ice) then the IPA simulations. This is clearly obvious, comparing simulations and measurements, what gives us reason to address the broadening partly to cloud inhomogeneities.

> *"The albedo map was used in the simulations implementing a cloud of $\tau = 5$ and a fixed $r_{eff} = 15$ µm, as derived from in situ measurements. With regard to the AMALi measurements, the cloud top altitude was set to $h_{cloud,\ top} = 200$ m. Compared to the simulations shown before, the best agreement between measurement and simulation is derived for this specific case for a cloud base altitude of $h_{cloud,\ base} = 100$ m and a slightly adjusted surface albedo ($\alpha_{water} = 0.09$, $\alpha_{ice} = 0.83$). Fig. 14 shows the frequency distributions of simulated and observed γ_λ. Comparing observation and simulation, the maximum of the ocean-water and sea-ice peak are found at equal γ_λ. In regions over dark ocean water as well as in regions over bright sea ice, the γ_λ of the observation show a broader distribution than the γ_λ of the simulation. Indeed, the magnitude of the simulated γ_λ peak above the sea-ice surface agrees well with the peak from the observation, while the difference above the dark ocean water is significantly larger. The different magnitude and the*

broader distribution of the observed single peaks compared to the simulation result most likely from simplifications in the simulations where a horizontally homogeneous cloud is assumed. Thus, variations of γ_λ due to cloud 3-D effects are not included here. Only the surface 3-D effects cause a broadening of the frequency distribution. However, while surface effects will fill up the gap between the two peaks only, cloud inhomogeneities can also result in values smaller (over water) and higher (over sea ice) than the IPA simulations."

Page 1445, lines 26-29: I recommend elaborating a bit more on the suggested technique, mainly to explain why a retrieval far from any sea ice would be needed for applying the correction factors in Figure 15 to pixels near clouds.

➔ We removed the statement on a possibility to correct these effects as in practice to many assumptions have to be used making a correction meaningless.

Page 1447, lines 10-12: I am not sure if I fully agree with the statement that the enhancement over water is stronger than the reduction over ice. It is true that in Table 1 the total reflectance is enhanced, so in this sense the "winning" effect is indeed the enhancement over water. However, the table also shows that the enhancements over water have smaller magnitudes than the reductions over ice. I suspect the enhancement of total reflectance occurs only because in the simulated cases ice covers much smaller areas than water does. So in cases of higher ice coverage the overall effect might be a net reduction, not enhancement.

➔ It is true that the total effect of enhancement above dark ocean water and reduction over bright sea ice is a function of the sea-ice coverage and floe size in the corresponding scene. In the simulations the water surface covers most of the scene biasing the averaged results. Therefore, we removed the original statement from the summary. However, for large ice floes which can be treated as an infinitely expanded ice edge as described in Section 4.2.1 and if the sea-ice and dark ocean coverage is of equal area, the reduction over the bright sea ice is stronger than the enhancement of the reflectivity over the dark ocean water. Please compare to Figure 8 in the resubmitted manuscript. For most scenarios with large flows this will result in a total reduction of the domain average radiance independent on the fraction of sea ice. As it cannot be ruled out that smaller flows result in an opposite effect, we removed this statement from the summary.

Wording:

Page 1424, lines 25-27: I suggest moving this sentence to the next paragraph, as it discusses the topic of that paragraph.

➔ The last sentence belongs to the next paragraph. We changed this according to the reviewers suggestion.

Page 1425, line 7: I suggest replacing "Here" by "In Section 2".

➔ Changed according to the reviewers suggestion

Page 1428 line 18, page 1429, lines 21 and 22: The word "both" should be replaced by "the two".

➔ Changed to "the two"

Page 1432, lines 2223: The words "in dependence" should be replaced by "as a function".

➔ Changed according to the reviewers suggestion

Page 1434, line 25: I suggest clarifying early which figure contains the grey lines, perhaps by mentioning Figure 7 in or around line 21.

➔ We have revised this part.

"The most general case of an ice edge is an infinitely straight ice edge. This case is comparable to Fig. 4a. Fig. 8 illustrates the results of the 1-D (grey lines) and 3-D (black lines) simulations. …"

Page 1437, line 3: I believe "geometrical" should be replaced by "optical", as Equation (4) does not include geometrical thickness, but the first sentence after the equation describes the way the equation coefficients change with optical thickness.

➔ At the given point, "geometrical" has to be replaced by "optical". We have revised this accordingly. Furthermore, there was a mistake with the labeling of the single curves. The legend was the wrong way around. Please find the revised version at Reply-Figure 1, for which one we have also included a second panel that presents the dependency of ΔL on the cloud geometrical thickness.

"For two model clouds with a geometrical thickness of 500 m and values of $\tau = 1$ and $\tau = 5$, Fig. 10a shows ΔL as a function of the cloud base altitude h_{cloud}. Similarly, Fig. 10b shows ΔL as a function of the cloud geometrical thickness Δh_{cloud} for low-level clouds with $\tau = 1$ and $\tau = 5$ and cloud base at 0 m. The increase of ΔL with increasing altitude of the cloud base (Fig. 10a) follows an almost linear function and can be parameterized by

$$\Delta L(h_{cloud}, \tau) = A(\tau) \cdot h_{cloud} + B(\tau). \quad (5)$$

For the parameters $A(\tau)$ and $B(\tau)$, the linear regression yields $A(\tau) = 2.00/1.6$ and $B(\tau) = 1000$ m/800 m for clouds with $\tau = 1/5$. This shows that the influence on ΔL is much larger for clouds at higher altitudes and lower τ. Comparing the results for $\tau = 1$ and $\tau = 5$ indicates that the slope A decreases with increasing τ. This proves that the influence of cloud geometry on ΔL is decreasing with increasing τ.
Similarly, ΔL increases almost linearly with increasing cloud geometrical thickness Δh_{cloud}. This relation can be parameterized by

$$\Delta L(\Delta h_{cloud}, \tau) = A(\tau) \cdot \Delta h_{cloud} + B(\tau). \quad (6)$$

The regression of the increase of ΔL with increasing cloud geometrical thickness yield $A(\tau) = 1.3/1.3$ and $B(\tau) = 300$ m/100 m for clouds with $\tau = 1/5$."

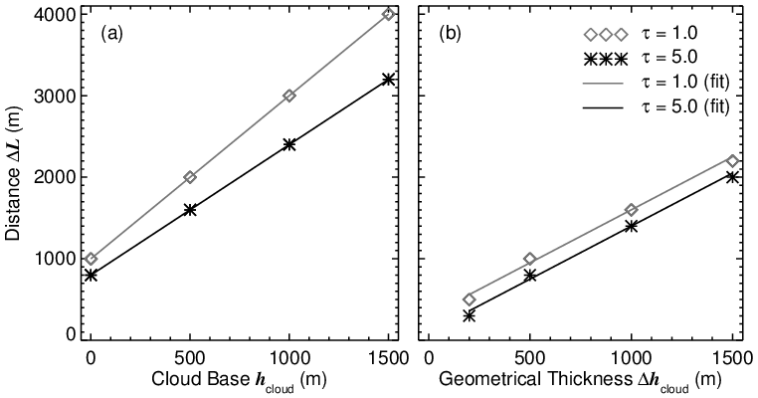

Reply-Figure 1: Revised Figure 9 (now Figure 10): *"(a) Distance ΔL as a function of the cloud base altitude h_{cloud} for a cloud with a geometrical thickness of Δh_{cloud} = 500 m and different τ. (b) Distance ΔL as a function of the cloud geometrical thickness Δh_{cloud} for a low-level cloud with cloud base at h_{cloud} = 0 m and different τ."*

Page 1437, line 5: "proofs" should be replaced by "proves".

➔ corrected

Page 1438, lines 10-15: I suggest refining the wording to make it clear that curvature affects both large and small ice floes.

➔ We have revised this by the following:

"For any water point near the ice edge, the ice area located close to this point is reduced with increasing curvature. The curvature affects both small and large ice floes and lowers the 3-D radiative effects slightly until the maximum effect, which is reached for an infinitely straight ice edge."

Page 1438, line 24: For clarity, I suggest mentioning the pixel size here.

➔ We have included remarks on the pixel size.

"This is due to the insufficient representation of the circular shape of the small ice floes by squared pixels with 50 m edge length."

Page 1443, line 24-26: To prevent any confusion, I suggest clarifying that Table 1 shows results for idealized scenarios.

➔ We have revised this according to the reviewers suggestion.

"In addition to the results from the idealized scenarios in Sect. 4.2.3, Table 1 shows the ratios $R_{3\text{-}D/IPA}$ between the results of the 3-D and IPA simulation for the realistic sea-ice scenario. Compared to the idealized scenarios in Sect. 4.2.3, for the realistic sea-ice scenario the differences between the IPA and 3-D simulations are larger above dark ocean water and smaller above bright sea ice."

Page 1444, line 8: "roll" should be replaced by "role".

➔ corrected

Reply to anonymous referee nr. 3 (review acpd-15-C667-2015):

We thank the reviewer for the helpful comments which we think have helped to improve the manuscript significantly. Especially, by removing the grammatical errors and misleading statements the revised manuscript will be easier to understand for the reader. The detailed replies on the reviewer comments are given below and structured as follows. Reviewer comments have bold letters, are labeled with the page number and line from the discussion paper, and are listed always in the beginning of each answer. The reviewer comments are followed by the author's comments with an explanation if necessary and revised parts of the paper. The revised parts of the paper are written in quotation marks and italic letters.

Sequential comments:

P1423, L4: The quoted reference, Bennartz et al. (2013) is a poor choice for substantiating the statement that clouds play a major role in projections of the future Arctic climate because it is observations-based and do not include climate model runs in any way.

➔ The reviewer is right. Bennartz et al. (2013) only state that clouds may play a major role in projections of the future Arctic climate, but not prove this by climate model runs. Therefore, we exchanged the reference Vavrus (2004), what is more suited for the given statement.

"Among others, Vavrus (2004) identified clouds as a major source of uncertainty in model predictions of the future Arctic climate."

L11: "In this regard, surface albedo: : :" since this follows after statement about the dominating influence of IR, one should perhaps clarify that this is for the solar wavelength range again - how about "For the solar wavelength range, surface albedo: : :"

➔ We agree that the wording in the original manuscript might confuse the reader. We adopted your suggestion and revised the section by:

"Depending on the time of year and their altitude, Arctic clouds may exert either a net warming or cooling effect. However, the low Sun in summer combined with a usually high surface albedo lead to a dominance of the terrestrial (infrared) radiative warming of low clouds (Intrieri et al., 2002b; Wendisch et al., 2013). For the solar wavelength range, surface albedo (sea ice coverage) is a major parameter determining whether a change of cloud amount in future climate is associated with a warming or cooling effect."

L14: ": : :Arctic stratus is nearly homogeneous: : :" This is an unsubstantiated claim if no reference is provided. Also, "from a microphysical point of view" is ambiguous. Does this mean in terms of droplet radius, thermodynamic phase, LWC/IWC? Wouldn't stratus be homogeneous in the macroscopic rather than microphysical sense?

➔ Thanks for pointing at this not properly discussed section. We now include references and clarified it more in detail, which parameters are described as homogeneous.

"While Arctic stratus often shows a horizontally homogeneous structure, both in macropyhsical (cloud base and top altitude) and microphysical properties, sea ice is often characterized by a

more heterogeneous horizontal distribution. Tsay and Jayaweera (1984) showed that Arctic stratus has a considerable horizontal homogeneity of cloud morphology, droplet diameter, concentration, and liquid water content, except for the cloud top layer. Here, mixing results in small-scale inhomogeneities identified by Lawson et al. (2001) and Klingebiel et al. (2015): bi-modal cloud particle size distributions at cloud top, while mono-modal distributions dominate the lower cloud layers representative for the adiabatic and homogeneous character of the clouds. In contrast, sea ice has irregular top and bottom surfaces and is broken into distinct pieces, called floes (Rothrock and Thorndike, 1984). …"

P1424, L4: Krijer et al. (2011) cannot be used to support the statement that "retrievals of Arctic cloud properties over bright surfaces [is] impossible". In fact, the opposite is true: Krijer et al. do state that with visible channels alone, this is not possible, but in their paper, they specifically mention that they overcome this limitation by introducing near-infrared channel(s) from SCIAMACHY.

➔ We totally agree with the reviewer. This is changed in the revised version. In particular, based on the comments by the reviewers, it is clear that we overemphasized the difficulties of cloud retrievals over bright surfaces and were wrong with the statement that cloud retrievals are not possible over ice surfaces. The reason for our misleading statement was that we focused only on the measurements with the imaging spectrometer AisaEAGLE, which covers only wavelength in the range from 400 nm to 1000 nm. For this spectral range, cloud retrievals over ice surfaces in fact are not possible without additional information (as it is stated by Krijger et al., 2011). But of course it has to be mentioned that this is only valid for the visible wavelength range and can be overcome by introducing near-infrared wavelength channels. We thank the reviewer for highlighting this lack of information, which necessarily must confuse the reader. We revised the relevant parts in the manuscript (also with respect to your later comments on MODIS) and introduced a series of new references including Platnick et al. (2001, 2004), Platnick and King (2003), and Krijger et al. (2011).

*"A highly variable Arctic surface albedo as observed during the VERDI campaign complicates the cloud retrieval introduced by Bierwirth et al. (2013). In fact, retrievals of cloud microphysical and optical properties using only visible wavelengths are strongly biased by a bright surface (Platnick et al., 2001, 2004; Platnick and King, 2003; Krijger et al., 2011). To overcome this limitation, near-infrared channels are introduced in the retrieval algorithms instead of the visible channel used over dark surfaces. E.g., for MODIS the 1.6 µm band reflectance is applied as a surrogate for the traditional non-absorbing band in conjunction with a stronger absorbing 2.1 or 3.7 µm band (Platnick et al., 2001, 2004; Platnick and King, 2003). However, an accurate separation between sea ice and open water needs to be performed before the retrieval algorithms are applied. Operational algorithms such as that for MODIS use NOAA's (**N**ational **O**ceanic and **A**tmospheric **A**dministration) microwave-derived daily 0.25° **N**ear Real-Time **I**ce and **S**now **E**xtent (NISE) dataset (Armstrong and Brodzik, 2001; Platnick and King, 2003) to identify snow- or ice-covered scenes."*

P1425, L16-L17: "Variations: : :will characterize: : :" unclear wording. Is the intention to say that changes in cloud altitude etc. will affect the transition? Or is the intention to describe what will be done in the paper?

➔ The wording in fact was unclear. We changed the relevant part to the following:

"Variations in cloud altitude, cloud geometrical thickness, r_{eff}, and surface albedo are investigated to characterize how strong these parameters influence the magnitude and distance of the γ_λ transition from high to low values."

P1426: This is an insufficient description of the instruments; while references can be used to "outsource" specific information, each paper needs to stand on its own, and at least the information that are crucial for understanding this paper need to be provided - for example the accuracy etc. of the instrumentation. For example, a google search reveals that AisaEAGLE covers wavelengths up to 1000 nm only - but later on in the paper, near-infrared wavelengths are used for applying the retrieval method by Werner et al. (2013).

➔ Thanks for showing that crucial information were missing. In the revised version we included those missing information (measured quantity, wavelength range, spectral resolution) to the description of the single instruments, which were used in this study. In order to do so, we decided to revise the order of paragraphs in this chapter as well to concentrate the instrument description to one section.

"The aircraft was equipped with an active and several passive remote-sensing systems. The active system was the Airborne Mobile Aerosol Lidar (AMALi; Stachlewska et al., 2010). It was operated in nadir viewing direction at 532 nm wavelength. Passive radiation measurements were carried out with the imaging spectrometer AisaEAGLE (manufactured by Specim Ltd. in Oulu, Finland; Schäfer et al., 2013). To analyze the 3-D radiative effects of ice edges in a cloudy atmosphere, we focus on measurements by this instrument. With 1024 spatial pixels, the single-line sensor provides a sufficiently high horizontal resolution to observe ice edges in detail. The flight altitude during the remote sensing legs was about 3 km above ground which is about 2 km above cloud top for typical boundary layer clouds with cloud top altitudes at about 1 km. For this geometry, the width of one AisaEAGLE pixel at cloud top is 3.5 m and the length is 4.2 m at an exposure time of 10 ms and a flight speed of 65 ms^{-1}. Each spatial pixel consists of 488 spectral pixels to detect spectra of radiance in the wavelength range from 400 to 970 nm with 1.25 nm full width at half maximum (FWHM). AisaEAGLE converts the detected photon counts into digitalized 12-bit numbers. By applying a spectral radiometric calibration, those numbers are transformed into radiances. The calibration, data handling, and necessary corrections are described by Schäfer et al. (2013). For radiance measurements, Schäfer et al. (2013) estimated an uncertainty of ±6 %. Assuming a fixed r_{eff}, those detected spectra of radiance can then be used to retrieve τ.
Further passive radiation measurements were carried out with the Spectral Modular Airborne Radiation measurement system (SMART-Albedometer; Wendisch et al., 2001), initially designed for albedo measurements, and a Sun tracking photometer. The SMART-Albedometer is horizontally stabilized and measures up-/downwelling spectral radiance I_λ and irradiance F_λ (λ = 350 − 2100 nm, 2-16 nm FWHM), while the Sun photometer covers aerosol optical thickness between λ = 367 − 1026 nm. The configuration was similar to that during the aircraft campaign SoRPIC described by Bierwirth et al. (2013). Additionally, dropsondes were used at selected waypoints to sample profiles of meteorological parameters (air pressure, air temperature, relative humidity) over the whole distance between the ground and the aircraft. For a more detailed description of the airborne instruments installed on Polar 5, see Bierwirth et al. (2013), Klingebiel et al. (2015) and Wendisch and Brenguier (2013).
In this study, the data from the AMALi and the dropsondes were used to determine the cloud-top altitude and geometrical thickness, whereas the data from the SMART-Albedometer were used to verify and validate the $I_\lambda^{\uparrow}$ measurements of AisaEAGLE. Furthermore, the SMART-Albedometer measurements of the downwelling irradiance $F_\lambda^{\downarrow}$ are used to transform the AisaEAGLE radiance $I_\lambda^{\uparrow}$ into the nadir reflectivity γ_λ, which is derived by: …"

➔ This comment by the reviewer may have evolved from a misunderstanding due to an insufficient introduction of this section. The reviewer is right that AisaEAGLE only covers the visible wavelength range of up to almost 1000 nm. However, in Section 5 no measurements were applied at all. The whole study is based on radiative transfer simulations as our measurements do not cover the wavelength needed to apply the retrieval method by Werner et al. (2013). We still have done this study as outlook with regard to future studies, when a near-infrared imaging

spectrometer (AisaHAWK, 1000-2500 nm wavelength) might be available. Intelligible, this is a legitimate question, since this information was not included in the manuscript yet. We have revised the manuscript and added a few more words at the point in the manuscript where we introduce the retrieval method by Werner et al. (2013).

"To quantify the magnitude of this overestimation, a synthetic cloud retrieval is investigated. The retrieval is based on simulations only in order to investigate also the uncertainties of retrieved r_{eff}, which cannot be derived from the current setup of AisaEAGLE measurements during VERDI. The limitation of AisaEAGLE to visible wavelengths restricts the retrieval to τ (Bierwirth et al., 2013). However, near-infrared measurements might be available by use of additional imaging spectrometers such as the AisaHAWK. Therefore, this study addresses both quantities τ and r_{eff}. To do so, the retrieval based on forward simulations is applied to the γ_λ field of a 3-D simulation where the cloud optical properties are known exactly."

Figure 1: What do the labels (1) and (2) mean (probably open ocean vs. ice, but it needs to be stated).

➔ Your assumption on label (1) and (2) is correct. We revised Figure 1 caption to more clearly point out the meaning of the labels.

*"**Figure 1.** VERDI flight track and true-colour MODIS image (Aqua; 250m resolution) from 17 May 2012. Numbers (1) and (2) label open ocean and sea ice, respectively."*

Figure 2: The authors may consider showing reflectance rather than radiance because the effects of SZA would then be removed, and the effect of optical thickness/surface albedo be isolated.

➔ Thanks for this helpful suggestion which we did follow in the revised manuscript. To do so, we transformed all radiance values appearing in the manuscript into reflectivities and introduced the definition.

$$\gamma_\lambda = \pi \cdot I_{\mathrm{Up}} / F_{\mathrm{down}}$$

For the calculation we used measured downwelling irradiance from the collocated SMART-Albedometer. For the transformation of the simulated radiance we additionally used simulated values for the downwelling irradiance.

To avoid any confusion by making use of the word reflectivity instead of reflectance (like it is used in your review), we like to justify our choice of "reflectivity". In our view all quantities with suffix "-ance" are radiometric quantities and have a dimension of, e.g., radiance (W m^{-2} sr^{-1}) or irradiance (W m^{-2}). Quantities which are the ratio of two radiometric quantities are dimensionless and own the suffix "..ivity" like transmissivity, emissivity. Contrarily, transmittance and emittance have the unit (W m^{-2} sr^{-1}). This nomenclature follows the discussion by Bohren and Clothiaux (2006). Following your suggestion, we revised all figures (Fig. 2, 3, 4, 5, 6, 7, 8, 12, 13, 14 following the numbering of the old manuscript) that showed measurements or simulations of the radiance. The use of the reflectivity clearly improved the interpretation of the graphs. As an example, the revised Figure 2 (see below Reply-Fig. 1) is shown here.

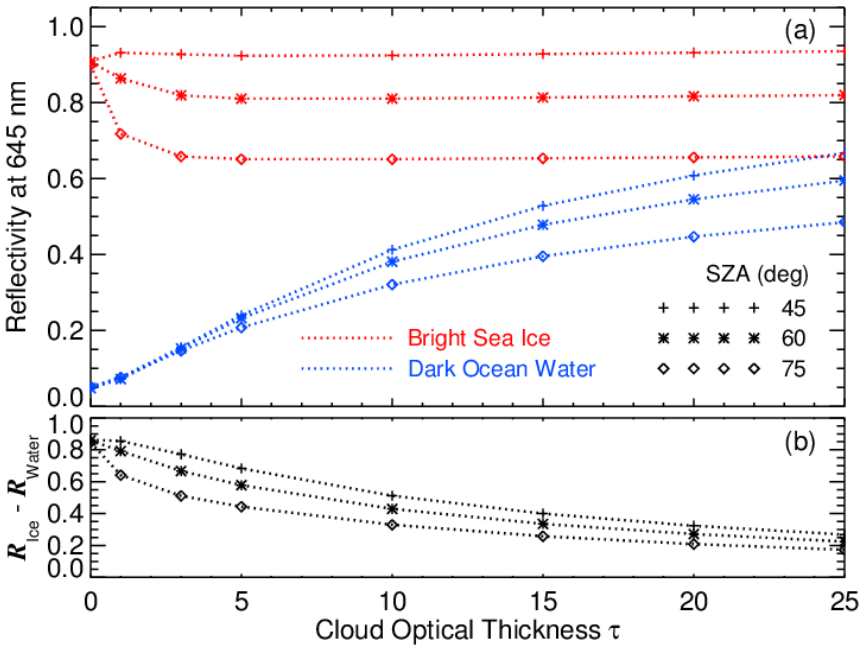

Reply-Figure 1: Revised Fig. 2.

Using the reflectivity instead of the radiance, the single simulations for different solar zenith angles (Θ) are much better separated from each other than before. However, the dependency on the Θ is not fully eliminated, what results from the non-lambertian scattering at cloud particles and the surface. Therefore, we keep the simulations for different Θ in this Figure.

P1427, L23: Unclear what this statement means. In fact, MODIS uses 860 nm, not 650 nm, for cloud retrievals over open ocean; 650 nm is used over land (when snow-free). MODIS retrievals over land (sea) ice and snow are a different story (see comment below).

➔ It is correct that MODIS retrieval over water uses the wavelength λ = 860 nm and not λ = 645 nm like we have done. However, our introduction into this section was quite misleading when we used a MODIS image to discuss the limitations of the Eagle measurements. Therefore, we revised the first part of this section to avoid any confusion. We also kept the choice of 645 nm as it was not our intention to relate the simulations to MODIS retrievals but to introduce a simple method to differentiate between ice and open water using the AisaEAGLE sensor. However, the statement at this point is not related to MODIS. In fact, we want to explain that we used the wavelength of λ = 645 nm because of its sensitivity to the cloud optical thickness. In addition, the use of the citation of Nakajima and King (1990) might be confusing, since they have used λ = 745 nm as their non-absorbing retrieval wavelength. We have revised this part and replaced the citation of Nakajima and King (1990) by Werner et al. (2013), who used the wavelength λ = 645 nm.

"The γ_λ presented in this paper are calculated at a wavelength of λ = 645 nm, where scattering is dominant and shows a strong sensitivity to τ (Werner et al., 2013)."

P1427, L18-19; P1428,L1-2: Statements of this kind are all over this manuscript and need to be carefully removed everywhere because the retrieval of cloud microphysics is, in fact, possible, and is done operationally by MODIS. Rather than Nakajima-King, it is based on near-infrared bands (1.6 and 2.1 microns) where snow is dark. This is discussed by King et al. (2004), among a few other papers. Why this is not mentioned anywhere in the manuscript is unclear. It appears that the authors are unaware of it, which seems impossible given the publication and research record of this group. Have they checked whether MODIS retrievals are, in fact, available, in addition to just looking at RGB images (Figure 1)? Attached as a supplement is a description of MODIS products, which demonstrates that MODIS does have skill to provide retrievals over snow and ice. Many more documents are publicly available. The question is what direction the manuscript would have taken, had the authors known of the existence of the MODIS algorithm. Since section 5 only refers to retrievals over the dark ocean in the vicinity of ice floes, but not over snow/ice itself, this paper is actually pertinent to the "classical" MODIS retrieval above dark surfaces. Back to the statement "A retrieval of cloud : : : properties : : : is not possible." and others of this kind: Please remove because they are incorrect.

➔ As mentioned above, the reviewer is absolutely correct with this criticism. Unfortunately we did overemphasis to motivate our study using the MODIS retrieval and did not refer to the current version of MODIS retrievals over sea ice. However, we think that our study on the 3D-effects does not necessarily needs to be motivated with satellite retrieval but is worthwhile to be presented as it is without strong link to satellite observations. Therefore, we carefully revised the whole manuscript for statements of this kind and clarified that cloud retrievals, in fact, are possible over ice surface. Only if sensors like the AisaEAGLE are used alone which do only cover visible wavelength, cloud retrieval are almost impossible over sea ice. Additionally to the before mentioned changes, the revised parts are the following:

"However, for 86 % of the cloud observations a cloud retrieval as described by Bierwirth et al. (2013) could not be applied as the surface albedo did not fulfill the constraint of being relatively dark. Either snow-covered ice almost eliminated the contrast between cloud and surface, or a mixture of ice and open water made a cloud retrieval following the strategy from Bierwirth et al. (2013) impossible."

"Using only the visible wavelength channels of the image, no visible contrast between sea ice and cloud remains. This is why near-infrared channels are applied in MODIS cloud retrievals over sea ice. However, with AisaEAGLE the observations are limited to wavelength below 1000 nm, where the contrast is weak (compare Fig. 4) and a retrieval of τ is not possible in those areas; it can only be performed above water surfaces.."

"Using those methods to estimate the threshold, ice masks were created to identify measurements of clouds above sea ice for which the cloud retrieval by Bierwirth et al. (2013) cannot be applied."

P1428, L24: "We estimate the cloud optical thickness: : :" What does this mean? Did the authors look at the level-2 MODIS products and got the number from there? Or did they visually estimate 5 from the RGB image? Why estimate if a retrieval is, in fact, available? Also, why did the authors not do their own retrieval of tau and reff, based on data from the instrumentation?

➔ We understand the confusion of the reviewer. “Estimate” is indeed a misleading word. We had a look at the closest level-2 MODIS product for cloud optical thickness (see Reply-Fig. 2). In the area of interest (red circle), the image shows values from 0 to 10 in cloud optical thickness. From this point of view we decided to use an areal average of the observation area which leads to a cloud optical thickness of 5. To point that out more clearly, we changes the sentence to:

> *"τ was obtained from AisaEAGLE measurements above open water far from any ice edge using the retrieval method presented by Bierwirth et al. (2013). An average value of τ = 5.3 ± 0.5 was derived, which agrees with the MODIS level-2 product showing values for τ between 0.02 and 15.5 (τ = 3.6 ± 2.5) in the investigated area.”*

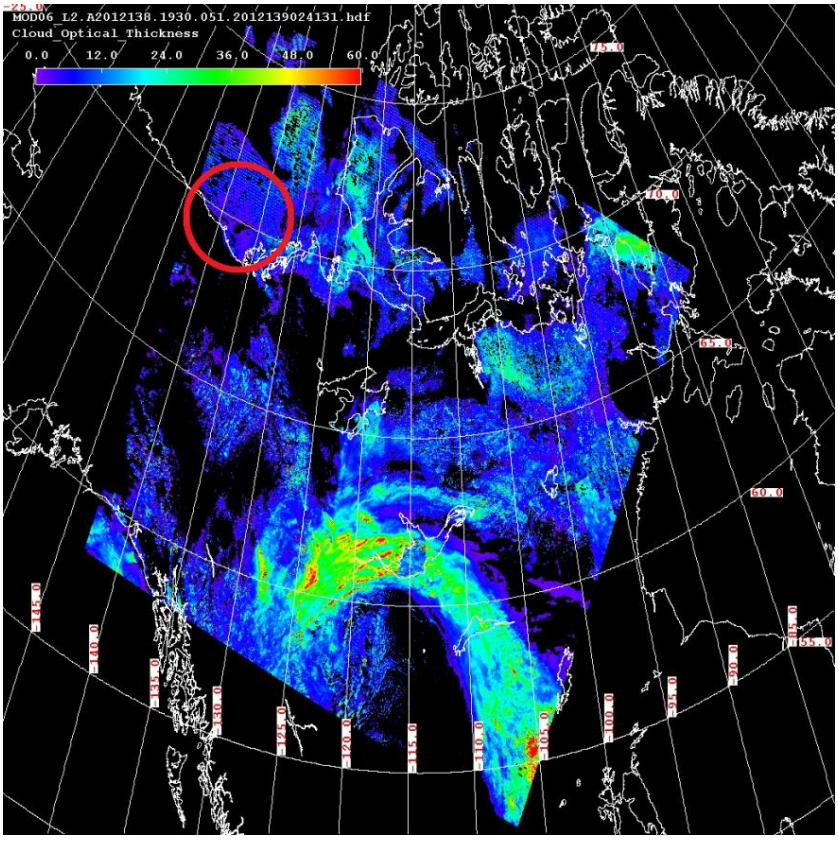

Reply-Figure 2: Level-2 MODIS product. Cloud optical thickness.

P1430, L20: One cannot see the effect of enhanced reflected radiance close to the sea ice from Figure 4b and d (mask results); better use Figure 6, which shows quantitative radiances.

➔ We agree, that the effect of enhanced reflected radiance close to the sea-ice edges was difficult to identify from Figure 4b and d. Therefore, we revised this Figure (see below Reply-Fig. 3) and color-coded the images. Due to the use of reflectivities instead of radiances, the span between extreme values became closer, which supports the use of the same legend for each image. The enhancement in the narrow bright bands around the sea-ice edges should now be easier to identify. However, we followed your suggestion to rather highlight the effect of enhanced reflected radiance close to the sea-ice edge in the text using Fig. 6 (now 7) than Fig. 4.

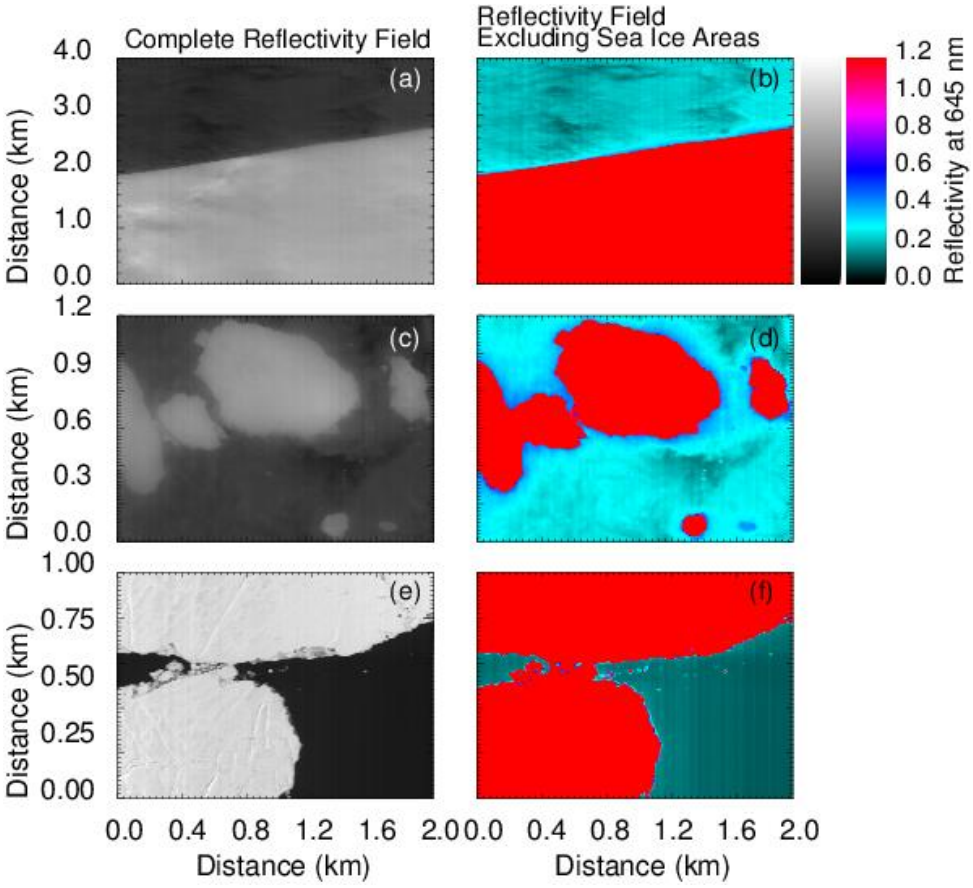

Reply-Figure 3: Revised Figure 4.

> *"Figure 7 shows the measured nadir radiance as function of the distance to the ice edge for the three scenes in Fig. 4. It shows that for the cases presented in Fig. 4b and d (red and blue in Fig. 7) close to the detected sea ice areas enhanced reflected radiance, i. e. narrow bright bands, are observed, which are most likely related to 3-D effects in clouds and the interaction between cloud and surface."*

Figure 6, Question 1: The question about Figure 6 that needs to be discussed is the significance of the local maximum of radiance at -50m.

➔ This is a justified question, which also arose to us, when we have seen this graph in the first time. However, the visibility of the local maximum of radiance at -50 m results only from the way we presented the measurements. Each gray line in the original figure represented one section across the ice edge out 488 total cross sections. The majority of the cross sections ranges close to the mean values and are superpose so that the few outlier weighted to strong by human eye. Those higher radiances are related to the small bright spot at x = 0.8 km and y = 2.0 km in Fig. 4a. In total, the number of data points that contribute to this enhanced radiance spot is less than 5 % of the total amount of data points. Nevertheless, we have revised this figure and show the standard deviation for each distance instead of all data points. Due to the small contribution of the bright spot to the standard deviation, the local maximum of radiance at -50 m does not appear anymore in the graph.

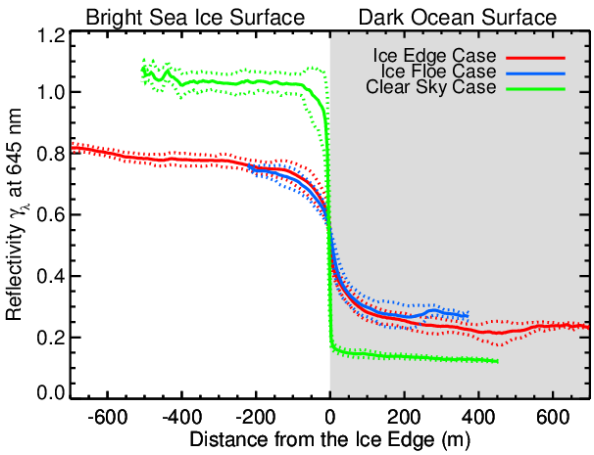

Reply-Figure 4: Revised Figure 6.

Figure 6, Question 2: The different cases shown are probably observed at different solar zenith angles. Could this be shown as reflectance instead to normalize with respect to mu?

➔ The reviewer is right. The different cases shown are observed at different solar zenith angles. In case of the same cloud properties, the reflectivity should be similar. Following one of your comments above, we have also exchanged the radiance values from this figure by reflectivities. Please see Reply-Fig. 4. The results for the first (red) and second (blue) measurement case (cloudy), which were measured almost during the same time with nearly equal Θ, are now approximately congruent. The results from the third (cloud-free) case (green) shows still different maximum and minimum values over the bright sea-ice and dark ocean water, compared to the two cloudy cases. The remaining differences result from the missing clouds in the clear sky case.

P1433, L12: No, The MODIS retrieval over water does not use this wavelength (see comment above).

➔ As replied to an earlier comment, we corrected the manuscript with regard to our choice of wavelength and the incorrect statements about MODIS.

"The input to the radiative transfer model (RTM) contains the optical properties of the atmosphere (e.g., extinction coefficients, single-scattering albedos, phase functions) and the 2-D surface albedo."

P1435, L7-8: Unclear statement

➔ With this part we wanted to address that the radiation, which is reflected by the sea ice, will travel into the direction in which it was scattered by the sea ice. On its way, the efficiency that it is scattered again into the nadir observation direction of the sensor is much lower for a clear atmosphere than for a cloudy atmosphere. We revised this part to point this out more clearly what is meant by this statement. Additionally, we included a schematic illustration of the 3-D effect in the revised version.

> *"…This indicates that the 3-D effect is dominated by horizontal photon transport between sea ice and clouds and the scattering processes by the cloud particles into the nadir observation direction. Without clouds, the horizontal photon transport above the isotropically reflecting surface is of similar magnitude to the cloudy case. However, due to the weak scattering in the clear atmosphere compared to the scattering by cloud particles, this effect is only significant for cloudy cases."*

P1435, L18: The purpose of Delta L and Delta L critical is misleading - why was Delta L critical (in addition to Delta L) introduced? Judging from Figures 9 and 10, it appears that the horizontal extent of the "vicinity zone" around ice floes decreases with cloud optical thickness, increases with cloud base/top height, (and geometrical thickness? - please add a table or Figure that shows this), as well as with the radius of the ice floe. It does not appear that Delta L critical is necessary because Delta L alone gives a clear picture.

➔ We chose the two different definitions, ΔL_{crit} (now ΔL_{HPT}) and ΔL, to address the influence on the horizontal photon transport on the one hand side and the influence of the 3-D effects on the cloud retrieval on other hand side. The first distance, ΔL_{HPT}, is a measure for the horizontal photon transport. This distance is increasing with increasing τ. Contrary, the second distance, ΔL, is a measure for the horizontal extent of the 3-D effects, within which cloud retrievals in the visible wavelength range above water are biased by the bright sea ice. We agree with the reviewer that this was not properly discussed in the original manuscript. In the resubmitted manuscript, we have revised the following parts:

> *"Over the water-covered area, an enhancement of γ_λ was measured close to the ice edge; while over the ice-covered area, γ_λ is reduced near the ice edge. We define two distances measured from the ice edge to quantify the enhancement effect. The first distance ΔL_{HPT} is introduced to quantify the range of horizontal photon transport. It characterizes the distance at which the transition from high $\gamma_{\lambda,ice}$ to low $\gamma_{\lambda,water}$ is $1/e^3$ of the initial difference between the mean γ_λ above ice ($\gamma_{\lambda,ice}$) and the mean γ_λ above open water ($\gamma_{\lambda,water}$):*
>
> $$\gamma_{\lambda,water}(\Delta L_{HPT}) = \gamma_{\lambda,water} + 1/e^3 \cdot \Delta IPA, \qquad (3)$$
>
> *with $\Delta IPA = \gamma_{\lambda,ice} - \gamma_{\lambda,water}$. By including ΔIPA, ΔL_{HPT} quantifies the range of horizontal photon transport independent on the difference of the surface albedo contrast. For the scene from Fig. 4a, ΔL_{HPT} indicated by the enhancement of γ_λ over the water surface extends to a distance of 200 m from the ice edge.*
> *Furthermore, a second distance to the ice edge ΔL is defined for which $\gamma_{\lambda,water}$ is enhanced by 6 % of the average γ_λ above open water.*
>
> $$\gamma_{\lambda,water}(\Delta L) = \gamma_{\lambda,water} + 0.06 \cdot \gamma_{\lambda,water}. \qquad (4)$$

The choice of the threshold results from the radiance measurement uncertainty (± 6 %) of the imaging spectrometer AisaEAGLE. Using this definition, ΔL is independent of γ_λ measured above the ice surface. It only accounts for the significance of the enhancement with respect to the measurement uncertainty. If the enhancement is higher than the measurement uncertainty, a cloud retrieval might be significantly biased when using the contaminated measurements. Therefore, ΔL is a measure for the horizontal extent within which the 3-D effects bias the cloud retrieval in the vicinity of an ice edge. For the special case of the measured γ_λ in Fig. 6, the ΔL = 300 m. Above open water, all measurements within that transition zone cannot be used for the cloud retrieval as the enhanced γ_λ will positively bias the retrieved τ."

''To compare the results with the measurement example in Fig. 6, the distance ΔL_{HPT} defined by Eq. (3) is analyzed. $\gamma_{\lambda,water}$ is set to the IPA values above water. For the cases presented in Fig. 8, ΔL_{HPT} increases with increasing τ from 100 m at τ = 1 to 250 m at τ = 5 and to 300 m at τ = 10. This shows that the horizontal photon transport increases with τ due to increased scattering inside the cloud layer. In contrast to ΔL_{HPT}, the distance ΔL defined by Eq. (4) decreases from 600 m (at τ = 1.0) to 400 m (at τ = 5.0) and to 250 m (at τ = 10.0). The decrease of ΔL suggests that the area in which γ_λ is enhanced and a cloud retrieval might be biased is smaller for optically thick clouds. This is related to the decrease in contrast between cloud covered sea ice and cloud covered ocean if τ increases. The difference Δ(IPA) between $\gamma_{\lambda,ice}$ and $\gamma_{\lambda,water}$ decreases from γ_λ = 0.87 for the clear-sky case to γ_λ = 0.44 for τ = 10, mainly due to the increasing reflection of incoming radiation by the cloud. If τ increases, $\gamma_{\lambda,water}$ increases which results in a higher uncertainty range exceeding the γ_λ enhancement also in areas closer to the ice edge. Therefore, the γ_λ enhancement becomes less significant for a cloud retrieval compared to the measurement uncertainties. Since we aim to retrieve τ above water areas enclosed by ice floes, in the following ΔL is used to quantify the 3-D effects.''

➔ The information that ΔL is increasing with an increase of the geometrical thickness, as it is written in the manuscript, is an artifact of a former version of the paper and actually not provable by Figure 9. Figure 9 only confirms that ΔL is increasing with increasing cloud base altitude. We revised Figure 9 (now Figure 10 in the resubmitted manuscript) to also include the information that ΔL is increasing with the geometrical thickness of the cloud. Furthermore, we corrected the labeling, which was the wrong way round in the former manuscript. Please see Reply-Fig. 6.

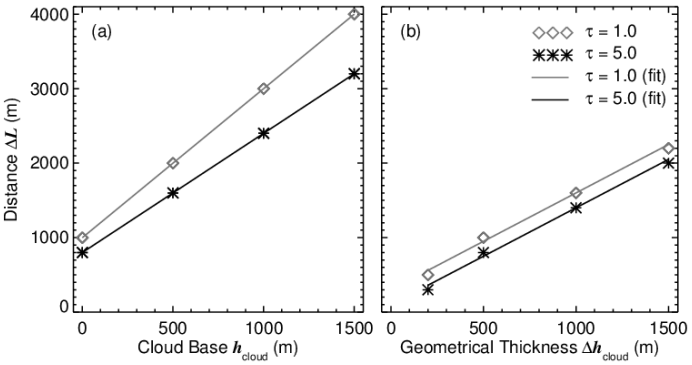

Reply-Figure 6: Revised Figure 9 (now Figure 10): *"(a) Distance ΔL as a function of the cloud base altitude h_{cloud} for a cloud with a geometrical thickness of Δh_{cloud} = 500 m and different τ. (b) Distance ΔL as a function of the cloud geometrical thickness Δh_{cloud} for a low-level cloud with cloud base at h_{cloud} = 0 m and different τ."*

"For two model clouds with a geometrical thickness of 500 m and values of τ = 1 and τ = 5, Fig. 10a shows ΔL as a function of the cloud base altitude h_{cloud}. Similarly, Fig. 10b shows ΔL as a function of the cloud geometrical thickness Δh_{cloud} for low-level clouds with τ = 1 and τ = 5 and cloud base at 0 m. The increase of ΔL with increasing altitude of the cloud base (Fig. 10a) follows an almost linear function and can be parameterized by

$$\Delta L(h_{cloud}, \tau) = A(\tau) \cdot h_{cloud} + B(\tau). \quad (5)$$

For the parameters A(τ) and B(τ), the linear regression yields A(τ) = 2.00/1.6 and B(τ) = 1000 m/800 m for clouds with τ = 1/5. This shows that the influence on ΔL is much larger for clouds at higher altitudes and lower τ. Comparing the results for τ = 1 and τ = 5 indicates that the slope A decreases with increasing τ. This proves that the influence of cloud geometry on ΔL is decreasing with increasing τ.
Similarly, ΔL increases almost linearly with increasing cloud geometrical thickness Δh_{cloud}. This relation can be parameterized by

$$\Delta L(\Delta h_{cloud}, \tau) = A(\tau) \cdot \Delta h_{cloud} + B(\tau). \quad (6)$$

The regression of the increase of ΔL with increasing cloud geometrical thickness yield A(τ) = 1.3/1.3 and B(τ) = 300 m/100 m for clouds with τ = 1/5."

Section 4.2.3: This section is too long, and there are many problems with repetition, language/grammar. Rather than listing the issues in detail, the authors are encouraged to shorten this section AND have this proof-read by the co-authors (something that should always be done). I would like to point out that the finding on P1442,L22-24 seems important, but would "shine more" if presented in a considerably shorter section 4.2.3.

➔ We have revised this section and significantly shortened it, especially by removing most of the repetitions or summarizing them in Section 4.2 (repetition of input parameters such as τ, cloud altitude or geometrical thickness) and 4.2.1 (general findings such as the description of the enhanced or reduced reflectivity in the vicinity of ice edges). Furthermore, we have resorted single paragraphs, which makes this section even shorter and avoids unnecessary back and forth switching between the single parameters. In the revised version, we try to separate the investigations of single parameters, before discussing the next one (ice edge length, sea-ice area,…). Due to the length of the changes we decide not to copy all new sections here. Please use the revised manuscript.

P1443, L21-23: Unclear what justifies the statement that cloud and surface heterogeneity effects "are in the same range". If that is true, please make this a quantitative statement and provide the respective ranges.

➔ We agree with the reviewer that the reason for the broader frequency distributions of the observations compared to the simulations cannot be substantiated by the last sentence of the corresponding paragraph – "Compared to the observations, this indicates that cloud heterogeneity effects and surface heterogeneity effects are in the same range". We have revised this sentence. However, we think that the broadening is due to differences in the cloud base altitude and due to cloud-inhomogeneity effects. While the cloud top is well defined by measurements with the AMALi, it cannot see the cloud base. Therefore, we performed some

tests with a different altitude of the cloud base. Additionally, we slightly varied the surface albedo. Doing so, we could achieve a better agreement between simulation and observation.
Furthermore, in the revised manuscript we changed the normalization of the distributions in Fig. 13 (now Fig. 14) to a total value of one. This makes the comparison more meaningful and highlights the different radiative effects. A broadening of the dark ocean water and sea-ice peak may result from both sea ice edge effect and cloud heterogeneities. However, while surface effects will fill up the gap between the two peaks only, clouds inhomogeneities can also result in values smaller (over water) and higher (over sea ice) then the IPA simulations. This is clearly obvious, comparing simulations and measurements, what gives us reason to address the broadening partly to cloud inhomogeneities. The revised version of this part is the following:

"The albedo map was used in the simulations implementing a cloud of $\tau = 5$ and a fixed $r_{eff} = 15\ \mu m$, as derived from in situ measurements. With regard to the AMALi measurements, the cloud top altitude was set to $h_{cloud,\ top} = 200$ m. Compared to the simulations shown before, the best agreement between measurement and simulation is derived for this specific case for a cloud base altitude of $h_{cloud,\ base} = 100$ m and a slightly adjusted surface albedo ($\alpha_{water} = 0.09$, $\alpha_{ice} = 0.83$). Fig. 14 shows the frequency distributions of simulated and observed γ_λ. Comparing observation and simulation, the maximum of the ocean-water and sea-ice peak are found at equal γ_λ. In regions over dark ocean water as well as in regions over bright sea ice, the γ_λ of the observation show a broader distribution than the γ_λ of the simulation. Indeed, the magnitude of the simulated γ_λ peak above the sea-ice surface agrees well with the peak from the observation, while the difference above the dark ocean water is significantly larger. The different magnitude and the broader distribution of the observed single peaks compared to the simulation result most likely from simplifications in the simulations where a horizontally homogeneous cloud is assumed. Thus, variations of γ_λ due to cloud 3-D effects are not included here. Only the surface 3-D effects cause a broadening of the frequency distribution. However, while surface effects will fill up the gap between the two peaks only, cloud inhomogeneities can also result in values smaller (over water) and higher (over sea ice) than the IPA simulations."

Section 5: I recommend removal of this section. In general, sections 5, 4.2.3, and 4.2.4 are of much lower quality than the rest of the paper. But regarding content, the applied retrieval technique actually does not replicate what MODIS is doing (if the goal is to improve/validate satellite retrievals). If this were the purpose of the study, the correct pairing of bands (860 nm + 2150 nm), should be used. It is unclear why Werner et al. (2013) is used here instead - why is Nakajima-King ambiguous (with respect to which retrieval parameters)? In addition, if the overestimation zone for cloud optical thickness is only 2 km, this would hardly be seen by MODIS anyway because its grid size is 1km. If anything, this will affect ONE pixel in the vicinity of an ice floe. This would be relevant for sub-grid-resolution ice floes though, which MAY bias the MODIS cloud retrievals high if they go undetected. But this does not seem to be the intent of the current study.

➔ The main focus and we hope that we could clarify this by the revisions discussed before is not to connect the observed 3-D effects to satellite observations. Still this is part of our motivation, but in this study the application of airborne measurements of imaging spectrometers is the main driver. Here the observed scales are much smaller and the 3-D effect might affect cloud retrievals. Therefore, in Section 5 a sensitivity study for such cloud retrieval is presented where we apply wavelengths and retrieval methods developed for airborne observation (Bierwirth et al. 2013, Werner et al., 2013) The motivation is to show how strong airborne derived cloud microphysical and optical properties with a high spatial resolution are affected by the 3-D effects.

Due to the missing near infrared wavelength in the measurements which are needed for retrieval of cloud particle effective radius, we decided to base this study purely on simulations. This is justified by the fact that in near future an imaging spectrometer for near infrared wavelength is available and will be used in future projects continuing the investigations of VERDI. From that point of view, we would like to keep this section and revised it throughout to avoid further misunderstandings. Additionally, we changed the title of the manuscript to clearly point out the focus on airborne measurements and avoid any confusion by the reader.

"Airborne observations and simulations of three-dimensional radiative interactions between Arctic boundary-layer clouds and ice floes"

➔ We also added an extra paragraph to the introduction, which shell clarify that the investigations are related to airborne measurements.

"As demonstrated by Bierwirth et al. (2013), airborne remote sensing using spectral imaging sensors is one promising method to characterize small scale inhomogeneities of clouds in the spatial range below 5 m. For airborne imaging spectrometer measurements over dark ocean surfaces, Bierwirth et al. (2013) introduced a novel five-wavelength cloud retrieval procedure that is based on the classic two-wavelength cloud retrieval by Nakajima and King (1990) and follows the multi-wavelength approach by Coddington et al. (2012) and King and Vaughan (2012). For airborne measurements performed during the international field campaign SoRPIC (Solar Radiation and Phase discrimination of ArctIc Clouds), Bierwirth et al. (2013) showed that accurate retrieval results can be obtained for the cloud optical thickness τ. However, due to the limitation of the instrument to wavelengths below 1000 nm a retrieval of r_{eff} was not feasible. Also, the application of the retrieval was restricted to areas of open water."

"Within the present study, the focus lies on those 3-D radiative effects that are related to the horizontal photon transport between cloud and surface due to isotropic reflection of the incident radiation on the bright sea ice. The goal is to quantify the magnitude and horizontal extent of those 3-D effects as well as their influence on cloud retrievals from the visible wavelength range with a high spatial resolution. In reality, such surface 3-D radiative effects will be combined with cloud 3-D radiative effects due to cloud inhomogeneities. …"

➔ The choice of the method by Werner et al. (2013) is justified by the following points. We refer to Werner et al (2013), because the general approach using ratios instead of absolute radiances was applied here as well. Second, the method is not restricted to cases when cirrus is above the aircraft (we have chosen data with clear sky conditions above the aircraft) but also improves retrieval uncertainties in this cases. It further improves the retrieval technique from Bierwirth et al. (2013) by using ratios of radiances instead of total radiance only. In comparison to the retrieval grid, derived by the two-wavelength retrieval from Bierwirth et al. (2013), the ratio method further results in a better orthogonality of the τ and r_{eff} solution space (please notice Reply-Figure 7). This leads to a better separation of the τ and r_{eff} solution space ("More unambiguous" was the wrong wording at this point. We revised it by the words "better separation"). For airborne investigations of τ and r_{eff} with large spatial coverage and high spatial resolution (as we want to perform it in future studies), this will result in a better accuracy of the retrieved values. To make our decision using the ratio method by Werner et al. (2013) more clear, we included the following part in the revised manuscript:

"The retrieval grid is constructed from the simulated γ_λ at 645 nm wavelength on the abscissa and the ratio of γ_λ at 1525 and 579 nm wavelength on the ordinate. This wavelength and the wavelength ratio was chosen in order to improve the retrieval method by Bierwirth et al. (2013). The choice of wavelength follows the method presented by Werner et al. (2013). This

method creates a retrieval grid with a more separated solution space for τ and r_{eff} than the classic two-wavelength method by Nakajima and King (1990) or Bierwirth et al. (2013). Furthermore, it effectively corrects the retrieval results for the influence of overlying cirrus and reduces the retrieval error for τ and r_{eff} caused by calibration uncertainties (Werner et al., 2013). For airborne investigations of τ and r_{eff} with large spatial coverage and high spatial resolution, this will result in a higher accuracy of the retrieved cloud properties."

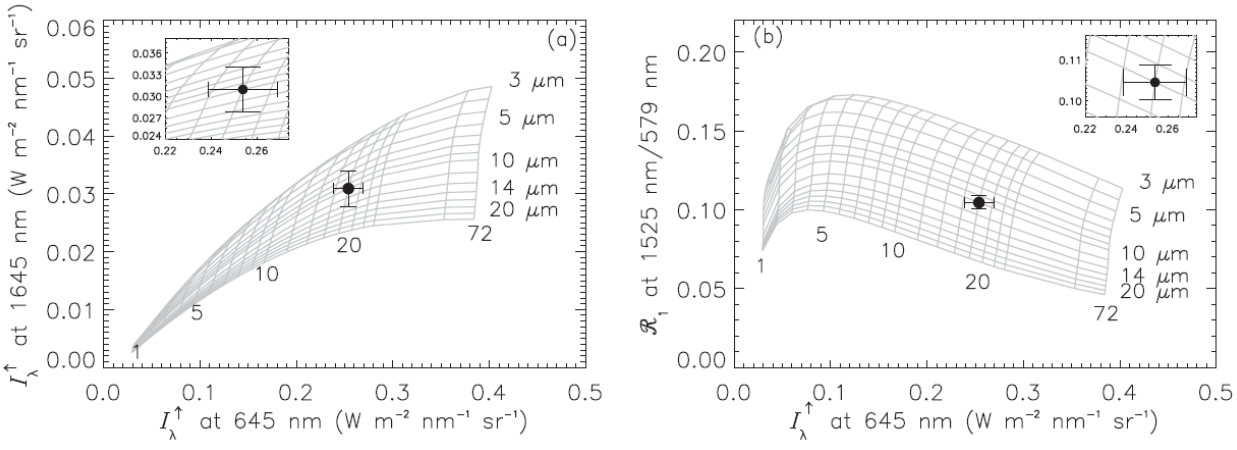

Reply-Figure 7: Comparison of classical two-wavelength retrial method by Nakajima and King (1990) and ratio method by Werner et al. (2013). Graphs adapted from Werner et al. (2013), not included in the manuscript.

P1445, L22-23: ": : :different patterns of : : : 3D effects can be larger at absorbing wavelengths". This statement needs to be substantiated. How do the different patterns suggest this?

➔ The reviewers confusion is justified. The statement as it is, is misleading. It is the wrong way around and contradicts the statements given before. Accordingly, we revised this part and also spend a few more words for the explanation.

"Furthermore, Fig. 16 shows that the overestimation of τ increases approximately exponentially starting at about 1.5 km distance, while the overestimation of r_{eff} increases more slowly and only extends up to a distance of 1.0 km. This indicates that the magnitude of the 3-D effects depends on the wavelengths. In all simulations shown in Sect. 4.2, a wavelength of 645 nm was used for the retrieval of τ. However, the retrieval of r_{eff} also requires simulations at 1 525 nm in the absorption band of liquid water. Therefore, the smaller magnitude and horizontal extent of the overestimation of r_{eff} compared to the magnitude and horizontal extent of the overestimation of τ suggest that the 3-D effects will be smaller at absorbing wavelengths."

P1446, L11-13: See comments above. Retrievals are possible over snow surfaces. Please review the literature.

➔ As stated before, we revised the whole article with respect to those justified comments. Here at this point, we removed this statement.

Conclusions: This section should be significantly shortened; after all, the purpose of this section should be to summarize the most important results.

➔ We agree with the reviewer that the summary in many instances was not written efficiently. We tried to follow the suggestions by the reviewer, revised this section and shortened it by almost the half summarizing only the most important results from the main part.

P1449, L14-L26: Remove (see comment above), or frame this differently, after having reviewed the cloud retrieval literature.

➔ As discussed above, we kept this section, clearly pointing out that it is representative only for the airborne measurements presented in the manuscript. We have revised the particular sentence by:

> *"The results from the simulations suggest that applying a 1-D cloud retrieval to airborne measurements over ocean areas located close to sea ice edges, τ and r_{eff} will be further overestimated the closer the pixel is located to the ice edge. …"*

Language/Spelling comments:

I am sure I did not capture all the language issues (especially in punctuation), the ones given below are representative. The manuscript needs to be revised by a native speaker and undergo ACP copy-editing.

➔ We thank the reviewer for the detailed list of language issues.

P1422, L2: add comma after "observations"
➔ inserted

L7: "instantaneously" –> "instantaneous"
➔ changed

L10: "with help" –> "with the help"
➔ changed

L13: "ground overlaying" sounds a bit awkward, can it be replaced with some other term or at least be hyphenated?

➔ The reviewer is right. "Ground overlaying" is a bad choice to characterize low-level clouds, which are touching the ground. However, we could not find an appropriate word, so we decided to replace "ground overlaying" by "low-level" and to add the altitude in quantitative numbers, from which it should become clear that the cloud is touching the ground. We changed it at each point where it occurred in the manuscript.

*"For a low-level cloud at 0–200 m altitude, as observed during the Arctic field campaign **VER**tical **D**istribution of **I**ce in Arctic clouds (VERDI) in 2012, an increase of the cloud optical thickness τ from 1 to 10 leads to a decrease of ΔL from 600 to 250 m."*

"From the two measurement cases presented here (τ = 5, h_{cloud} = 0–200 m), a distance ΔL of 400 m was observed."

***"Figure 8.** Simulated mean γ_λ across an ice edge for clear-sky conditions as well as for low-level clouds between 0 and 200 m altitude, τ = 1/5/10, and r_{eff} = 15 µm. …"*

***"Figure 10.** (a) Distance ΔL as a function of the cloud base altitude h_{cloud} for a cloud with a geometrical thickness of Δh_{cloud} = 500 m and different τ. (b) Distance ΔL as a function of the cloud geometrical thickness Δh_{cloud} for a low-level cloud with cloud base at h_{cloud} = 0 m and different τ."*

L13: "in 0-200m altitude" –> "at 0-200m altitude" (multiple occurrences throughout manuscript)
➔ We have changed this (see above) and revised the whole manuscript for similar mistakes.

L13: "on both, cloud and sea" - remove comma
➔ Removed

L21: "infinite" –> "infinitely"
➔ We have changed it and revised the whole manuscript for similar occurrences.

P1424, L19: "superposed" – use a more suitable word such as "combined"
➔ We changed it to the reviewers suggestion "combined".

P1425, L12: add comma after "(2013)"
➔ inserted

L13: add comma after "simulations"
➔ inserted

L23 and L27: add comma after "(VERDI)"
➔ inserted

P1426, L3: "aimed at" –> "was aimed at"
➔ changed

P1426, L22: "obverse" –> "observe"
➔ corrected

P1434, L11: "effects affect" - improve language
➔ We have replaced “affect” with “influence”.

L16: "will be simulated" – please fix the usage of tense throughout the paper. The simulations have already been performed, so future tense is inappropriate.

L21: "have been" –> "were"?
➔ Changed to were

P1435, L1: add comma after "observations"
➔ inserted

L2: add comma after "ice"
➔ inserted

L9: add comma after "general"
➔ inserted

L16: add comma after "7"
➔ inserted

L20: "That" –> "This"
➔ corrected

P1437, L5: "That proofs" –> "This proves"
➔ corrected

P1439, P1443: R_(3-D-IPA) is misleading, this should be relabeled R_(3D)/R_(IPA) (Currently, this looks like a difference, but it’s a ratio).

➔ The reviewer is right that this was misleading in the old manuscript and could confuse the reader. We have changed and R_(3-D-IPA) to R_(3D)/R_(IPA) at each point where it occurred in the manuscript.

P1444, L8: "roll" –> "role"
➔ corrected

P1445, L17: Replace "kind of" - this is slang
➔ changed to “approximately”

P1446, L19: "This causes horizontal photon transport, which : : : is scattered" It is not the transport that is scattered but the radiation (fix structure).

> *“This reflection causes horizontal photon transport, before the radiation is scattered by cloud particles into the direction of observation.”*

References cited in this reply:

Bohren, C. F. and Clothiaux, E. E.: Fundamentals of atmospheric radiation, Wiley-VCH Verlag GmbH & Co. KGaA, Weinheim, 2006.

Ehrlich, A., Bierwirth, E., Wendisch, M., Herber, A., and Gayet, J.-F., Airborne hyperspectral observations of surface and cloud directional reflectivity using a commercial digital camera, Atmos. Chem. Phys. , 12, 3493-3510, doi:10.5194/acp-12-3493-2012, 2012

Nakajima, T., and M. King (1990), Determination of the optical thickness and effective particle radius of clouds from reflectedsolar radiation measurements. Part I: Theory, *J. Atmos. Sci.*, *47*, 1878–1893.

Vavrus, S.: The Impact of Cloud Feedbacks on Arctic Climate under Greenhouse Forcing, J. Climate., 17, 603–615, 2004.

Werner, F., Siebert, H., Pilewskie, P., Schmeissner, T., Shaw, R. A., and Wendisch, M.: New airborne retrieval approach for trade wind cumulus properties under overlying cirrus, J. Geophys. Res., 118, 1–16, doi:10.1002/jgrd.50334, 2013.

Manuscript prepared for Atmos. Chem. Phys. Discuss.
with version 2015/04/24 7.83 Copernicus papers of the LaTeX class copernicus.cls.
Date: 9 June 2015

Airborne observations and simulations of three-dimensional radiative interactions between Arctic boundary-layer clouds and ice floes

M. Schäfer[1], E. Bierwirth[1,2], A. Ehrlich[1], E. Jäkel[1], and M. Wendisch[1]

[1]Leipzig Institute for Meteorology, University of Leipzig, Leipzig, Germany
[2]now at: PIER-ELECTRONIC GmbH, Nassaustr. 33–35, 65719 Hofheim-Wallau, Germany

Correspondence to: M. Schäfer (michael.schaefer@uni-leipzig.de)

Abstract

Based on airborne spectral imaging observations, three-dimensional (3-D) radiative effects between Arctic boundary layer clouds and highly variable Arctic surfaces were identified and quantified. A method is presented to discriminate between sea ice and open water under cloudy conditions based on airborne nadir reflectivity γ_λ measurements in the visible spectral range. In cloudy cases the transition of γ_λ from open water to sea ice is not instantaneous but horizontally smoothed. In general, clouds reduce γ_λ above bright surfaces in the vicinity of open water, while γ_λ above open sea is enhanced. With the help of observations and 3-D radiative transfer simulations, this effect was quantified to range between 0 and 2200 m distance to the sea ice edge (for a dark-ocean albedo of $\alpha_{\text{water}} = 0.042$ and a sea-ice albedo of $\alpha_{\text{ice}} = 0.91$ at 645 nm wavelength). The affected distance ΔL was found to depend on both cloud and sea ice properties. For a low-level cloud at 0–200 m altitude, as observed during the Arctic field campaign **VER**tical **D**istribution of **I**ce in Arctic clouds (VERDI) in 2012, an increase of the cloud optical thickness τ from 1 to 10 leads to a decrease of ΔL from 600 to 250 m. An increase of the cloud base altitude or cloud geometrical thickness results in an increase of ΔL; for $\tau = 1/10$ $\Delta L = 2200$ m/1250 m in case of a cloud in 500–1000 m altitude. To quantify the effect for different shapes and sizes of ice floes, radiative transfer simulations were performed with various albedo fields (infinitely long straight ice edge, circular ice floes, squares, realistic ice floe field). The simulations show that ΔL increases with increasing radius of the ice floe and reaches maximum values for ice floes with radii larger than 6 km (500–1000 m cloud altitude), which matches the results found for an infinitely long, straight ice edge.

Furthermore, the influence of these 3-D radiative effects on the retrieved cloud optical properties was investigated. The enhanced brightness of a dark pixel next to an ice edge results in uncertainties of up to 90 and 30 % in retrievals of τ and effective radius r_{eff}, respectively. With the help of ΔL, an estimate of the distance to the ice edge is given, where the retrieval uncertainties due to 3-D radiative effects are negligible.

1 Introduction

As shown by observations and simulations, the Arctic climate changes faster and stronger than the global climate (e. g., Sanderson et al., 2011; Overland et al., 2011). Among others, Vavrus (2004) identified clouds as a major source of uncertainty in model predictions of the future Arctic climate. Therefore, understanding the effects of clouds in the Arctic climate system is of utmost importance. Depending on the time of year and their altitude, Arctic clouds may exert either a net warming or cooling effect. However, the low Sun in summer combined with a usually high surface albedo lead to a dominance of the terrestrial (infrared) radiative warming of low clouds (Intrieri et al., 2002b; Wendisch et al., 2013). For the solar wavelength range, the surface albedo (sea ice coverage) is a major parameter determining whether a change of cloud amount in future climate is associated with a warming or cooling effect.

While Arctic stratus often shows a horizontally homogeneous structure, both in macrophysical (cloud base and top altitude) and microphysical properties, sea ice is often characterized by a more heterogeneous horizontal distribution. Tsay and Jayaweera (1984) showed that Arctic stratus has a considerable horizontal homogeneity of cloud morphology, droplet diameter, concentration, and liquid water content, except for the cloud top layer. Here, mixing results in small-scale inhomogeneities identified by Lawson et al. (2001) and Klingebiel et al. (2015): bi-modal cloud particle size distributions at cloud top, while monomodal distributions dominate the lower cloud layers representative for the adiabatic and homogeneous character of the clouds. In contrast, sea ice has irregular top and bottom surfaces and is broken into distinct pieces, called floes (Rothrock and Thorndike, 1984). Openings in the ice surface (cracks, leads, and polynias) are often present especially in the transition zone between sea ice and open water, often accompanied by fields of scattered ice floes. The albedo contrast in such areas is the highest we can observe on Earth. For visible wavelengths, the albedo of open water is low (0.042 at 645 nm; Bowker et al., 1985), while that of ice-/snow-covered ocean is high (0.91 at 645 nm; Bowker et al., 1985). These differences significantly decrease in the near-infrared wavelength range ($\alpha_{\text{water}} = 0.01$ and

$\alpha_{\text{snow}} = 0.04$ at $\lambda = 1.6\,\mu\text{m}$ wavelength; Bowker et al., 1985), but still slightly alter the radiative transfer.

Using Advanced Very High Resolution Radiometer (AVHRR) data from the polar-orbiting satellites NOAA-IO and NOAA-11, Lindsay and Rothrock (1994) analyzed the albedos of 145 different $200\,\text{km}^2$ cells in the Arctic. The mean values for the cloud-free portions of individual cells range from 0.18 to 0.91 and were found to be highly variable at monthly and annual time scales (Lindsay and Rothrock, 1994).

As demonstrated by Bierwirth et al. (2013), airborne remote sensing using spectral imaging sensors is one promising method to characterize small scale inhomogeneities of clouds in the spatial range below 5 m. For airborne imaging spectrometer measurements over dark ocean surfaces, Bierwirth et al. (2013) introduced a novel five-wavelength cloud retrieval procedure that is based on the classic two-wavelength cloud retrieval by Nakajima and King (1990) and follows the multi-wavelength approach by Coddington et al. (2012) and King and Vaughan (2012). For airborne measurements performed during the international field campaign SoRPIC (**So**lar **R**adiation and **P**hase discrimination of Arct**I**c **C**louds), Bierwirth et al. (2013) showed that accurate retrieval results can be obtained for the cloud optical thickness τ. However, due to the limitation of the instrument to wavelengths below 1000 nm a retrieval of r_{eff} was not feasible. Also, the application of the retrieval was restricted to areas of open water.

A highly variable Arctic surface albedo as observed during the VERDI campaign complicates the cloud retrieval introduced by Bierwirth et al. (2013). In fact, retrievals of cloud microphysical and optical properties using only visible wavelengths are strongly biased by a bright surface (Platnick et al., 2001, 2004; Platnick and King, 2003; Krijger et al., 2011). To overcome this limitation, near-infrared channels are introduced in the retrieval algorithms instead of the visible channel used over dark surfaces. E.g., for MODIS the $1.6\,\mu\text{m}$ band reflectance is applied as a surrogate for the traditional non-absorbing band in conjunction with a stronger absorbing 2.1 or $3.7\,\mu\text{m}$ band (Platnick et al., 2001, 2004; Platnick and King, 2003). However, an accurate separation between sea ice and open water needs to be performed before the retrieval algorithms are applied. Operational algo-

rithms such as that for MODIS use NOAA's (National Oceanic and Atmospheric Administration) microwave-derived daily 0.25° **N**ear Real-Time **I**ce and **S**now **E**xtent (NISE) dataset (Armstrong and Brodzik, 2001; Platnick and King, 2003) to identify snow- or ice-covered scenes. For the typical scale of ice floes which can be observed from aircraft, this pixel size is not sufficient. Algorithms using the resolution of the radiance measurements have to be applied.

However, even when ice and ice-free areas are perfectly separated by the retrieval algorithms, 3-D radiative effects may still affect the cloud retrieval over ice-free pixels close to the ice edge. With respect to the large temporal and spatial variability of the Arctic surface albedo as described by Lindsay and Rothrock (1994), the investigation of the 3-D effects becomes even more important. Lyapustin (2001) and Lyapustin and Kaufman (2001) investigated the impact of the strong contrast of the surface albedo between open sea and adjacent sea-ice or snow on the retrieval of Arctic cloud properties. Adjacency effects were found to reduce the apparent surface contrast by decreasing the top-of-the-atmosphere γ_λ over bright pixels and increasing the brightness of dark pixels, which becomes important for land remote-sensing applications developed for usage with both dark or bright targets.

Within the present study, the focus lies on those 3-D radiative effects that are related to the horizontal photon transport between cloud and surface due to isotropic reflection of the incident radiation on the bright sea ice. The goal is to quantify the magnitude and horizontal extent of those 3-D effects as well as their influence on cloud retrievals from the visible wavelength range with a high spatial resolution. In reality, such surface 3-D radiative effects will be combined with cloud 3-D radiative effects due to cloud inhomogeneities. However, in the case of Arctic stratus, the individual cloud 3-D effect is of minor importance. For a solar zenith angle (Θ) of 45°, Zinner et al. (2010) found that the remote sensing of stratocumulus was not biased by 3-D effects, while that of scattered cumulus was sensitive to horizontal heterogeneities. This leads to the assumption that retrievals of cloud microphysical and optical properties can be treated by 1-D simulations if the distance to ice-open water boundaries is sufficiently large. However, measurements in Arctic regions are often performed for solar zenith angles larger than 45°. In such cases, 3-D radiative effects gen-

erated by the cloud structures become important. Using plane-parallel 1-D simulations of clouds, Loeb and Davis (1996) stated that the cloud optical thickness shows a systematic shift towards larger values with increasing solar zenith angle. This dependence is still weak ($\leq 10\,\%$) for thin clouds ($\tau \leq 6$) and $\Theta \leq 63^\circ$. Grosvenor and Wood (2014) confirmed this statement. They investigated MODIS satellite retrieval biases of τ and stated that τ is fairly constant between $\Theta = 50^\circ$ and $\approx$65–70°, but then increases rapidly with an increase of over 70 % between the lowest and highest Θ.

The individual 3-D effect of heterogeneous surfaces in cloud-free situations was investigated by Jäkel et al. (2013). They quantified the effect of local surface-albedo heterogeneity and aerosol parameters on the retrieved area-averaged surface albedo from airborne upward and downward irradiance measurements. For adjacent land and sea, Jäkel et al. (2013) defined a critical distance d_c at which the retrieved area-averaged surface albedo deviates by 10 % or less from the given local surface albedo. It was found that d_c ranges in the order of 2.4 km for a flight altitude of 2 km and is larger for albedo fields with higher surface albedo contrast. In the case of clouds with an optical thickness larger than that of aerosol particles, this effect is expected to increase significantly.

In Sect. 2 we present airborne observations of γ_λ derived from imaging spectrometer measurements of upwelling radiance $I_\lambda^\uparrow$ and spectrometer measurements of downwelling irradiance $F_\lambda^\downarrow$. A robust algorithm separating sea-ice and open-water surfaces under cloud cover is introduced in Sect. 3 and applied to the measurements. Observations and simulations of the 3-D radiative effects are analyzed in Sect. 4. Similar to Jäkel et al. (2013), a critical distance from the ice edge is defined to quantify the horizontal range of the effects. For the model simulations, idealized surface albedo fields (infinitely long straight ice edge, circular ice floes of different sizes, groups of ice floes) are generated and investigated for cases of clear sky and for $\tau = 1/5/10$. Variations in cloud altitude, cloud geometrical thickness, r_eff, and surface albedo are investigated to characterize how strong these parameters influence the magnitude and distance of the γ_λ transition from high to low values. In Sect. 5 we investigate how these 3-D radiative effects bias 1-D retrievals of τ and r_eff.

2 Airborne measurements of spectral reflectivity γ_λ

The measurements used in this study were performed during the international Arctic field campaign VERDI, which took place in Inuvik, Northwest Territories, Canada, in April and May 2012. The instruments were installed on Polar 5, an aircraft used for scientific research by the Alfred Wegener Institute Helmholtz Centre for Polar and Marine Research (AWI), Bremerhaven. During VERDI, the Polar 5 was operated out of the Inuvik Mike Zubko Airport (YEV). Most flights were performed over the Beaufort Sea, partly covered by sea ice interspersed with open leads and polynias which grew bigger towards the end of the campaign.

The measurement strategy during VERDI was aimed at combining remote sensing and in situ cloud observations. Therefore, the same clouds were subsequently sampled by a set of in situ (see Klingebiel et al. (2015)) and remote-sensing instruments on board of Polar 5. The aircraft was equipped with an active and several passive remote-sensing systems. The active system was the **A**irborne **M**obile **A**erosol **Li**dar (AMALi; Stachlewska et al., 2010). It was operated in nadir viewing direction at 532 nm wavelength. Passive radiation measurements were carried out with the imaging spectrometer AisaEAGLE (manufactured by Specim Ltd. in Oulu, Finland; Schäfer et al., 2013). To analyze the 3-D radiative effects of ice edges in a cloudy atmosphere, we focus on measurements by this instrument. With 1024 spatial pixels, the single-line sensor provides a sufficiently high horizontal resolution to observe ice edges in detail. The flight altitude during the remote sensing legs was about 3 km above ground which is about 2 km above cloud top for typical boundary layer clouds with cloud top altitudes at about 1 km. For this geometry, the width of one AisaEAGLE pixel at cloud top is 3.5 m and the length is 4.2 m at an exposure time of 10 ms and a flight speed of 65 $\mathrm{m\,s^{-1}}$. Each spatial pixel consists of 488 spectral pixels to detect spectra of radiance in the wavelength range from 400 to 970 nm with 1.25 nm full width at half maximum (FWHM). AisaEAGLE converts the detected photon counts into digitalized 12-bit numbers. By applying a spectral radiometric calibration, those numbers are transformed into radiances. The calibration, data handling, and necessary corrections are described by

Schäfer et al. (2013). For radiance measurements, Schäfer et al. (2013) estimated an uncertainty of $\pm 6\,\%$. Assuming a fixed r_{eff}, those detected spectra of radiance can then be used to retrieve τ.

Further passive radiation measurements were carried out with the **S**pectral **M**odular **A**irborne **R**adiation measurement syst**e**m (SMART-Albedometer; Wendisch et al., 2001), initially designed for albedo measurements, and a Sun tracking photometer. The SMART-Albedometer is horizontally stabilized and measures up-/downwelling spectral radiance I_λ and irradiance F_λ ($\lambda = 350 - 2100\,\text{nm}$, 2-16 nm FWHM), while the Sun photometer covers aerosol optical thickness between $\lambda = 367 - 1026\,\text{nm}$. The configuration was similar to that during the aircraft campaign SoRPIC described by Bierwirth et al. (2013). Additionally, dropsondes were used at selected waypoints to sample profiles of meteorological parameters (air pressure, air temperature, relative humidity) over the whole distance between the ground and the aircraft. For a more detailed description of the airborne instruments installed on Polar 5, see Bierwirth et al. (2013), Klingebiel et al. (2015) and Wendisch and Brenguier (2013).

In this study, the data from the AMALi and the dropsondes were used to determine the cloud-top altitude and geometrical thickness, whereas the data from the SMART-Albedometer were used to verify and validate the $I_\lambda^\uparrow$ measurements of AisaEAGLE. Furthermore, the SMART-Albedometer measurements of the downwelling irradiance $F_\lambda^\downarrow$ are used to transform the AisaEAGLE radiance $I_\lambda^\uparrow$ into the nadir reflectivity γ_λ, which is derived by:

$$\gamma_\lambda(\tau, r_{\text{eff}}) = \frac{\pi \cdot I_\lambda^\uparrow(\tau, r_{\text{eff}})}{F_\lambda^\downarrow(\tau, r_{\text{eff}})}, \tag{1}$$

and is a function of r_{eff} and τ. The γ_λ presented in this paper are calculated at a wavelength of $\lambda = 645\,\text{nm}$, where scattering is dominant and shows a strong sensitivity to τ (Werner et al., 2013).

During all 15 flights of VERDI, 130 recordings (25 h, 11 min, 29 s) of cloud-top and surface reflectance were collected with AisaEAGLE. 78 % of the observation time was spent

above clouds. However, for 86 % of the cloud observations a cloud retrieval as described by Bierwirth et al. (2013) could not be applied as the surface albedo did not fulfil the constraint of being relatively dark. Either snow-covered ice almost eliminated the contrast between cloud and surface, or a mixture of ice and open water made a cloud retrieval following the strategy from Bierwirth et al. (2013) impossible. The latter occurred in 42 % of all observations and is analyzed in this paper in more detail to quantify how strong cloud retrievals are biased above such heterogeneous surfaces.

3 Identification of ice and open water

A typical scene showing a mixture of sea ice and open ocean surfaces covered by an optically thin stratus is shown in Fig. 1. Using only the visible wavelength channels of the image, no visible contrast between sea ice and cloud remains. This is why near-infrared channels are applied in MODIS cloud retrievals over sea ice. However, with AisaEAGLE the observations are limited to wavelength below 1000 nm, where the contrast is weak (compare Fig. 4) and a retrieval of τ is not possible in those areas; it can only be performed above water surfaces.

The limitation of AisaEAGLE in case of bright surfaces is illustrated in Fig. 2 showing the calculated γ_λ at 645 nm for clouds with different values of τ over a dark ocean surface (blue lines) and a bright sea-ice surface (red lines). The calculations were performed for different solar zenith angles Θ of 45°, 60°, and 75° (the range during VERDI measurements).

The upper panel shows that the separation of γ_λ for clouds of different τ above sea ice are not significant and far below the measurement uncertainties of most optical sensors. This illustrates that no physical information on the cloud optical thickness is given by γ_λ at this visible wavelength of 645 nm. Therefore, a retrieval of τ based on 645 nm reflectivity is not possible. For the same clouds placed above a dark ocean surface, γ_λ is a strong function of τ, which is the basis of the cloud retrieval following the method by Nakajima and King (1990); Bierwirth et al. (2013); Werner et al. (2013).

In order to select the dark-surface pixels for which a cloud retrieval can be attempted, a sea-ice mask has to be derived. Figure 2 clearly shows that even for optically thick clouds γ_λ is significantly larger ($\geq 25\,\%$ at $\tau = 25$ and $\Theta = 60°$) above bright sea ice than over a dark ocean surface. This gap can be used as a threshold to distinguish between measurements of clouds above the dark ocean surface and a bright sea ice surface. To define this threshold, it has to be considered that the differences between γ_λ measured above a dark ocean surface or a bright sea ice surface is smaller for larger solar zenith angles and also decreases with increasing τ (lower panel of Fig. 2). However, the differences are still significant at large solar zenith angles of $\Theta = 60°$ and $\tau = 25$ (lower panel). For VERDI, where Θ was in the range of 55° to 75° for most of the observations, the particular threshold is defined as the center value between the two simulations:

$$\gamma_{\lambda,\mathrm{thresh}} = \frac{\gamma_{\lambda,\mathrm{ice}} + \gamma_{\lambda,\mathrm{water}}}{2}. \tag{2}$$

To test this threshold, a section of a VERDI flight on 17 May 2012 (Fig. 1) was analyzed. The flight was divided into a remote-sensing leg A at 2920 m altitude (red in Fig. 1) and an in-situ leg B inside the cloud at 150 m altitude (blue in Fig. 1). The solar zenith angle was $\Theta = 58°$. τ was obtained from AisaEAGLE measurements above open water far from any ice edge using the retrieval method presented by Bierwirth et al. (2013). An average value of $\tau = 5.3 \pm 0.5$ was derived, which agrees with the MODIS level-2 product showing values for τ between 0.02 and 15.5 ($\overline{\tau} = 3.6 \pm 2.5$) in the investigated area. In that case, the simulated $\gamma_{\lambda,\mathrm{ice}} = 0.8$ and $\gamma_{\lambda,\mathrm{water}} = 0.2$ from Fig. 2 give a threshold of $\gamma_{\lambda,\mathrm{thresh}} = 0.5$.

Figure 3 shows a histogram of the measured γ_λ at 645 nm from leg A. There are two maxima with a distinct separation which correspond to measurements above bright sea ice and dark ocean. Either the minimum between the two maxima or the mean of those two most frequent values of γ_λ can be used as an alternative estimate of the threshold for the ice mask. In this particular case the threshold estimated from the frequency distribution is $\gamma_{\lambda,\mathrm{thresh}} = 0.5$, which confirms the theoretical value derived from the radiative transfer simulations.

Using those methods to estimate the threshold, ice masks were created to identify measurements of clouds above sea ice for which the cloud retrieval by Bierwirth et al. (2013) cannot be applied. Figure 4 shows three examples of γ_λ derived from the nadir radiance and zenith irradiance measurements. Figures 4a and 4b show a long ice edge, while Fig. 4c and 4d show an accumulated ice floe field, all observed on 17 May 2012 around 17:00 UTC ($\Theta = 58°$). In both cases, a cloud layer was located between the ground and the aircraft. Figures 4e and 4f show ice floes without cloud cover, observed on 14 May 2012 at 21:00 UTC. The corresponding ice masks are shown on the right panel in Fig. 4. In those images, all pixels identified as sea ice are shown as red areas.

Fig. 5 shows the frequency distributions for the three cases presented in Fig. 4 (solid black lines). All frequency distributions are normalized so that the maximum is 1. In each case, two maxima are separated by a distinct minimum which defines the ice/water threshold value. For the cloudy cases in Fig. 5a and b the dark-surface peak is broadened asymmetrically towards higher γ_λ values, while the bright-surface peak is broadened towards lower γ_λ values. For the clear-sky case in Fig. 5c, the peaks representing dark ocean and sea-ice surfaces are clearly separated.

To analyze the impact of the ice edge, frequency distributions for a selection of pixels far from the ice edge are included in Fig. 5 for each particular scene, separated into dark open-water pixels (dashed blue lines) and bright sea-ice pixels (dashed red lines). In Fig. 5a and 5b, the peaks of the selective frequency distributions are much sharper than the original peaks. For the clear-sky case in Fig. 5c, these selective frequency distributions are almost congruent with the single peaks of the entire frequency distribution. This means that in this case the ice edge has no impact on γ_λ of adjacent pixels, or in other words, there is no significant horizontal photon transport. Between the remote selected pixels and the ice edge there are many pixels where γ_λ is enhanced (over open water) or reduced (over sea ice) compared to the values at the remote pixels. This particular enhancement and reduction of the measured γ_λ is related to 3-D radiative effects in clouds and the reflection between clouds and the surface. This influence of the ice edge on the pixels' reflectivity will significantly influence cloud retrievals based on 1-D simulations in such scenes. In the following,

those 3-D effects are investigated at first only by analyzing γ_λ and then with respect to the retrieved cloud optical properties. To characterize the magnitude of the enhancement and reduction of the measured γ_λ, 3-D radiative transfer simulations are performed in Sect. 4 and are used to identify the most important parameters that control this 3-D effect. Afterwards, a 1-D cloud retrieval is performed in Sect. 5 to quantify the influence of the 3-D effects on the retrieved τ and r_{eff}.

4 3-D radiative effects of clouds near ice edges

4.1 Measurements from VERDI

Figure 6 illustrates the measured γ_λ (solid lines) and its standard deviation (dotted lines) as a function of the distance to the ice edge for the three scenes presented in Fig. 4. It shows that for the cases presented in Fig. 4b and d (red and blue in Fig. 6), close to the detected sea ice areas, narrow bright bands of enhanced γ_λ are observed, which are most likely related to 3-D radiative effects in clouds and the interaction between clouds and surface. In this study, only the latter case is considered, namely, the 3-D radiative effects related to the pathway of the photons between cloud and surface. Horizontal photon transport in the layer between surface and cloud smoothes the abrupt decrease of the surface albedo from large values above sea ice to low values above the open water. For measurements without clouds (Fig. 4f, green in Fig. 6) we could not find similar areas with enhanced γ_λ above the water close to the ice edge.

The theory explaining the 3-D radiative effect, which cause the enhancement of γ_λ, is illustrated in Fig. 7. The incident radiation ($F_0 \cdot \cos(\Theta)$) impinges on the cloud, where scattering and absorption processes take place. Part of the incident radiation is transmitted through the cloud and scattered into the direction of the ice edge (bold black arrow). Sea ice acts similar to a Lambertian reflector and reflects the incoming radiation almost uniformly in all directions (grey arrows). The reflected radiation penetrates the cloud at a certain altitude (red or blue arrows), from where parts of it are scattered into the observation direction.

Without sea ice in the vicinity of the measurements, the reflected radiance would be influenced only by the cloud and dark ocean water. The measured nadir radiance $I_\lambda^\uparrow$ above the cloud parcel is enhanced due to the additional radiation reflected from the sea ice into the direction of the last scattering point in the cloud. This effect is significant only for cloudy cases, because of the weak scattering efficiency of the clear atmosphere compared to that of clouds. If we compare the 3-D effect for clouds of different altitude (Fig. 7), the horizontal photon path of the reflected radiation is extended (compare for cloud A (red) and cloud B (blue)). Hence, the range of the 3-D effect increases with cloud altitude.

For the case of the straight ice edge (Fig. 4a), the distances presented here are almost in line with the flight track which was perpendicular to the ice edge. The spatial range of 1400 m perpendicular to the ice edge corresponds to 1418 m distance along the flight track. With a frame rate of 30 Hz and an aircraft speed of 65 m s^{-1} this results in 700 measurements along the 1418 m for each of the 1024 spatial pixels. This large amount of data provides good statistics for the mean γ_λ illustrated as a solid red line in Fig. 6. In general, γ_λ decreases by about two thirds from $\gamma_\lambda = 0.75$ above bright sea ice to about $\gamma_\lambda = 0.25$ above dark ocean surface. For scene (a) and (b) the decrease does not occur sharply at the ice edge, but gradually starts at about 400 m distance from the ice edge and ends at 400 m distance from the ice edge over open water. In the cloud-free case, the asymptotic values above sea ice and water are reached much closer to the ice edge at about 50 m.

Over the water-covered area, an enhancement of γ_λ was measured close to the ice edge; while over the ice-covered area, γ_λ is reduced near the ice edge. We define two distances measured from the ice edge to quantify the enhancement effect. The first distance ΔL_{HPT} is introduced to quantify the range of horizontal photon transport. It characterizes the distance at which the transition from high $\gamma_{\lambda,\mathsf{ice}}$ to low $\gamma_{\lambda,\mathsf{water}}$ is $1/e^3$ of the initial difference between the mean γ_λ above ice ($\overline{\gamma}_{\lambda,\mathsf{ice}}$) and the mean γ_λ above open water ($\overline{\gamma}_{\lambda,\mathsf{water}}$):

$$\gamma_{\lambda,\mathsf{water}}(\Delta L_{\mathsf{HPT}}) = \overline{\gamma}_{\lambda,\mathsf{water}} + \frac{1}{e^3} \cdot \Delta\mathsf{IPA}, \tag{3}$$

with $\Delta\mathsf{IPA} = \overline{\gamma}_{\lambda,\mathsf{ice}} - \overline{\gamma}_{\lambda,\mathsf{water}}$. By including $\Delta\mathsf{IPA}$, ΔL_{HPT} quantifies the range of horizontal photon transport independent on the difference of the surface albedo contrast. For the

scene from Fig. 4a, ΔL_{HPT} indicated by the enhancement of γ_λ over the water surface extends to a distance of 200 m from the ice edge.

Furthermore, a second distance to the ice edge ΔL is defined for which $\gamma_{\lambda,\mathrm{water}}$ is enhanced by 6 % of the average γ_λ above open water.

$$\gamma_{\lambda,\mathrm{water}}(\Delta L) = \overline{\gamma}_{\lambda,\mathrm{water}} + 0.06 \cdot \overline{\gamma}_{\lambda,\mathrm{water}}. \quad (4)$$

The choice of the threshold results from the radiance measurement uncertainty (± 6 %) of the imaging spectrometer AisaEAGLE. Using this definition, ΔL is independent of γ_λ measured above the ice surface. It only accounts for the significance of the enhancement with respect to the measurement uncertainty. If the enhancement is higher than the measurement uncertainty, a cloud retrieval might be significantly biased when using the contaminated measurements. Therefore, ΔL is a measure for the horizontal extent within which the 3-D effects bias the cloud retrieval in the vicinity of an ice edge. For the special case of the measured γ_λ in Fig. 6, the $\Delta L = 300$ m. Above open water, all measurements within that transition zone cannot be used for the cloud retrieval as the enhanced γ_λ will positively bias the retrieved τ.

For the isolated ice floes of Fig. 4c, the values of the averaged γ_λ (solid blue line) in Fig. 6 are comparable to the values from the scenario in Fig. 4a. Furthermore, Fig. 6 shows a similar analysis (solid green line) for the cloud-free scenario on 14 May 2012 (Fig. 4f). Here, the decrease of γ_λ at the ice edge is significantly sharper than for the cloud-covered scenes. This indicates that in the cloudy scenes horizontal photon transport is taking place in the layer between the bright surface and cloud base, leading to a smoother transition between bright sea ice and dark ocean water.

4.2 Model studies

To better quantify the observations of 3-D radiative effects at ice edges, we applied a 3-D radiative transfer model. The simulations are used to determine ΔL and ΔL_{HPT} as a function of different cloud properties. We expect that the interaction between clouds and sea-ice surface varies with varying τ, geometrical thickness, and cloud altitude. Furthermore, the

simulations are used to clarify whether these 3-D radiative effects result in an enhancement of the mean γ_λ for a certain area or if the enhancement is, on average, counterbalanced by the decrease of γ_λ above the sea ice. Different idealized sea-ice geometries are studied to investigate the horizontal pattern and average of the 3-D effects.

The radiative transfer simulations of the upwelling radiance $I_\lambda^\uparrow$ and downwelling irradiance $F_\lambda^\downarrow$ to derive γ_λ are performed with the open-source **M**onte **C**arlo **A**tmospheric **Ra**diative **T**ransfer **S**imulator (MCARaTS) which is a forward-propagating Monte Carlo photon-transport model (Iwabuchi, 2006; Iwabuchi and Kobayashi, 2008). It traces individual photons on their path through the 3-D atmosphere. To reduce the computational effort for radiance simulations, MCARaTS uses several variance-reduction techniques, such as a modified local-estimate method or a truncation approximation for highly anisotropic phase functions (Iwabuchi, 2006). The input to the radiative transfer model contains the optical properties of atmospheric contributions such as clouds and trace gases (e.g., extinction coefficients, single-scattering albedos, phase functions) and the 2-D surface albedo. The model requires a predefined albedo field. For this purpose we create a field of 20 000 m by 20 000 m with a pixel size of 50 m by 50 m (400 pixels in both horizontal dimensions). Depending on the given sea-ice distribution, the albedo of individual pixels is set to sea-ice albedo (0.910 at 645 nm; Bowker et al., 1985) or water albedo (0.042 at 645 nm; Bowker et al., 1985). The pixel size of the 3-D model is about ten times larger than that of AisaEAGLE. However, model results and measurements are still comparable as the investigated 3-D effects occur in the range of a few hundred meters on either side of the ice edge. Accordingly, the AisaEAGLE data is averaged for comparing the model results with the measurements. 2.2×10^9 photons were used in each single model run, which resulted in a noise level of the 3-D simulations of less than 1 %. This value is much lower than the measurement uncertainties of AisaEAGLE.

Other input parameters for the model are adapted to the measurement conditions on 17 May 2012 around 17:00 UTC with a solar zenith angle of 58° and the solar azimuth angle of 113°. The extraterrestrial solar spectrum was taken from Gueymard (2004). The output altitude for $I_\lambda^\uparrow$ and $F_\lambda^\downarrow$ is 2920 m (10 000 ft flight altitude). To represent the observed clouds in an

idealized way, a horizontally and vertically homogeneous liquid water cloud was assumed between 0 and 200 m altitude. Besides reference simulations for clear-sky conditions, the cloud optical thickness was varied between $\tau = 1$ and $\tau = 10$ as observed by MODIS in the surroundings of the measurement area. Based on the observations, the effective radius of the liquid water droplets was set to $r_{\text{eff}} = 15\,\mu\text{m}$. The microphysical properties of the liquid water clouds are converted to optical properties by Mie calculations. Furthermore, profiles of the atmospheric pressure, temperature, density, and gases are taken from profiles given by Anderson et al. (1986). Gas absorption was modelled by LOWTRAN (**Low** Resolution **Tran**smission Model parametrization, Pierluissi and Peng, 1985), as adapted from SBDART (**S**anta **B**arbara **D**ISORT **A**tmospheric **R**adiative **T**ransfer, Ricchiazzi and Gautier, 1998).

Additionally, 1-D simulations which use the independent pixel approximation (IPA) are applied to the particular cases. The IPA simulations were performed with the same 3-D model, but with a homogeneous surface albedo – either dark ocean water or bright sea ice. All other parameters remain the same as in the 3-D simulations.

4.2.1 Infinitely straight ice edge

The most general case of an ice edge is an infinitely straight ice edge. This case is comparable to Fig. 4a. Fig. 8 illustrates the results of the 1-D (grey lines) and 3-D (black lines) simulations. Similar to the observations, γ_λ from the 3-D simulations decreases above the bright sea ice, and increases above the dark ocean surface. The effect is larger the closer the pixel is located to the ice edge. In the clear-sky simulations this effect is small; 3-D and IPA simulations are almost identical. This indicates that the 3-D effect is dominated by horizontal photon transport between sea ice and clouds and the scattering processes by the cloud particles into the nadir observation direction. Without clouds, the horizontal photon transport above the isotropically reflecting surface is of similar magnitude to the cloudy case. However, due to the weak scattering in the clear atmosphere compared to the scattering by cloud particles, this effect is only significant for cloudy cases. Similar investigations are presented by Marshak et al. (2008) with respect to aerosol-cloud interactions. In the vicinity of clouds, they found that the radiance in cloud-free columns is increased due to

a cloud-induced enhancement of the Rayleigh scattering. In general, Fig. 8 shows that with increasing τ the slope of the decrease of γ_λ next to the ice edge is flattened. This is a result of the reduction in contrast between the dark ocean surface and bright sea ice surface by the overlying clouds.

To compare the results with the measurement example in Fig. 6, the distance ΔL_{HPT} defined by Eq. (3) is analyzed. $\overline{\gamma}_{\lambda,\mathsf{water}}$ is set to the IPA values above water. For the cases presented in Fig. 8, ΔL_{HPT} increases with increasing τ from 100 m at $\tau = 1$ to 250 m at $\tau = 5$ and to 300 m at $\tau = 10$. This shows that the horizontal photon transport increases with τ due to increased scattering inside the cloud layer.

In contrast to ΔL_{HPT}, the distance ΔL defined by Eq. (4) decreases from 600 m (at $\tau = 1.0$) to 400 m (at $\tau = 5.0$) and to 250 m (at $\tau = 10.0$). The decrease of ΔL suggests that the area in which γ_λ is enhanced and a cloud retrieval might be biased is smaller for optically thick clouds. This is related to the decrease in contrast between cloud covered sea ice and cloud covered ocean if τ increases. The difference Δ(IPA) between $\gamma_{\lambda,\mathsf{ice}}$ and $\gamma_{\lambda,\mathsf{water}}$ decreases from $\gamma_\lambda = 0.87$ for the clear-sky case to $\gamma_\lambda = 0.44$ for $\tau = 10$, mainly due to the increasing reflection of incoming radiation by the cloud. If τ increases, $\gamma_{\lambda,\mathsf{water}}$ increases which results in a higher uncertainty range exceeding the γ_λ enhancement also in areas closer to the ice edge. Therefore, the γ_λ enhancement becomes less significant for a cloud retrieval compared to the measurement uncertainties. Since we aim to retrieve τ above water areas enclosed by ice floes, in the following ΔL is used to quantify the 3-D effects.

Additionally, the sensitivity of the results to the assumption of a constant r_{eff} was analyzed by running simulations with an r_{eff} of 10, 15, 20, and 30 µm (not shown here). The results showed that ΔL is almost independent of r_{eff}. This indicates that a variation of r_{eff} does not need to be considered when estimating the 3-D radiative effects described here.

Furthermore, simulations with varied values of the surface albedo were performed (not shown). Based on the measurement uncertainty of AisaEAGLE, the surface albedo of the dark ocean water and bright sea ice was varied by $\pm 6\,\%$. Over the dark ocean area, the simulations show almost identical results with differences far below 1 % in γ_λ. Compared

to the measurement uncertainties, those differences in the surface albedo are of less significance for ΔL. Indeed, the albedo has a larger effect over the sea-ice surface (up to 10 %) due to changing the albedo value relative with 6 %, which corresponds to an absolute change of ± 0.05 compared to 0.002 absolute change for the water surface. For the investigations presented here, the effect over the dark ocean area is relevant only.

Other important aspects which influence the results are the cloud altitude and cloud geometrical thickness. The horizontal photon transport resulting from the horizontal displacement of the location where a photon is isotropically scattered at the surface and the location in the cloud where it is scattered afterwards into the viewing direction, changes if the cloud geometry changes. Figure 9 shows the simulated γ_λ for clouds of different altitude (Fig. 9a) and clouds of different geometrical thickness (Fig. 9b). Increasing the cloud base of a cloud with a geometrical thickness of 500 m and $\tau = 1$ from $h_{\text{cloud}} = 0$ m to $h_{\text{cloud}} = 1500$ m, ΔL increases from 1000 m to 4000 m. For $\tau = 5$ ΔL increases from 800 m to 3200 m. Similarly, ΔL increases with increasing geometrical thickness. For $\tau = 1$, ΔL increases from 500 m to 2200 m when the cloud geometrical thickness changes from 200 m to 1500 m. For $\tau = 5$, ΔL increases from 300 m to 2000 m. Compared to the influence of τ, the cloud altitude and cloud geometrical thickness have a similar impact on ΔL and cannot be neglected.

For two model clouds with a geometrical thickness of 500 m and values of $\tau = 1$ and $\tau = 5$, Fig. 10a shows ΔL as a function of the cloud base altitude h_{cloud}. Similarly, Fig. 10b shows ΔL as a function of the cloud geometrical thickness Δh_{cloud} for low-level clouds with $\tau = 1$ and $\tau = 5$ and cloud base at 0 m. The increase of ΔL with increasing altitude of the cloud base (Fig. 10a) follows an almost linear function and can be parameterized by

$$\Delta L(h_{\text{cloud}}, \tau) = A(\tau) \cdot h_{\text{cloud}} + B(\tau). \quad (5)$$

For the parameters $A(\tau)$ and $B(\tau)$, the linear regression yields $A(\tau) = 2.00/1.6$ and $B(\tau) = 1000$ m/800 m for clouds with $\tau = 1/5$. This shows that the influence on ΔL is much larger for clouds at higher altitudes and lower τ. Comparing the results for $\tau = 1$ and $\tau = 5$ indicates that the slope A decreases with increasing τ. This proves that the influence of cloud geometry on ΔL is decreasing with increasing τ.

Similarly, ΔL increases almost linearly with increasing cloud geometrical thickness Δh_{cloud}. This relation can be parameterized by

$$\Delta L(\Delta h_{\text{cloud}}, \tau) = A(\tau) \cdot \Delta h_{\text{cloud}} + B(\tau). \quad (6)$$

The regression of the increase of ΔL with increasing cloud geometrical thickness yield $A(\tau) = 1.3/1.3$ and $B(\tau) = 300\,\text{m}/100\,\text{m}$ for clouds with $\tau = 1/5$.

The cloud bases of all boundary layer clouds observed during VERDI ranged between 0 and 650 m which is in agreement with the climatology presented by Shupe et al. (2011). To demonstrate the potential effects of clouds with higher cloud base, the following simulations cover two clouds, one similar to the observed cases from Fig. 4a–d ($h_{\text{cloud}} = 0$–200) m and one with cloud base at 500 m and cloud top at 1000 m.

4.2.2 Single circular ice floes

An infinitely straight ice edge as discussed in Sect. 4.2.1 does not represent reality in all aspects. Scattered ice floes of different size are often observed (see Fig. 4c). In this case, we expect a reduced 3-D effect above open water due to the curvature of the ice edge.

To analyze and quantify this reduction of 3-D radiative effects, we simulated single circular ice floes of different sizes. The radius of the circular ice floe was varied from 100 to 1000 m in steps of 100 m and from 1 to 9 km in steps of 1 km. The center of the circular ice floe was placed in the middle of the model domain. For reasons of symmetry, a cross section through the center of the model domain was used for the data evaluation. Figure 11 shows the influence of the ice-floe size on ΔL.

As expected, ΔL is lower for small ice floes than for the infinitely ice edge simulated in Sect. 4.2.1. For all simulated τ, ΔL increases with an increasing radius of the ice floe, asymptotically reaching a maximum value which is identical to the results of the infinitely ice edge ($r = \infty$). This shows that all ice floes larger than about 6 km can be treated like the infinitely straight ice edge (for the given cloud and observation geometry).

The reduction of ΔL for smaller ice floes can be explained by two effects. For ice floes with radii smaller than the distance ΔL of the infinitely straight ice edge, $r_{\text{floe}} < \Delta L(\tau)$, the

size of the ice area is too small for the γ_λ above the ice to reach the IPA γ_λ at any place. All areas of the ice floe are affected by 3-D effects. On the other hand, the area of the ice floe is too small to fully affect the adjacent water area. The water area behind the ice floe limits its effect. For ice floes with a radius larger than ΔL, the IPA γ_λ will be reached at some point on the ice floe. Only the curvature of the floe reduces the 3-D effect above open water. For any water point near the ice edge, the ice area located close to this point is reduced with increasing curvature. The curvature affects both small and large ice floes and lowers the 3-D radiative effects slightly until the maximum effect, which is reached for an infinitely straight ice edge.

Combining these two effects and assuming an exponential relationship between ΔL and the ice flow size r_{floe}, we parameterized the results presented in Fig. 11 by

$$\Delta L = \frac{2}{3} \cdot \Delta L_{\max}(\tau) \cdot \left[1 - \exp\left(-\frac{r_{\text{floe}}^2}{C^2}\right)\right] + \frac{1}{3} \cdot \Delta L_{\max}(\tau) \cdot \left[1 - \exp\left(-\frac{r_{\text{floe}}}{\Delta L_{\max}(\tau)}\right)\right]. \quad (7)$$

The distances for the infinitely straight ice edge, $\Delta L_{\max}(\tau)$, are taken from Sect. 4.2.1. For the exponential parameter C, the fit yields $C = 1000\,\text{m}$ for clouds with $\tau = 1/5/10$. The parametrization is valid for ice floes with radii r_{floe} larger than 300 m. For those ice floes the uncertainty is less than 5 %. For ice floes with radii r_{floe} less than 300 m, the uncertainty increases rapidly and reaches up to 100 %. This is due to the insufficient representation of the circular shape of the small ice floes by squared pixels with 50 m edge length.

4.2.3 Groups of ice floes

To get closer to reality, we have to consider ice floes of different sizes creating an irregular mixture of ice and water surfaces. In this case, the size of the ice floes, their shape and the distance to each other influence the described 3-D effects. To address these more complex cases, we ran four simulations with the same model setup as in Sects. 4.2.1 and 4.2.2, but changed the shape and the number of the ice floes. In total, four scenarios with ice floes represented by squares (total sea-ice area A_{x}, total ice edge length l_{x}) were investigated to quantify the influence of A_{x} and l_{x} on the 3-D effects.

In Scenario 1, which serves as a reference, an ice floe with a size of 5 km by 5 km ($A_1 = 25\,\text{km}^2$, $l_1 = 20\,\text{km}$) was placed in the center of the model domain. For Scenario 2, the total sea-ice area was conserved ($A_2 = A_1 = 25\,\text{km}^2$) and the total ice edge length doubled ($l_2 = 2 \cdot l_1 = 40\,\text{km}$). This was realized by four smaller ice floes (2.5 km by 2.5 km), separated by a distance of 5 km from each other. Scenario 3 simulates two small ice floes (2.5 km by 2.5 km) for which the total ice edge length has been conserved ($A_3 = 0.5 \cdot A_1 = 12.5\,\text{km}^2$, $l_3 = l_1 = 20\,\text{km}$). Scenario 4 was designed to investigate the effect of the distance between the single ice floes. The two ice floes of Scenario 3 ($A_4 = 0.5 \cdot A_1 = 12.5\,\text{km}^2$, $l_4 = l_1 = 20\,\text{km}$) were copied, but placed next to each other.

To highlight the 3-D radiative effects, the ratios $R_{\text{3-D/IPA}}$ of the 3-D and IPA results are calculated. If both simulations are equal, the ratio is $R_{\text{3-D/IPA}} = 1$. Compared to the IPA simulations, a ratio of $R_{\text{3-D/IPA}} > 1$ represents an enhancement of γ_λ. Table 1 lists $R_{\text{3-D/IPA}}$ for all simulated τ and h_{cloud}. Figure 12 displays the $R_{\text{3-D/IPA}}$ for a cloud with $\tau = 5$ at $h_{\text{cloud}} =$ 500–1000 m, since the 3-D effects are more evident for larger τ and higher cloud altitudes. Yet, the overall 3-D effect is relatively small with $R_{\text{3-D/IPA}}$ ranging from 96.5 to 98.4 %, but is still significantly above the noise level of the 3-D simulations. The small values are caused by the large model domain and the relatively small ice fraction. Most pixels are ice-free and at a distance to the ice floes where 3-D effects are negligible.

As expected, in each scenario the contrast at the ice floe boundaries is reduced by the 3-D effects. To quantify the 3-D radiative effect in the entire model domain, average and standard deviations (SD) of γ_λ are calculated (not listed). The average γ_λ is largest for Scenario 1 and smallest for Scenarios 3 and 4. This is not surprising since the area of the ice floes in Scenario 3 and 4 is half the area of the reference scenario. In all scenarios, evidence of the 3-D radiative effect is found in a slight reduction of the average γ_λ ($R_{\text{total}} < 1$). This reduction originates from the absorption of the radiation, which is scattered by the cloud base back into the direction of the dark ocean surface. This part of absorption does not exist in the IPA simulations, which in comparison leads to a lower scene average reflection in the 3-D simulations. The SDs in the 3-D simulations are also lower than in the IPA results, which corresponds to the smoothing at the ice edges.

In Scenarios 1–3, the individual ice floes do not affect each other, as the distance between them is too large. Here, similar 3-D effects are observed. The corners of the ice floes are smoothed out and the γ_λ field around the ice floe becomes more circular. This results in larger ΔL values at the center of the ice edges and in smaller ΔL values close to the corners. For the large ice floe of Scenario 1, $\Delta L = 1400\,\mathrm{m}$ at the center of each side. In agreement with Fig. 11, ΔL for the small ice floes in Scenario 2 and 3 is smaller (1200 m). Along the normal line of the corners, ΔL is reduced to 900 m for Scenario 1 and 700 m for Scenario 2 and 3. In Scenario 4, the ice floes cause a different pattern close to their point of contact. Here, ΔL is largest measured tangential to the connected corners and reaches 2000 m as the 3-D radiative effects of both floes add up for these points.

In addition, Fig. 13 shows frequency distributions of γ_λ for the four scenarios. Since the clouds in the simulations are homogeneous, the γ_λ in areas unaffected by 3-D effects are identical to the γ_λ from the IPA simulation. For the open-water pixels, this causes a single peak at $\gamma_\lambda(\tau = 5) = 0.24$. For pixels above ice, no single peak corresponding to the IPA $\gamma_\lambda(\tau = 5) = 0.84$ is observed. This is due to the small size of the ice floes, above which the IPA γ_λ is not reached. All γ_λ values that are not included in the single water peak result from the 3-D effects. Above ice, the distributions of Scenarios 2–4 are shifted to lower γ_λ compared to Scenario 1. This is because the diameter of the floes is even smaller than in Scenario 1. Thus, the large reflectivity values of Scenario 1 cannot be reached by Scenarios 2–4 (compare Fig. 11). Comparing the frequency distribution of Scenarios 1 and 2, Fig. 13a reveals the effect of the increased ice edge length in Scenario 2. More pixels are affected by 3-D effects and show values different from IPA. Furthermore, with four times the number of corners in Scenario 2, γ_λ above water is slightly shifted to lower values compared to the reference case. Similar effects can be observed in Scenario 3. In Scenario 4, the combined effect of both floes leads to larger enhancements above ocean water than in Scenarios 2 and 3.

In order to identify the relevant effects, we separately calculated the ratios $R_{\text{3-D/IPA}}$ for ice-free (R_{water}) and ice-covered (R_{ice}) areas (Tab. 1). The reduction of γ_λ above ice is much larger ($R_{\text{ice}} = 82$–$88\,\%$) than the enhancement above water ($R_{\text{water}} = 107$–$113\,\%$), which

again is partly a result of the larger water area. But also the small size of the ice floes leads to the stronger effects above sea ice, as the IPA γ_λ is never reached. Interestingly, with increasing τ, the deviations from IPA increase for the ice area but decrease for the dark ocean area. This effect is related to the asymmetry of enhancement and reduction for clouds of high τ, as shown in Fig. 8.

The average reduction over sea–ice areas (R_{ice}) is largest for Scenario 1. For all other scenarios, smaller values are obtained, with Scenarios 2 and 3 showing values identical to each other. This indicates that the particular distance between the ice floes in Scenarios 2 and 3 is large enough to suppress any influence of the single ice floes on each other. Contrarily, Scenario 4 gives the second largest R_{ice}. Compared to Scenario 1 and Scenario 3, this confirms that the distance between the ice floes can have a significant influence on the enhancement of γ_λ over dark ocean water in the vicinity of ice edges.

R_{water} is almost equal for Scenarios 1 and 3, although the ice-covered area differs by a factor of two. For Scenario 2, with a doubled ice boundary length, this ratio is significantly larger. This leads to the conclusion that the ice boundary length has a significantly larger effect on the enhancement of γ_λ (over the water next to an ice edge) than the size of the area covered by sea ice.

4.2.4 Realistic sea-ice scenario

In order to combine all aspects of the 3-D effects demonstrated before, γ_λ was simulated above an albedo field generated from the observation shown in Fig. 4c. To simulate ice floes in the same size range as for the measurements, the pixel size of the albedo map was adjusted to the pixel number and size of the AisaEAGLE measurements (488 by 601 pixels with 5 m edge length).

The albedo map was used in the simulations implementing a cloud of $\tau = 5$ and a fixed $r_{\text{eff}} = 15\,\mu\text{m}$, as derived from in situ measurements. With regard to the AMALi measurements, the cloud top altitude was set to $h_{\text{cloud, top}} = 200\,\text{m}$. Compared to the simulations shown before, the best agreement between measurement and simulation is derived for this specific case for a cloud base altitude of $h_{\text{cloud, base}} = 100\,\text{m}$ and a slightly adjusted surface

albedo ($\alpha_{\text{water}} = 0.09$, $\alpha_{\text{ice}} = 0.83$). Fig. 14 shows the frequency distributions of simulated and observed γ_λ. Comparing observation and simulation, the maximum of the ocean-water and sea-ice peak are found at equal γ_λ. In regions over dark ocean water as well as in regions over bright sea ice, the γ_λ of the observation show a broader distribution than the γ_λ of the simulation. Indeed, the magnitude of the simulated γ_λ peak above the sea-ice surface agrees well with the peak from the observation, while the difference above the dark ocean water is significantly larger. The different magnitude and the broader distribution of the observed single peaks compared to the simulation result most likely from simplifications in the simulations where a horizontally homogeneous cloud is assumed. Thus, variations of γ_λ due to cloud 3-D effects are not included here. Only the surface 3-D effects cause a broadening of the frequency distribution. However, while surface effects will fill up the gap between the two peaks only, cloud inhomogeneities can also result in values smaller (over water) and higher (over sea ice) than the IPA simulations.

In addition to the results from the idealized scenarios in Sect. 4.2.3, Table 1 shows the ratios $R_{\text{3-D/IPA}}$ between the results of the 3-D and IPA simulation for the realistic sea-ice scenario. Compared to the idealized scenarios in Sect. 4.2.3, for the realistic sea-ice scenario the differences between the IPA and 3-D simulations are larger above dark ocean water and smaller above bright sea ice. This behaviour is related to the larger sea-ice fraction in the realistic sea-ice distribution, where water pixels are surrounded by more ice area compared to the isolated sea-ice floes of Sect. 4.2.3. On the one hand, it shows that the main characteristics of the ice-edge induced 3-D radiative effects in clouds can be studied by using idealized surface albedo fields. On the other hand, in case of a real sea-ice distribution from measurements, it is also necessary to consider the real surface-albedo distribution for deriving ΔL and the overestimation in the retrieved τ and r_{eff}. No fixed values for ΔL and the overestimation can be given as a function of τ and cloud altitude alone. The surface-albedo distribution plays a major role as well and has to be known.

5 Retrieval of cloud optical thickness τ and effective radius r_{eff}

All simulations in Sect. 4.2 showed that γ_λ over open water areas close to sea ice can be enhanced drastically if clouds are present. For a cloud retrieval following the strategy by Bierwirth et al. (2013), this enhancement suggests that τ will be overestimated in this area when a surface albedo of water is assumed. To quantify the magnitude of this overestimation, a synthetic cloud retrieval is investigated. The retrieval is based on simulations only in order to investigate also the uncertainties of retrieved r_{eff}, which cannot be derived from the current setup of AisaEAGLE measurements during VERDI. The limitation of AisaEAGLE to visible wavelengths restricts the retrieval to τ (Bierwirth et al., 2013). However, near-infrared measurements might be available by use of additional imaging spectrometers such as the AisaHAWK. Therefore, this study addresses both quantities τ and r_{eff}. To do so, the retrieval based on forward simulations is applied to the γ_λ field of a 3-D simulation where the cloud optical properties are known exactly. To study a simple case, in the 3-D simulation an isolated ice floe with a radius of 6 km (Sect. 4.2.2) was chosen and a homogeneous cloud with $\tau = 10$ and $r_{\text{eff}} = 15\,\mu\text{m}$ was placed above it at an altitude of 500 to 1000 m. With a radius of 6 km the ice floe has an effect similar to that of an infinitely straight ice edge which leads to the maximum range of 3-D effects with the largest ΔL (see Fig. 11). The retrieval is only performed over the dark ocean surface. The forward simulations of the γ_λ look-up table are based on 1-D simulations. τ and r_{eff} are varied in the range of 1–25 and 10–25 µm, respectively; see Fig. 15. The retrieval grid is constructed from the simulated γ_λ at 645 nm wavelength on the abscissa and the ratio of γ_λ at 1525 and 579 nm wavelength on the ordinate. This wavelength and the wavelength ratio was chosen in order to improve the retrieval method by Bierwirth et al. (2013). The choice of wavelength follows the method presented by Werner et al. (2013). This method creates a retrieval grid with a more separated solution space for τ and r_{eff} than the classic two-wavelength method by Nakajima and King (1990) or Bierwirth et al. (2013). Furthermore, it effectively corrects the retrieval results for the influence of overlying cirrus and reduces the retrieval error for τ and r_{eff} caused by calibration uncertainties (Werner et al., 2013). For airborne investigations of

τ and r_{eff} with large spatial coverage and high spatial resolution, this will result in a higher accuracy of the retrieved cloud properties.

The γ_λ of the 3-D simulation is plotted in Fig. 15 as dots colour-coded with the distance to the ice edge. The exact result of a cloud with $\tau = 10$ and $r_{\text{eff}} = 15\,\mu\text{m}$ is marked with a black cross. The results imply a significant overestimation of τ and r_{eff} at distances below 2 km from the ice edge (dark blue dots). The overestimation increases with decreasing distance to the ice edge. As expected, for distances larger than 2 km from the ice edge (light blue to red dots) the γ_λ is close to the IPA value (black cross). Small deviations are results of noise in the 3-D simulations. For the range below $\Delta L = 2\,\text{km}$, the mean τ and r_{eff} (solid lines) and their standard deviation (dotted lines) derived from the retrieval are shown as a function of the distance to the ice edge in Fig. 16.

The graph shows that the overestimation of τ increases up to 90 % while r_{eff} is biased by up to 30 % close to the ice edge. Both values are valid only for the cloud used in the simulations ($\tau = 10$ and $r_{\text{eff}} = 15\,\mu\text{m}$). For a lower τ, the effect will be lower. Furthermore, Fig. 16 shows that the overestimation of τ increases approximately exponentially starting at about 1.5 km distance, while the overestimation of r_{eff} increases more slowly and only extends up to a distance of 1.0 km. This indicates that the magnitude of the 3-D effects depends on the wavelengths. In all simulations shown in Sect. 4.2, a wavelength of 645 nm was used for the retrieval of τ. However, the retrieval of r_{eff} also requires simulations at 1 525 nm in the absorption band of liquid water. Therefore, the smaller magnitude and horizontal extent of the overestimation of r_{eff} compared to the magnitude and horizontal extent of the overestimation of τ suggest that the 3-D effects will be smaller at absorbing wavelengths.

6 Summary and conclusions

During the international field campaign VERDI, airborne measurements of γ_λ were performed with the imaging spectrometer AisaEAGLE and the SMART-Albedometer spectrometer system. In particular, measurements above clouds in situations with heterogeneous surface albedo were analyzed in order to retrieve τ. Due to the high contrast in the sur-

face albedo of sea ice and open water, the data showed a distinct difference between γ_λ above water and sea ice surfaces. This transition was used to distinguish between areas of both surfaces. Threshold γ_λ values derived from both measurements and radiative transfer simulations are in good agreement and were found to be robust for the separation of the surfaces.

In the vicinity of the separated ice edges, we found that γ_λ is reduced/enhanced above the bright sea ice/dark ocean surface. This is related to 3-D effects, which result from isotropic reflection on the bright sea ice. This reflection causes horizontal photon transport, before the radiation is scattered by cloud particles into the direction of observation. With focus on the applicability of a cloud retrieval in such areas of open water close to ice floes, this 3-D radiative effect was quantified using γ_λ measurements from the VERDI campaign and 3-D radiative transfer simulations performed with MCARaTS for a clear-sky case and clouds of $\tau = 1/5/10$ located above various surface albedo fields. Two distances ΔL_{HPT} and ΔL were defined to characterize the extent of the horizontal photon transport (ΔL_{HPT}) and to estimate the distance to the ice edge within which the retrieval of τ and r_{eff} is biased by the 3-D effects stronger than by measurement uncertainties (ΔL).

From the two measurement cases presented here ($\tau = 5$, $h_{\text{cloud}} = 0$–200 m), a distance ΔL of 400 m was observed. Radiative transfer simulations, adapted to the observed cloud and sea-ice situation, confirmed this value. For the case of the infinitely straight ice edge, a distance $\Delta L_{\text{HPT}} = 100$ m/250 m/300 m was found for $\tau = 1/5/10$. The increase of ΔL_{HPT} shows that the horizontal photon transport is increasing with increasing τ. However, the minimum distance ΔL to the ice edge, where a 1-D cloud retrieval can be applied is decreasing with increasing τ ($\Delta L = 600$ m/400 m/250 m at $\tau = 1/5/10$) due to the stronger impact of measurement uncertainties in case of thicker clouds (higher γ_λ).

Furthermore, it was found that variations in r_{eff} do not have to be considered. The simulations did not show significant differences of ΔL_{HPT} and ΔL assuming various r_{eff} between 10–30 µm. Besides cloud properties, the influence of the magnitude of the albedo contrast was tested. Varying the simulated surface albedo of the bright sea ice and dark ocean water by $\pm 6\,\%$, ΔL_{HPT} and ΔL were found to vary less by $< 1\,\%$ which is less than the given

measurement uncertainty of 6 %. This indicates that ΔL_{HPT} and ΔL are a robust measures to quantify the horizontal extent of the 3-D radiative effect at various albedo contrasts and can be applied as well for e.g. albedo contrast in regions with heterogeneous distributions of forest and deforested areas.

The cloud altitude and cloud geometrical thickness were found to be parameters significantly influencing ΔL. The distance ΔL increases linearly with an increasing cloud base altitude (for $\tau = 5$ from 800 to 3200 m for a 500 m thick cloud with cloud base at 0 m and 1500 m). The same increase of ΔL holds for an increasing cloud geometrical thickness (for $\tau = 5$ from 300 to 2000 m for a 200 m and 1500 m thick cloud). Therefore, the cloud base altitude and cloud geometrical thickness have to be known exactly while performing 3-D radiative transfer simulations of clouds above ice edges.

The size of the individual ice floe has an influence on ΔL, which increases with an increasing radius of the ice floe, until it asymptotically reaches a maximum value ($\Delta L =$ 2200 m/1500 m/1250 m for $\tau =$ 1/5/10, $h_{\mathrm{cloud}} =$ 500–1000 m, and $r_{\mathrm{floe}} \geq 6$ km).

To investigate any changes in the 3-D radiative effect due to changes in the ice-edge boundary length or sea-ice area, area-averaged γ_λ were calculated for different idealized cases of sea-ice distributions. A larger enhancement of the area-averaged γ_λ was found for longer ice edge lengths. Changes in the sea-ice area are of less importance. Placing the ice floes directly next to each other, an enhancement of the area-averaged γ_λ was found as well, although the sea-ice area and ice-edge length remained the same.

For the direct comparison of simulation and measurement, a realistic ice floe field was modelled. The frequency distributions of observations and simulations agree within the measurement uncertainties. However, the area-averaged γ_λ showed stronger 3-D effects for the real case compared to the idealized cases simulated before. This indicates that an exact quantification of the appearing 3-D radiative effects in clouds above ice edges can only be derived by simulations if realistic surface albedo fields are applied. However, a parameterization of the influence of individual parameters is only possible by using such simplified surface albedo fields.

The results from the simulations suggest that applying a 1-D cloud retrieval to airborne measurements over ocean areas located close to sea ice edges, τ and r_{eff} will be further overestimated the closer the pixel is located to the ice edge. This overestimation was calculated for a liquid water cloud with $\tau = 10.0$ and $r_{\text{eff}} = 15\,\mu\text{m}$. In that case, the overestimation of the retrieved τ reaches up to a distance of 2 km from the ice edge, with a maximum overestimation of 90 % directly beside the ice edge. For r_{eff}, an overestimation of 30 % was found in the direct vicinity of the ice edge. 3-D influences on the retrieval of r_{eff} are observable up to a distance of 1.5 km from the ice edge. This is slightly lower compared to the distance where τ is biased, which indicates that the 3-D effect probably depends on wavelength. Further investigations and the application of similar studies to satellite observations and retrievals of cloud properties in Arctic regions will be part of future studies which dealing with 3-D radiative effects of heterogeneous surface albedo.

Acknowledgements. We are grateful of the Alfred Wegener Institute Helmholtz Centre for Polar and Marine Research, Bremerhaven, Germany for supporting the VERDI campaign with the aircraft and manpower. In addition we like to thank Kenn Borek Air Ltd., Calgary, Canada for the great pilots who made the complicated measurements possible. For excellent ground support with offices and accommodations during the campaign we are grateful of the Aurora Research Institute, Inuvik, Canada.

References

Anderson, G., Clough, S., Kneizys, F., Chetwynd, J., and Shettle, E.: AFGL Atmospheric Constituent Profiles (0–120 km), Tech. Rep. AFGL-TR-86-0110, AFGL (OPI), Hanscom AFB, MA 01736, 1986.

Armstrong, R. L. and Brodzik, M. J.: Recent Northern Hemisphere Snow Extent: A Comparison of Data Derived from Visible and Microwave Satellite Sensors, Geophy. Res. Lett., 28, 3673–3676, 2001.

Bierwirth, E., Ehrlich, A., Wendisch, M., Gayet, J.-F., Gourbeyre, C., Dupuy, R., Herber, A., Neuber, R., and Lampert, A.: Optical thickness and effective radius of Arctic boundary-layer clouds retrieved from airborne nadir and imaging spectrometry, Atmos. Meas. Tech., 6, 1189–1200, doi:10.5194/amt-6-1189-2013, 2013.

Bowker, D., Davis, R., Myrick, D., Stacy, K., and Jones, W.: Spectral Reflectances of Natural Targets for Use in Remote Sensing Studies, NASA RP-1139, NASA Langley Research Center, Hampton (VA), USA, 1985.

Coddington, O. M., Pilewskie, P., and Vukicevic, T.: The Shannon information content of hyperspectral shortwave cloud albedo measurements: Quantification and practical applications, J. Geophy. Res., 117, D04205, doi:10.1029/2011JD016771, 2012.

Curry, J. A., Rossow, W. B., Randall, D., and Schramm, J. L.: Overview of Arctic cloud and radiation characteristics, J. Climate, 9, 1731–1764, 1996.

Grosvenor, D. P. and Wood, R.: The effect of solar zenith angle on MODIS cloud optical and microphysical retrievals within marine liquid water clouds, Atmos. Chem. Phys., 14, 7291–7321, doi:10.5194/acp-14-7291-2014, 2014.

Gueymard, C. A.: The sun's total and spectral irradiance for solar energy applications and solar radiation models, Sol. Energy, 76, 423–453, 2004.

Intrieri, J. M., Fairall, C. W., Shupe, M. D., Persson, P. O. G., Andreas, E. L., Guest, P. S., and Moritz, R. E.: An annual cycle of Arctic surface cloud forcing at SHEBA, J. Geophys. Res., 107, SHE 13-1-SHE 13-14, doi:10.1029/2000JC000439, 2002a.

Intrieri, J. M., Shupe, M. D., Uttal, T., and McCarty, B. J.: An annual cycle of Arctic cloud characteristics observed by radar and lidar at SHEBA, J. Geophys. Res., 107, SHE 5-1-SHE 5-15, doi:10.1029/2000JC000423, 2002b.

Iwabuchi, H.: Efficient Monte Carlo methods for radiative transfer modeling, J. Atmos. Sci., 63, 2324–2339, 2006.

Iwabuchi, H. and Kobayashi, H.: Modeling of radiative transfer in cloudy atmospheres and plant canopies using Monte Carlo methods, Tech. Rep. 8, 199 pp., FRCGC, 2008.

Jäkel, E., Wendisch, M., and Mayer, B.: Influence of spatial heterogeneity of local surface albedo on the area-averaged surface albedo retrieved from airborne irradiance measurements, Atmos. Meas. Tech., 6, 527–537, doi:10.5194/amt-6-527-2013, 2013.

King, N. J., and Vaughan, G.: Using passive remote sensing to retrieve the vertical variation of cloud droplet size in marine stratocumulus: An assessment of information content and the potential for improved retrievals from hyperspectral measurements, J. Geophys. Res., 117, D15206, doi:10.1029/2012JD017896, 2012.

Klingebiel, M., de Lozar, A., Molleker, S., Weigel, R., Roth, A., Schmidt, L., Mayer, J., Ehrlich, A., Neuber, R., Wendisch, M., and Borrmann, S.: Arctic low-level boundary layer clouds: in situ measurements and simulations of mono- and bimodal supercooled droplet size distributions at the top

layer of liquid phase clouds, Atmos. Chem. Phys., 15, 617–631, doi:10.5194/acp-15-617-2015, 2015.

Krijger, J. M., Tol, P., Istomina, L. G., Schlundt, C., Schrijver, H., and Aben, I.: Improved identification of clouds and ice/snow covered surfaces in SCIAMACHY observations, Atmos. Meas. Technol., 4, 2213–2224, doi:10.5194/amt-4-2213-2011, 2011.

Lawson, R. P., Baker, B. A., and Schmitt, C. G.: An overview of microphysical properties of Arctic clouds observed in May and July 1998 during FIRE ACE, J. Geophys. Res., 106, 14989–15014, 2001.

Lindsay, R. W. and Rothrock, D. A.: Arctic sea–ice albedo from Avhrr, J. Climate, 7, 1737–1749, doi:10.1175/1520-0442(1994)007<1737:ASIAFA>2.0.CO;2, 1994.

Loeb, N. G. and Davis, R.: Observational evidence of plane parallel model biases: Apparent dependence of cloud optical depth on solar zenith angle, J. Geophys. Res., 101, 1621–1634, 1996.

Lyapustin, A.: Three-dimensional effects in the remote sensing of surface albedo, IEEE T. Geosci. Remote, 39, 254–263, 2001.

Lyapustin, A. and Kaufman, Y.: Role of adjacency effect in the remote sensing of aerosol, J. Geophys. Res., 106, 11909–11916, 2001.

Marshak, A., Wen, G., Coakley Jr., J. A., Remer, L. A., Loeb, N. G., and Cahalan, R. F.: A simple model for the cloud adjacency effect and the apparent bluing of aerosols near clouds, J. Geophys. Res., 113, D14S17, doi:10.1029/2007JD009196, 2008.

Nakajima, T. and King, M.: Determination of the optical thickness and effective particle radius of clouds from reflected solar radiation measurements. Part I: Theory, J. Atmos. Sci., 47, 1878–1893, 1990.

Overland, J. E., Wood, K. R., and Wang, M.: Warm Arctic–cold continents: impacts of the newly open Arctic Sea, Polar Res., 30, 15787, doi:10.3402/polar.v30i0.15787, 2011.

Pierluissi, J. and Peng, G.-S.: New molecular transmission band models for LOWTRAN, Opt. Eng., 24, 541–547, 1985.

Platnick, S., Li, J. Y., King, M. D., Gerber, H. and Hobbs, P. V.: A solar reflectance method for retrieving the optical thickness and droplet size of liquid water clouds over snow and ice surfaces, J. Geophys. Res., 106, 15,185–15,199, 2001.

Platnick, S., King, M. D., Wind, B., Gray, M. and Hubanks, P.: An initial analysis of pixel-level uncertainty in global MODIS cloud optical thickness and effective particle size retrievals, Proc. of SPIE, 5652, doi: 10.1117/12.578353, 2004.

Platnick, S. and King, M. D.: The MODIS Cloud Products: Algorithms and Examples From Terra, IEEE T. Geosci. Remote. 41, 459–473, 2003.

Ricchiazzi, P. and Gautier, C.: Investigation of the effect of surface heterogeneity and topography on the radiation environment of Palmer Station, Antarctica, with a hybrid 3-D radiative transfer model, J. Geophys. Res., 103, 6161–6178, 1998.

Rothrock, D. A. and Thorndike, A. S.: Measuring the sea ice floe size distribution, J. Geophys. Res., 89, 6477–6486, 1984.

Sanderson, M. G., Hemming, D. L., and Betts, R. A.: Regional temperature and precipitation changes under high-end ($\geq$ 4 degrees C) global warming, Philos. T. R. Soc. A., 369, 85–98, doi:10.1098/rsta.2010.0283, 2011.

Schäfer, M., Bierwirth, E., Ehrlich, A., Heyner, F., and Wendisch, M.: Retrieval of cirrus optical thickness and assessment of ice crystal shape from ground-based imaging spectrometry, Atmos. Meas. Tech., 6, 1855–1868, doi:10.5194/amt-6-1855-2013, 2013.

Shonk, J. K. P., Hogan, R. J., Edwards, J. M., and Mace, G. G.: Effect of improving representation of horizontal and vertical cloud structure on the Earth's global radiation budget. Part I: Review and parametrization, Q. J. Roy. Meteor. Soc., 136, 1191–1204, doi:10.1002/qj.647, 2010.

Shupe, M. D. and Intrieri, J. M.: Cloud radiative forcing of the Arctic surface: The influence of cloud properties, surface albedo, and solar zenith angle, J. Climate, 17, 616–628, 2004.

Shupe, M. D., Matrosov, S. Y., and Uttal, T.: Arctic mixed-phase cloud properties derived from surface-based sensors at SHEBA, J. Atmos. Sci., 63, 697–711, 2006.

Shupe, M. D., Walden, V. P., Eloranta, E., Uttal, T., Campbell, J. R., Starkweather, S. M., and Shiobara, M.: Clouds at Arctic atmospheric observatories. Part I: Occurrence and macrophysical properties, J. Appl. Meteorol. Clim., 50, 626–644, doi:10.1175/2010JAMC2467.1, 2011.

Stachlewska, I. S., Neuber, R., Lampert, A., Ritter, C., and Wehrle, G.: AMALi – the Airborne Mobile Aerosol Lidar for Arctic research, Atmos. Chem. Phys., 10, 2947–2963, doi:10.5194/acp-10-2947-2010, 2010.

Tsay, S.-C. and Jayaweera, K.: Physical Characteristics of Arctic Stratus Clouds, J. Clim. Appl. Meteorol., 23, 584–596, 2013.

Vavrus, S.: The Impact of Cloud Feedbacks on Arctic Climate under Greenhouse Forcing, J. Climate., 17, 603–615, 2004.

Wendisch, M. and Brenguier, J.-L.: Airborne Measurements for Environmental Research – Methods and Instruments, Wiley–VCH Verlag GmbH & Co. KGaA, Weinheim, Germany, 2013.

Wendisch, M., Müller, D., Schell, D., and Heintzenberg, J.: An airborne spectral albedometer with active horizontal stabilization, J. Atmos. Ocean. Tech., 18, 1856–1866, 2001.

Wendisch, M., Pilewskie, P., Jäkel, E., Schmidt, S., Pommier, J., Howard, S., Jonsson, H. H., Guan, H., Schröder, M., and Mayer, B.: Airborne measurements of areal spectral surface albedo over different sea and land surfaces, J. Geophys. Res., 109, D08203, doi:10.1029/2003JD004392, 2004.

Wendisch, M., Yang, P., and Ehrlich, A., (Eds.): Amplified climate changes in the Arctic: Role of clouds and atmospheric radiation, vol. 132, 1–34, Sitzungsberichte der Sächsischen Akademie der Wissenschaften zu Leipzig. Mathematisch-Naturwissenschaftliche Klasse, S. Hirzel Verlag, Stuttgart/Leipzig, 2013.

Werner, F., Siebert, H., Pilewskie, P., Schmeissner, T., Shaw, R. A., and Wendisch, M.: New airborne retrieval approach for trade wind cumulus properties under overlying cirrus, J. Geophys. Res., 118, 1–16, doi:10.1002/jgrd.50334, 2013.

Zinner, T., Wind, G., Platnick, S., and Ackerman, A. S.: Testing remote sensing on artificial observations: impact of drizzle and 3-D cloud structure on effective radius retrievals, Atmos. Chem. Phys., 10, 9535–9549, doi:10.5194/acp-10-9535-2010, 2010.

Table 1. Ratio $R_{\text{3-D/IPA}}$ (in %) of γ_λ for the total scene area (R_{total}), for the sea-ice covered area (R_{ice}), and for the dark ocean covered area (R_{water}) of all scenarios from Sect. 4.2.3 and 4.2.4. The simulations are performed with clouds of $\tau = 1$ and $\tau = 5$ at an altitude of 0–200 and 500–1000 m.

0–200 m	Case	$\tau = 1$ R_{total} (%)	R_{ice} (%)	R_{water} (%)	$\tau = 5$ R_{total} (%)	R_{ice} (%)	R_{water} (%)
	1	99.7	96.1	103.0	99.5	95.1	100.7
	2	99.1	94.1	104.3	99.1	91.7	101.6
	3	100.0	94.0	103.0	99.5	91.7	100.7
	4	100.1	94.2	104.8	99.5	91.8	101.2
	Real Case	–	–	–	92.6	73.2	124.0

500–1000 m	Case	$\tau = 1$ R_{total} (%)	R_{ice} (%)	R_{water} (%)	$\tau = 5$ R_{total} (%)	R_{ice} (%)	R_{water} (%)
	1	97.4	87.5	107.2	97.4	77.5	103.2
	2	96.5	82.5	112.8	96.5	66.5	106.0
	3	98.4	82.3	106.7	97.9	66.5	102.8
	4	98.4	82.9	109.4	98.1	67.5	103.9

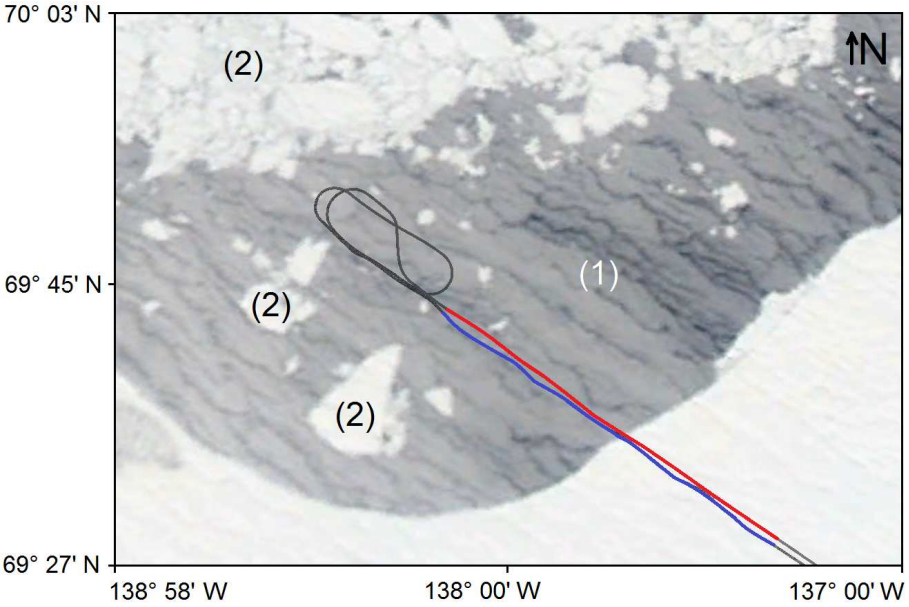

Figure 1. VERDI flight track and true-colour MODIS image (Aqua; 250 m resolution) from 17 May 2012. Numbers (1) and (2) label open ocean and sea ice, respectively.

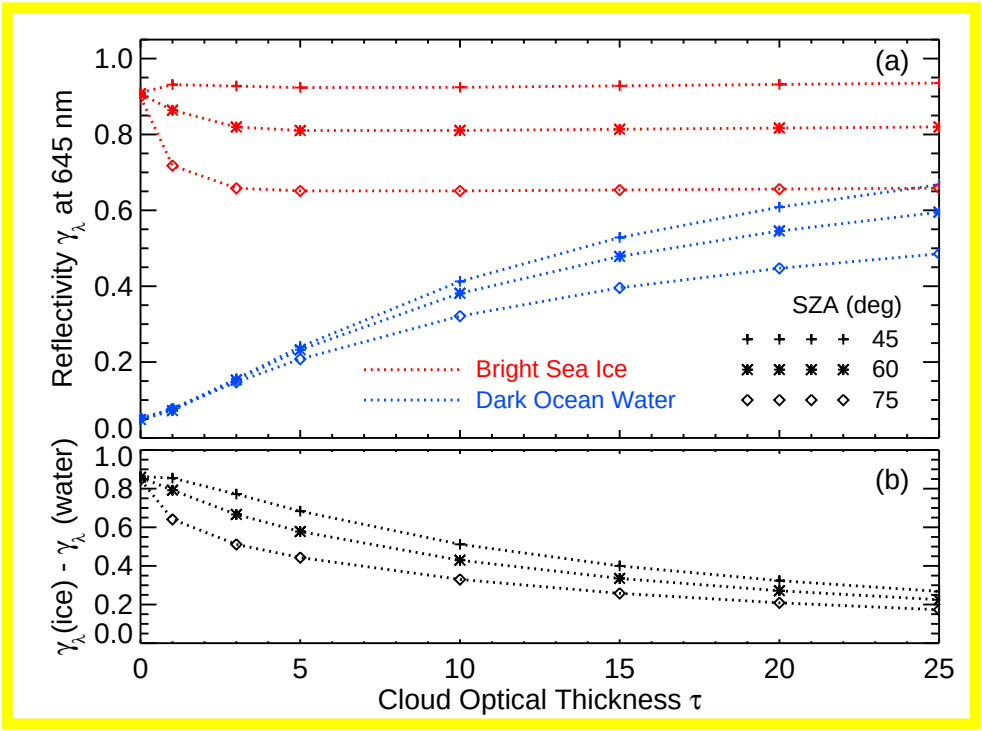

Figure 2. (a) Simulated γ_λ at 645 nm calculated for different τ ranging from 0 to 25 and cloud particles with a fixed r_{eff} of 15 µm. The calculations were performed for different Θ of 45, 60, and 75° over a highly reflecting ice surface and a dark ocean surface. **(b)** Difference between the simulated γ_λ over bright sea ice surface and dark ocean surface from **(a)**.

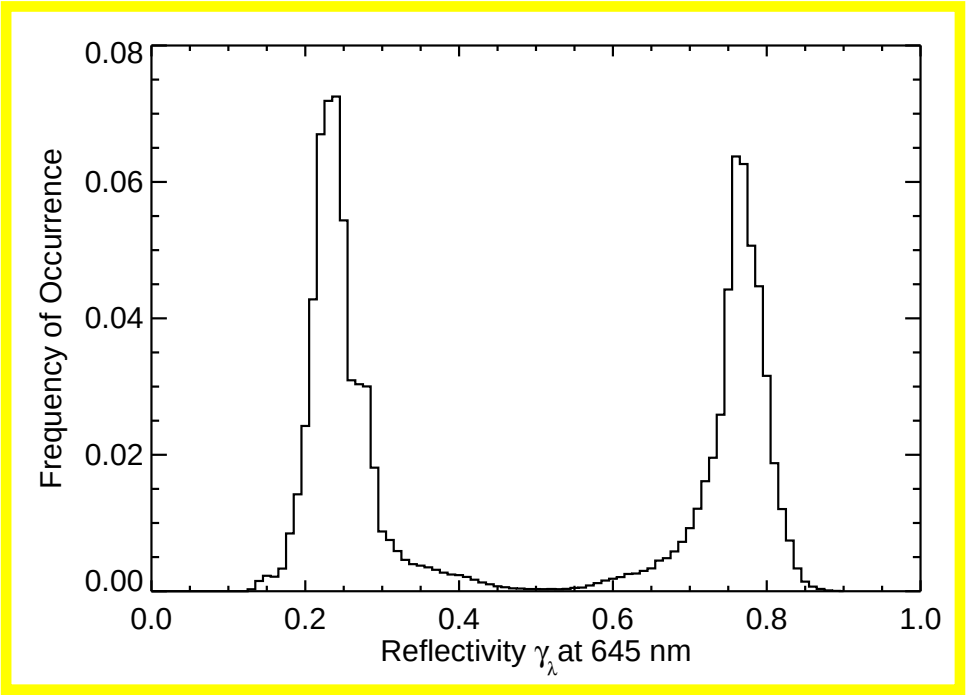

Figure 3. Fraction of occurrence of the measured γ_λ at 645 nm, given in the example of Fig. 4a. The bin size is 0.01.

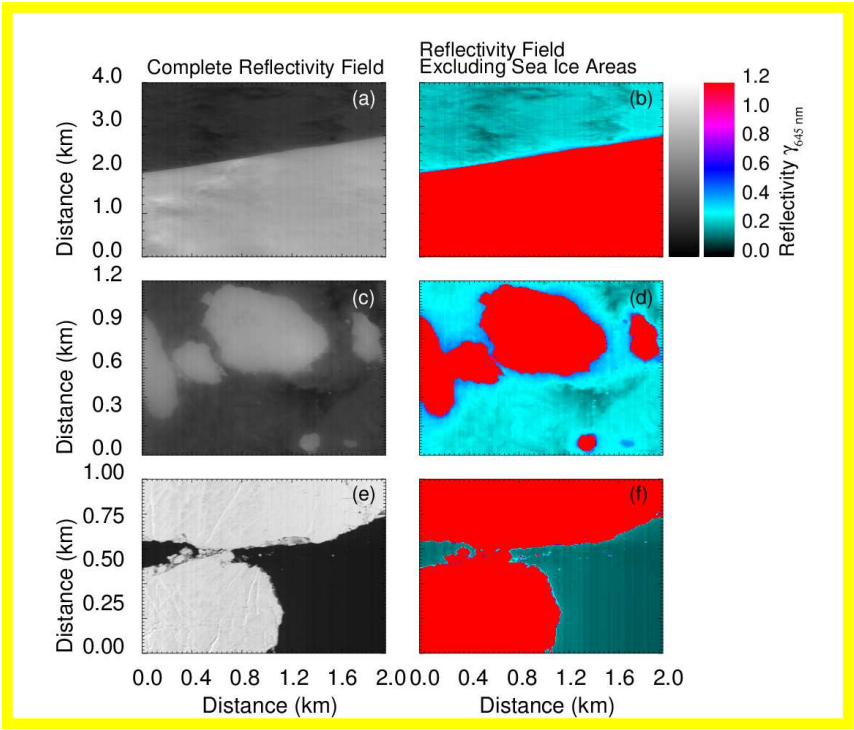

Figure 4. Left Side: Fields of γ_λ at 645 nm, measured with the imaging spectrometer AisaEAGLE. The measurements were performed on 17 May 2012 during the international field campaign VERDI. Right side: The same as on the left side in colour-scale and with ice mask overlay.

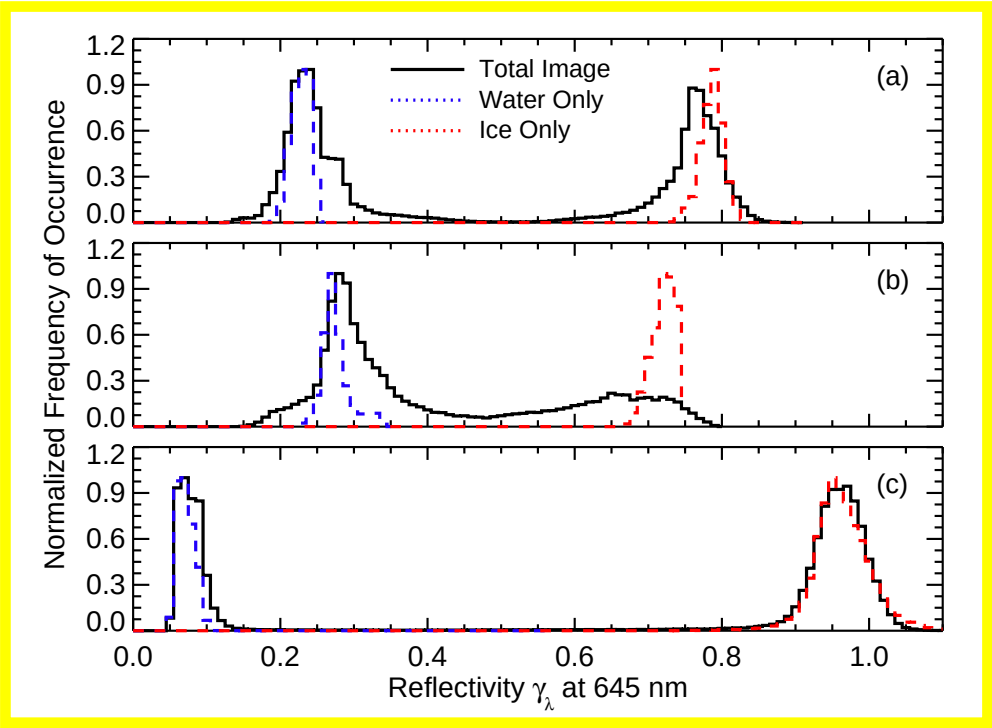

Figure 5. Normalized distributions of the frequency of occurrence of γ_λ measured during the three cases presented in Fig. 4. Additionally included are the frequency distributions over sea ice and dark ocean water only.

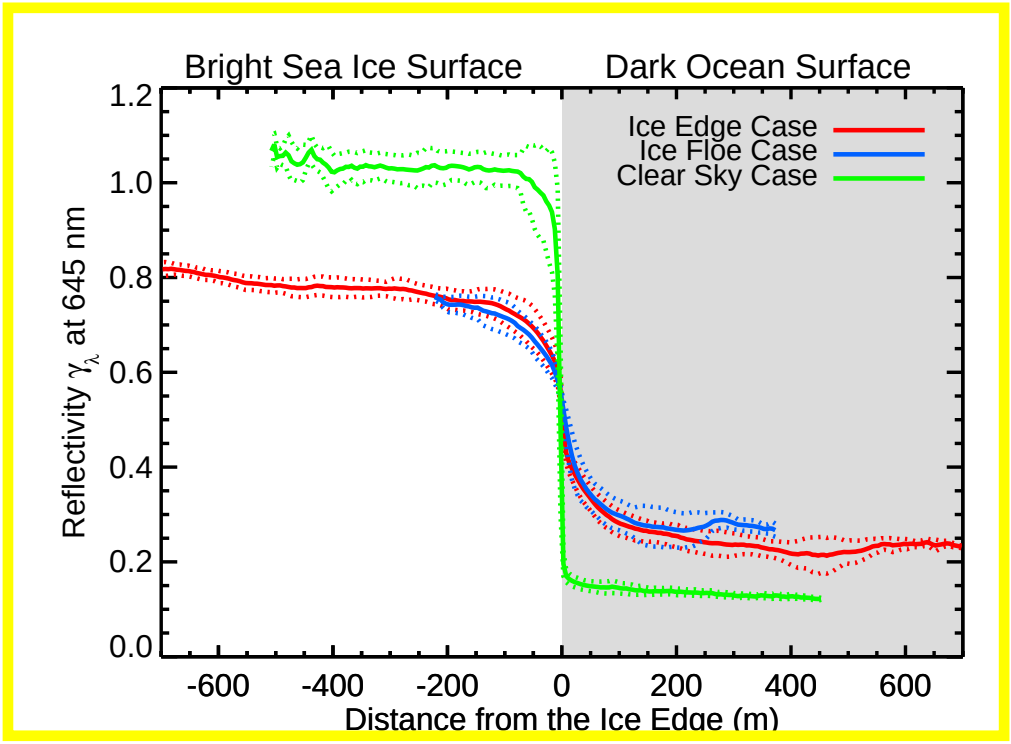

Figure 6. Averaged γ_λ (solid lines) $\pm 6\%$ measurement uncertainty of γ_λ (dashed lines) at 645 nm wavelength, measured perpendicular to the ice edges shown in Fig. 4.

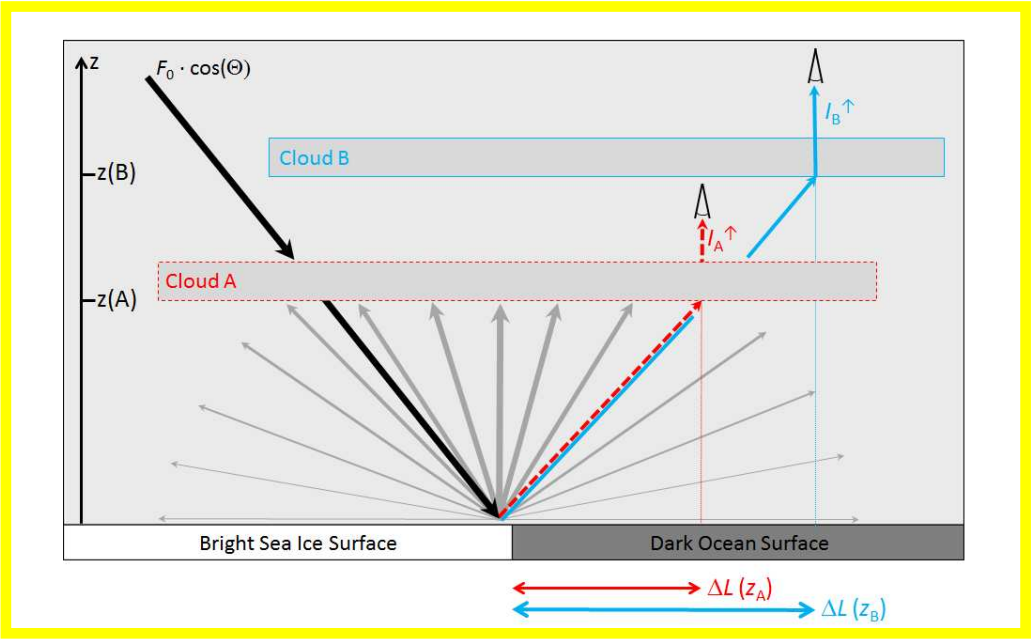

Figure 7. Sketch of the 3-D radiative effects between clouds at two different altitudes and the surface in the vicinity of an ice edge. The arrows illustrate the pathway of the photons between source, cloud, surface, and sensor.

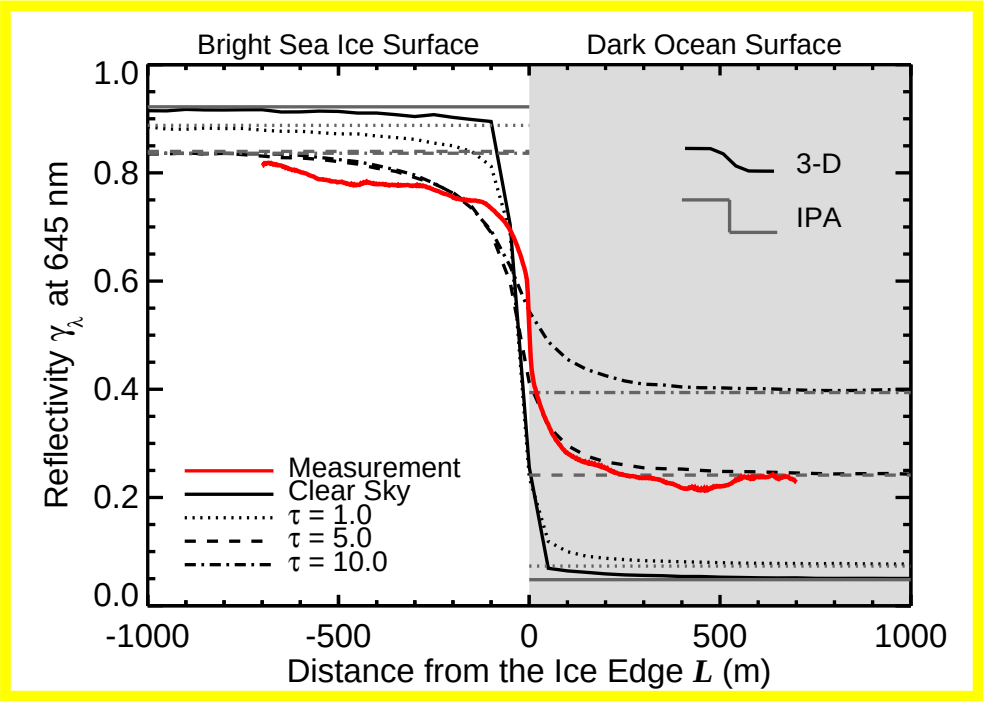

Figure 8. Simulated mean γ_λ across an ice edge for clear-sky conditions as well as for low-level clouds between 0 and 200 m altitude, $\tau = 1/5/10$, and $r_{\text{eff}} = 15\,\mu\text{m}$. The white area illustrates the bright sea ice, the grey area the dark ocean water. Included are the results of the 3-D and IPA simulation, as well as the average of γ_λ, measured perpendicular to the ice edge in Fig. 4a.

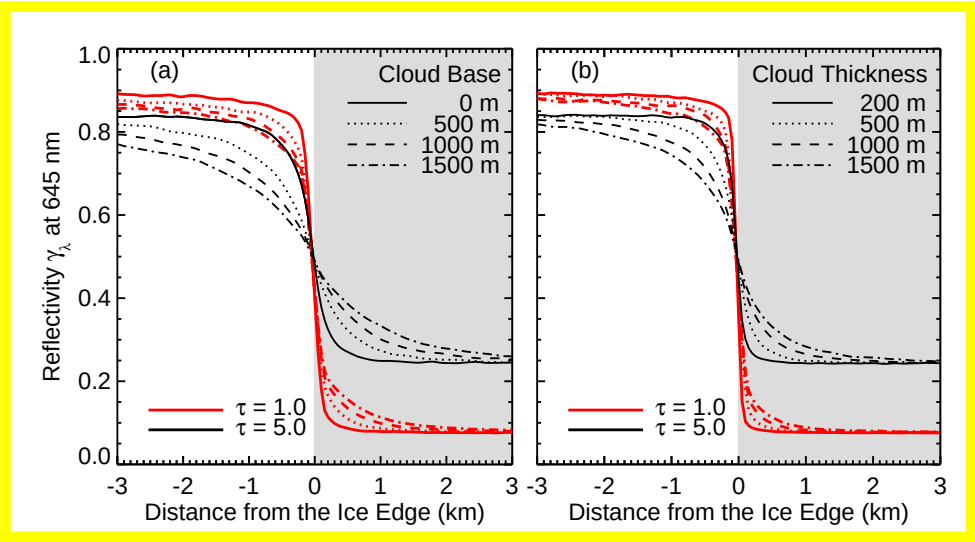

Figure 9. Simulated γ_λ for clouds at different altitudes and with different geometrical thickness for the passage from a highly reflecting ice-covered region to a darker region of open water. The white area illustrates the ice stripe. **(a)** The cloud geometrical thickness is 500 m. **(b)** Cloud base at 0 m.

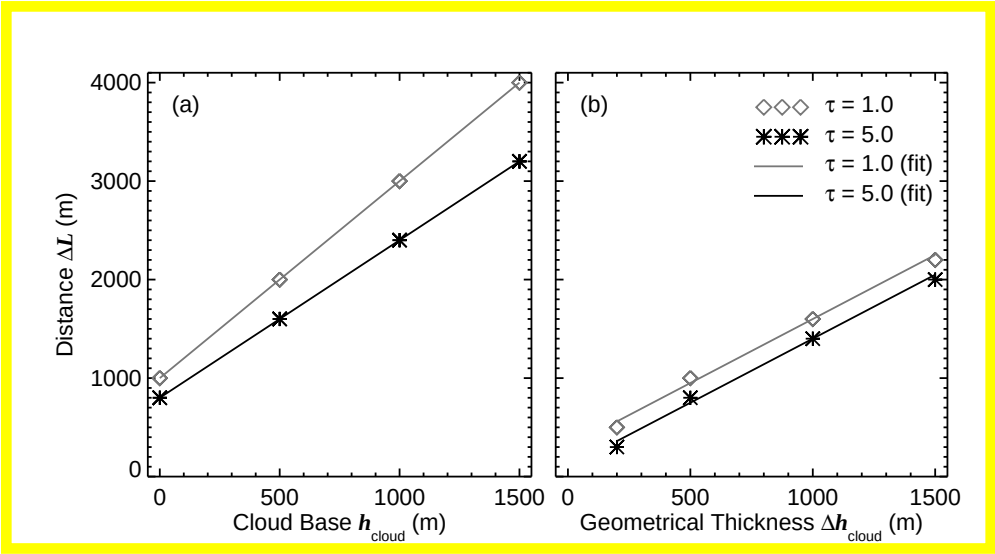

Figure 10. (a) Distance ΔL as a function of the cloud base altitude h_{cloud} for a cloud with a geometrical thickness of $\Delta h_{\text{cloud}} = 500$ m and different τ. (b) Distance ΔL as a function of the cloud geometrical thickness Δh_{cloud} for a low-level cloud with cloud base at $h_{\text{cloud}} = 0$ m and different τ.

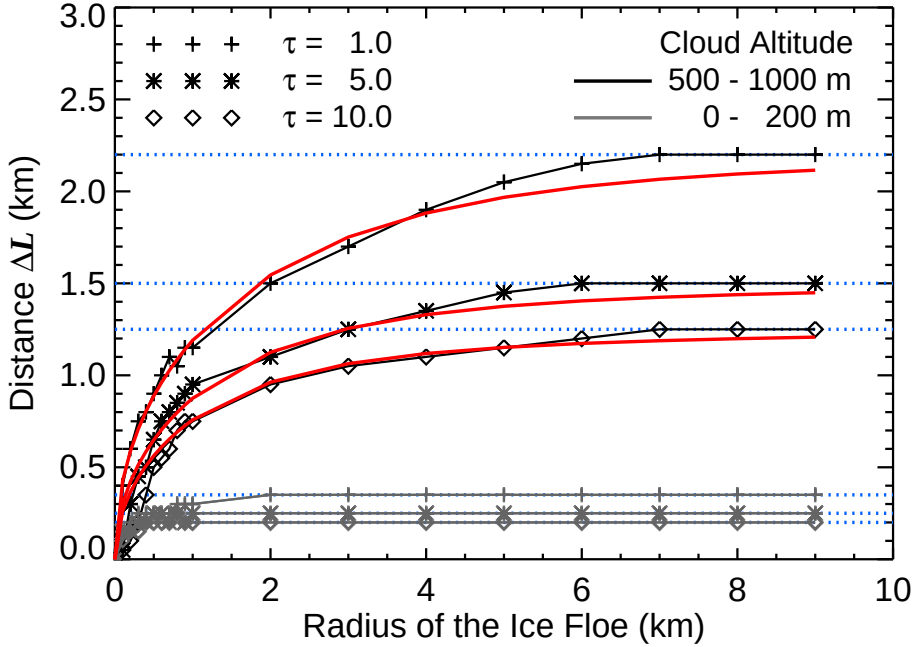

Figure 11. Simulations (grey and black lines) and parametrisations (red lines) of ΔL as a function of the ice floe size, different τ, and different cloud altitudes. Asymptotic maximum values of ΔL are marked with dotted blue lines.

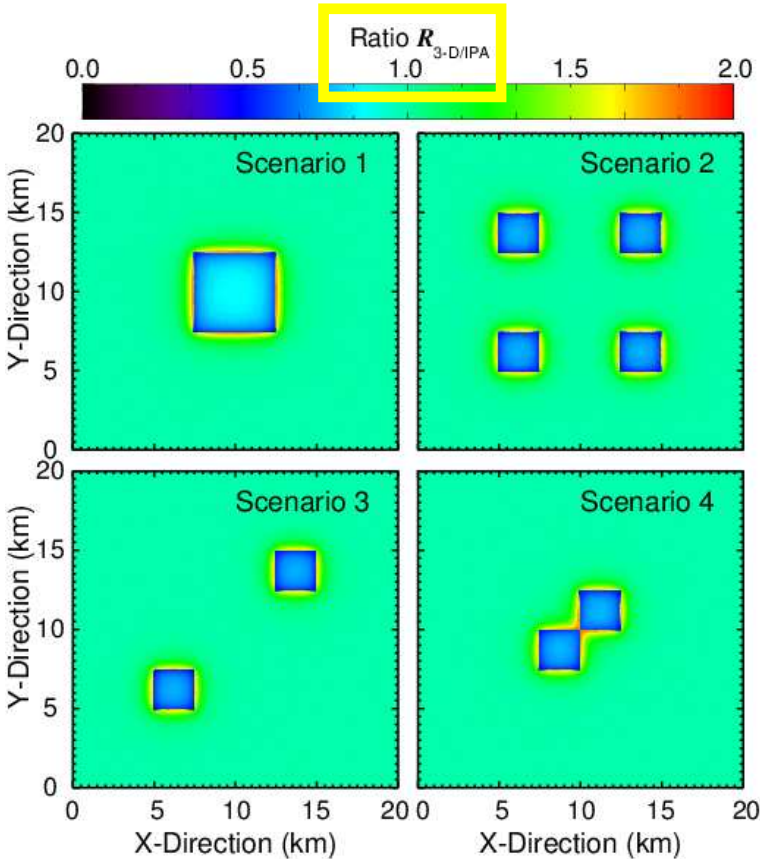

Figure 12. Ratio $R_{\text{3-D/IPA}}$ of γ_λ of the 3-D and IPA simulation at $\tau = 5$ and for a cloud between 500 and 1000 m altitude. Each panel displays one of the four scenarios.

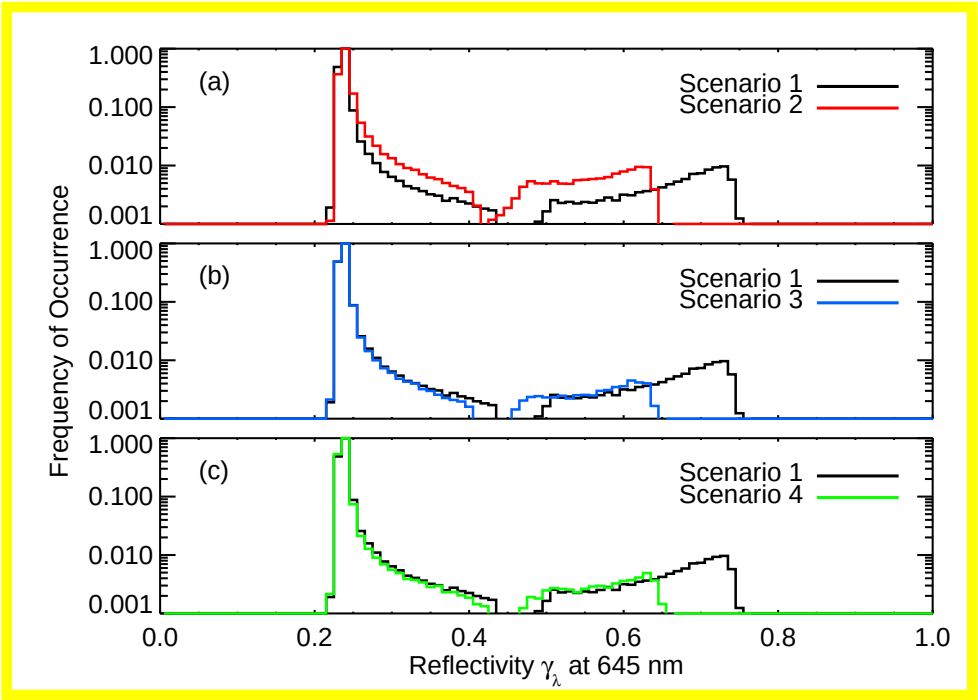

Figure 13. Single logarithmic frequency distributions of the modelled γ_λ from all four scenarios displayed in Fig. 12.

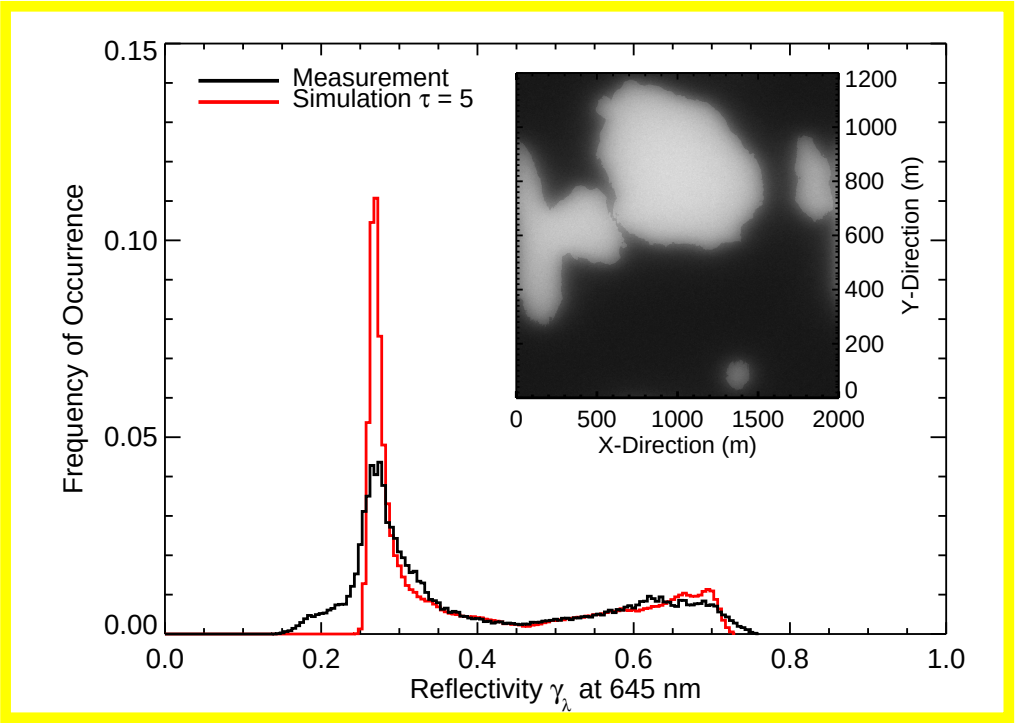

Figure 14. Frequency distributions of measurement and simulation. 3-D simulation performed for the second measurement case, presented in Fig. 4 and Sect. 3. The bin size in γ_λ is 0.005.

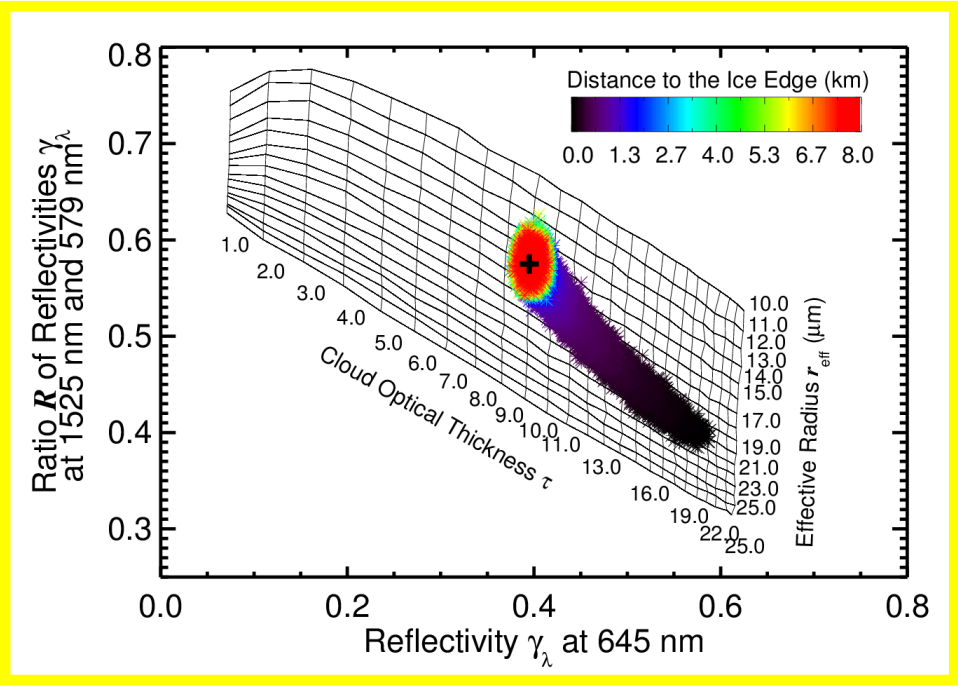

Figure 15. Retrieval grid using γ_λ at 645 nm and the ratio of γ_λ at $\lambda_1/\lambda_2 = 1525\,\text{nm}/579\,\text{nm}$. γ_λ of the 3-D simulation are illustrated by colour-coded dots as a function of distance to the ice-floe edge. The black cross marks the exact cloud properties $\tau = 10$ and $r_{\text{eff}} = 15\,\mu\text{m}$ used in the 3-D simulation for the cloud at 500 to 1000 m altitude.

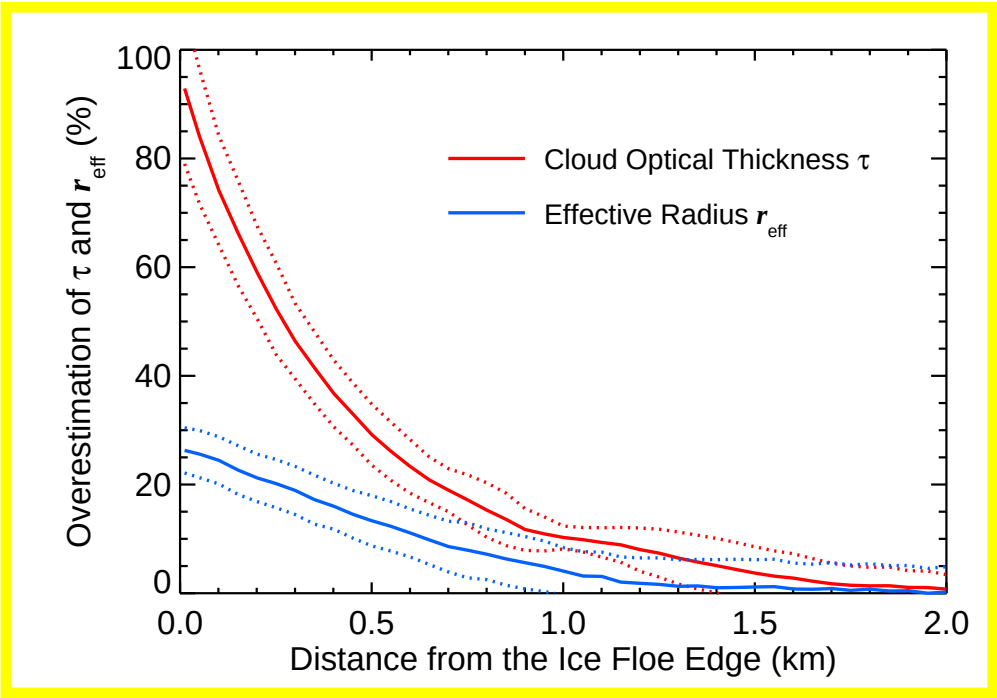

Figure 16. Overestimation (average and standard deviation) of τ and r_{eff} as a function of the distance to the edge of the ice floe. The model cloud at an altitude of 500 to 1000 m had $\tau = 10$ and $r_{\text{eff}} = 15\,\mu\text{m}$.